CASE WESTERN RESERVE UNIVERSITY

GRADUATE STUDIES

We hereby approve the thesis of

Matthew Stephen Johnson

candidate for the Master of Science in Dentistry degree.

Signed: V. KAZRA (Chairman)

Date 8/13/90

ACCOUNT NO. 00-104-07

TITLE NO.

ISSN NUMBER

VOL/YR

FREQUENCY

PICKUP

NEW TITLE ☐ RUB SENT ☐ SAMPLE SENT ☐

	F	R	NP		IN	OUT	EX.
TITLE PAGE				FRONT COVER			
TABLE CONT.				REAR COVER			
INDEX				ADVERTISING			

COLLATE INST.

POCKET	YES NO	SEW-THRU-FOLD	YES NO
SINGLES S.T.F.	YES NO	DON'T RESEW	YES NO
ADHESIVE BIND	YES NO	EXTRA TIME	

STAMP INST.

SLOT | TITLE

JOHNSO . S.

28 | 1990

STYLE TH

CALL NUMBER

PRINT COLOR G

TRIM HEIGHT

BUCKRAM COLOR 2075

BUCKRAM SIZE

LIBRARY IMPRINT

49 91 355CS 0 104 7 TH 4308

THESIS

INFORMATION CONSERVATION, INC.
GENERAL BOOKBINDING CO.

BOOK ☐ BINDERY COPY 1

CASE WESTERN RESERVE UNIVERSITY

GRADUATE STUDIES

We hereby approve the thesis of

Matthew Stephen Johnson

candidate for the Master of Science in Dentistry degree.

Signed: V. KAZRA (Chairman)

Date 8/13/90

ESTHETIC ORTHODONTIC ARCH WIRES: A QUEST FOR MATERIALS AND A PRE-CLINICAL MECHANICAL PROPERTIES TESTING PROTOCOL

by

MATTHEW STEPHEN JOHNSON

Submitted in partial fulfillment of the requirements

for the Degree of Master of Science in Dentistry

Department of Orthodontics

School of Dentistry

CASE WESTERN RESERVE UNIVERSITY

AUGUST 1990

ESTHETIC ORTHODONTIC ARCH WIRES: A QUEST FOR MATERIALS AND A PRE-CLINICAL MECHANICAL PROPERTIES TESTING PROTOCOL

Abstract

by

Matthew Stephen Johnson

With the obvious demand for a maximally esthetic fixed orthodontic appliance, as was indicated by the popularity of clear esthetic orthodontic brackets, an effort was initiated to develope complementary esthetic orthodontic arch wires. An initial assessment of various esthetic materials, those which were clear or tooth colored, demonstrated that esthetic polymer compounds were already used in commercial products with similar dimensions to orthodontic arch wires. The search for esthetic materials involved contacting numerous polymer suppliers and manufacturers in an effort to obtain sample specimens for mechanical properties testing if they were available in configurations similar to orthodontic arch wires.

A tensile test and a three-point-bend test were developed which were capable of determining the actual material mechanical properties of the esthetic materials that were received and considered adequate for testing. The spectrum of commonly used metal wires; stainless steel, cobalt-chromium-nickel, beta titanium-molybdenum, nickel-titanium, and multistranded stainless steel wires were tested in order to verify the testing protocol and establish a direct means of standard comparison for the selected esthetic materials. Stress-strain diagrams were constructed from data derived from tensile tests and load-deflection

diagram were constructed from bend test data. In Addition, Approximated flexural stress-strain diagrams were constructed indirectly from the bend test data by using the definition of the modulus of elasticity (E), $E=\sigma/\varepsilon$, where, σ, is the stress and, ε, is the engineering stain, as an approximation. The true stain, ε, was used in the case of tensile stress-strain diagrams.

Values for the tensile modulus of elasticity (E_t), the yield strength at the 0.2% offset and the corresponding stain at the 0.2% offset, were reported from the tensile data. The values for the flexural modulus of elasticity (E_f), and with use of the approximated flexural stress-strain diargams, the yield strength at the 0.2% offset, the corresponding strain at the 0.2% offset, the load corresponding to the 0.2% strain offset, and the deflection corresponding to the 0.2% strain offset, were reported from bend test data. Although the selection of the yield point at the 0.2% offset was initially done in order to be consistent with engineering literature, it proved to be a clinically relevant parameter since it not only approximated the point at which elastic behavior ends and plastic deformation starts as customarily, but in addition, this yield point at the 0.2% offset strain occurred were the corresponding amount of deflection was within the threshold that is visually obvious in clinical terms, occurring here for the various materials studies in a range from 0.0103 inch (0.26 mm) to 0.0595 inch (1.51 mm).

Experimental values for the reported properties of the commonly used metal wires fell within established values and thus the test protocol was verified for accuracy and a means of a standard for comparison established. The tensile modulus of elasticity (E_t) for overall average of 0.0.14", 0.016", 0.018", and 0.020" Tru-Chrome®, stainless steel; 0.018" TMA®, 0.018" beta-titanium molybdenum; 0.018" Titanal®, nickel-titanium metal wires were found to

be 24.2 ± 0.6x10^6 psi (166.7 ± 10.0x10^9 N/m^2), 11.9 ±0.4x10^6 psi (82.1 ± 2.6x10^9 N/m^2), 5.0 ± 0.47x10^6 psi (34.4 ± 3.2x10^9 N/m^2), and the flexural modulus of elasticity (E_f), was 28.1 ± 0.7x10^6 psi (193.6 ± 4.6x10^9 N/m^2), 12.9 ± 0.4x10^6 psi (89.1 ± 2.6x10^9 N/m^2), 6.78 ± 0.56x10^6 psi (46.7 ± 3.8x10^9 N/m^2), respectively, just to name a few of the materials studies. In addition, the flexural modulus of elasticity (E_f) of 0.0175" *Respond® 6-stranded multistranded stainless steel wire was 1.64 ± 0.02x10^6 psi (11.3 ± 0.11x10^9 N/m^2).

The flexural modulus of elasticity (E_f) for some of the esthetic materials tested, **MX-501 (PEEK) polyether ether ketone, **WOX-3 (PEEK) polyether ether ketone, **WP-320 (PET) polyethylene terephthalate, **WP-89 (PET) polyethylene terephthalate, were 0.97 ± 0.03x10^6 psi (6.68 ± 0.22x10^9 N/m^2), 1.05 ± 0.11x10^6 psi (7.26 ± 0.74x10^9 N/m^2), 2.24 ± 0.02x10^6 psi (15.4 ± 0.16x10^9 N/m^2), and 2.43 ± 0.04x10^6 psi (16.7 ± 0.26x10^9 N/m^2), respectively, to name a few of the polymers that preformed comparatively well during mechanical testing in terms of the flexural modulus of elasticity (E_f).

Since Burstone *et al.* (1983) reported the flexural modulus of elasticity (E_f) for the 0.016" x 0.022" *D-Rect®, 9-stranded braided multistranded stainless steel rectangular wire at 0.89 ± 0.08x10^6 psi when tested parallel to the large cross section of the wire and additionally since the values of the flexural modulus of elasticity (E_f) reported herein for the 0.0175" *Respond® 6-stranded multistranded stainless steel wire, it appear likely that the formentioned polymers

---

*Ormco Corporation, Glendora, Calif.

**Shakespeare Monofilament, Columbia, S.C.

wires can deliver a clinical efficacy similar to these metal wires on the basis of comparing the values for the flexural modulus of elasticity (E_f). The *Optiflex™ an esthetic fiber glass orthodontic wire; **Glastic®, another fiber glass composite wire; and a ***Nylon 6/6 wire were the other esthetic wires tested.

The *** (PET) polyethylene terephthalate polyester wires, which had the highest values for the flexural modulus of elasticity (E_f) for unfilled polymers studied are available from the manufacturer in variable colors including clear and can be form into any requested diameter. Since this type of material is commonly used in the food packaging industry (*e.g.*, plastic bottles), and has a low water absorption, 0.2%, factors of biocompatibility may be favorable for use in the oral cavity as an initial leveling and aligning orthodontic arch wire.

Polymers, particularly unfilled polymers, have mechanical properties that are highly dependent on time, temperature, and conditions of stressing (Nielsen, 1974). Before the unfilled polymers, in particular, can be recommend for intraoral use as initial leveling and aligning wires, it is recommended that strain cycling and flexural cycling tests be done to understand the fatigue and springback behavior, and creep data be accumulated to address the effects of time and temperature on these materials.

---

*Ormco Corporation, Glendora, Calif.

**Glastic Corporation, Cleveland, Ohio

***Shakespeare Monofilament, Columbia, S.C.

ACKNOWLEDGEMENTS

The author wishes to express his sincere appreciation to the following individuals and companies:

Dr. Varun Kalra, Director of the Orthodontic Clinic, for sharing some of his original ideas which made this thesis possible, and accepting the responsibility of acting as chairman of the thesis committee. His friendship and guidance eased the journey toward completing this study.

Dr. Mark Hans, Program Director of the Orthodontic Department, for being a thesis advisor and his constructive comments of the preparation of the manuscript. His dedication to our orthodontic education is obvious in the direction that he has given to the department and to all of us.

Dr. Peter Lagerlof, Professor of Material Science and Engineering, for being a thesis advisor and his expert guidance with the technical material science and engineering aspects of this study. His commitment to science and truly superb teaching manner dramatically influenced the quality of this work.

Mr. Chris Tuma, Instron Mechanical Properties Laboratory Technician, for training me and giving me guidance with the Instron instrumentation involved with the study.

Mr. John Jaroscak, Machinist in the Chemistry and Physics Machine Shop, for his exceptional ideas and work in construction of the three-point-bend fixture and modification of the tensile clamps.

To the following companies that graciously donated wires samples: GAC International, Inc.; Glastic Corporation, Inc.; Lancer Orthodontics, Inc.; Ormco Corporation, Inc.; Rocky Mountain Orthodontics, Inc.; Shakespeare Monofilament, Inc.; and TP Orthodontics, Inc.

Drs. Jose Chaques-Asensi, Valerie Martone, George Souris, George Rosenczweig, and Sophie Rosenczweig, with whom I enjoyed their commraderie the last two years as residents in the graduate orthodontic program. Their friendship will not be forgotten.

DEDICATION

TO

My parents,

who helped make my education possible,

and for instilling in me the determination

to have come this far.

TABLE OF CONTENTS

Page

ABSTRACT. ii

ACKNOWLEDGEMENTS. vi

DEDICATION. viii

LIST OF TABLES. x

LIST OF FIGURES. xi

INTRODUCTION. 1

LITERATURE REVIEW. 4

STATEMENT OF THESIS. 42

MATERIALS AND METHODS. 43

RESULTS. 87

DISCUSSION. 136

SUMMARY AND CONCLUSIONS. 160

LITERATURE CITED. 164

LIST OF TABLES

Tables Page

I. The Mechanical Properties of Metal Arch Wires as Reported in the Orthodontic Literature. 37

II. The Metal Wires that were Tested. 69

III. The Esthetic Wires that were Tested. 70

IV. The Tensile Modulus of Elasticity, E_t, Uniaxial Tensile Test. 87

V. The Tensile Yield Strength at the 0.2% Offset, YS, Uniaxial Tensile Test. 88

VI. The Tensile Strain at the 0.2% Offset, Uniaxial Tensile Test. 89

VII. The Flexural Modulus of Elasticity, E_f, Three-Point-Bend Test, 0.5" Span Length. 90

VIII. The Flexural Yield Strength at the 0.2% Offset, FYS, Three-Point-Bend Test, 0.5" Span Length. 91

IX. The Flexural Strain at the 0.2% Offset, Three-Point-Bend Test, 0.5" Span Length. 92

X. The Load Corresponding to the Flexural Yield Strength at the 0.2% Offset, FYS, Three-Point-Bend Test, 0.5" Span Length. 93

XI. The Deflection Corresponding to the Flexural Yield Strength at the 0.2% Offset, FYS, Three-Point-Bend Test, 0.5" Span Length. 94

LIST OF FIGURES

Figure Page

1. A Typical Stress-Strain Diagram for a 0.018" Stainless Steel Orthodontic Arch wire (Tru-Chrome®). 38

2. A Stress-Strain Diagram for a Mild Steel Which Demonstrates the Proportional Limit, the Actual Yield Strength, and Ultimate Yield Strength. 39

3. A Demonstration of the 0.2% Yield Strength Offset Method. 40

4. An Example of Typical Stress-Strain Curves for a Fiber, a Plastic, and an Elastomer. 41

5. The Tensile Clamps, Grips, and Extensometer in Place on the Instron Universal Testing Machine with a Wire Specimen in Position and Ready for Testing and the Extensometer Calibrator is Shown at the Lower Left. 72

6. An Oblique View of the Modified Grip Faces with the Wire Specimen and Extensometer in Place. 74

7. A Close-up View of the Modified Grip Faces with the Wire Specimen and Extensometer in Place. 76

8. A Close-up View of the Extensometer on the Wire Specimen Ready for Testing. 78

LIST OF FIGURES continued

Figure Page

9. An Frontal View of The Three-Point-Bend Test Fixture with a Wire Specimen and Crosshead Positioned to Begin Testing on the Instron Universal Testing Machine. 80

10. An Oblique View of The Three-Point-Bend Test Fixture with a Wire Specimen and Crosshead Positioned to Begin Testing on the Instron Universal Testing Machine. 82

11. A Top View of The Three-Point-Bend Test Fixture with a Wire Specimen and Crosshead Positioned to Begin Testing on the Instron Universal Testing Machine. 84

12. A Close-up View of The Three-Point-Bend Test Fixture with a Wire Specimen and Crosshead Positioned to Begin Testing on the Instron Universal Testing Machine. 86

13. Comparison of Tensile Test Stress/Strain Diagrams --
(a) Tru-Chrome® 0.020", Tru-Chrome® 0.018", Tru-Chrome® 0.016", and Tru-Chrome® 0.014";
(b) Tru-Chrome® 0.018", A. J. Wilcox Australian Regular 0.018", and A. J. Wilcox Australian Special+ 0.018". 99

14. Comparison of Tensile Test Stress/Strain Diagrams --
(a) Tru-Chrome® 0.018", Blue Elgiloy®0.018", and Red Elgiloy® 0.018";
(b) Tru-Chrome® 0.018", Titanal® 0.018" and Titanal® XR 0.018". 100

LIST OF FIGURES continued

Figure Page

15. Comparison of Tensile Test Stress/Strain Diagrams --
(a) Tru-Chrome® 0.018", Neo-Sentalloy® 0.018" x 0.025",
Sentalloy® Light 0.018", Sentalloy® Medium 0.018", and Sentalloy® Heavy 0.018";
(b) Neo-Sentalloy® 0.018" x 0.025",
Sentalloy® Light 0.018", Sentalloy® Medium 0.018",
and Sentalloy® Heavy 0.018". 101

16. Comparison of Tensile Test Stress/Strain Diagrams --
(a) Tru-Chrome® 0.018", WP-320 (PET) Polyester Monofilament
0.0157", and Sentalloy® Light 0.018";
(b) Tru-Chrome® 0.018", WP-89 (PET) Polyester Monofilament 0.0138",
and Sentalloy® Light 0.018". 102

17. Comparison of Tensile Test Stress/Strain Diagrams --
(a) Tru-Chrome® 0.018", MX-501 (PEEK) Monofilament
0.0236", and Sentalloy® Light 0.018";
(b) Tru-Chrome® 0.018", WOX-3 (PEEK) Monofilament 0.0157",
and Sentalloy® Light 0.018". 103

18. Comparison of Tensile Test Stress/Strain Diagrams --
(a) Tru-Chrome 0.018", WN-101 Nylon 6/6 Monofilament 0.014",
and Sentalloy® Light 0.018";
(b) Tru-Chrome 0.018",Tripleflex™ 0.0195", TMA® 0.018",
NiTi™ 0.018", and Respond® 0.0175". 104

19. Comparison of Tensile Test Stress/Strain Diagrams --
(a) Tru-Chrome® 0.018", Optiflex™ Fiber Glass Composite 0.020",
and Sentalloy® Light 0.018"; and
(b) Tru-Chrome® 0.018", Glastic® Fiber Glass Composite 0.030",
and Sentalloy® Light 0.018". 105

LIST OF FIGURES continued

Figure Page

20. Comparison of Tensile Test Stress/Strain Diagrams -- WP-89 (PET) Polyester Monofilament 0.0138", WP-320 (PET) Polyester Monofilament 0.0157", WOX-3 (PEEK) Monofilament 0.0157", MX-501 (PEEK) Monofilament 0.0236", and WN-101 Nylon 6/6 Monofilament 0.014". 106

21. Tensile Test Stress/Strain Diagrams for Individual Materials --
(a) Tru-Chrome® 0.020",
(b) Tru-Chrome® 0.018",
(c) Tru-Chrome® 0.016", and
(d) Tru-Chrome® 0.014". 107

22. Tensile Test Stress/Strain Diagrams for Individual Materials --
(a) A. J. Wilcox Australian Regular 0.018",
(b) A. J. Wilcox Australian Special+ 0.018",
(c) Blue Elgiloy®0.018", and
(d) Red Elgiloy® 0.018". 108

23. Tensile Test Stress/Strain Diagrams for Individual Materials --
(a) TMA® 0.018",
(b) Respond® 0.0175",
(c) Tripleflex™ 0.0195", and
(d) NiTi™ 0.018". 109

24. Tensile Test Stress/Strain Diagrams for Individual Materials --
(a) Neo-Sentalloy® 0.018" x 0.025",
(b) Sentalloy® Light 0.018",
(c) Sentalloy® Medium 0.018", and
(d) Sentalloy® Heavy 0.018". 110

LIST OF FIGURES continued

Figure Page

25. Tensile Test Stress/Strain Diagrams for Individual Materials --
(a) Titanal® 0.018",
(b) Titanal® XR 0.018",
(c) Optiflex™ Fiber Glass Composite 0.020", and
(d) WN-101 Nylon 6/6 Monofilament 0.014". 111

26. Tensile Test Stress/Strain Diagrams for Individual Materials --
(a) MX-501 (PEEK) Monofilament 0.0236",
(b) WOX-3 (PEEK) Monofilament 0.0157",
(c) WP-89 (PET) Polyester Monofilament 0.0138", and
(d) WP-320 (PET) Polyester Monofilament 0.0157". 112

27. Tensile Test Stress/Strain Diagrams for Individual Materials --
Glastic® Fiber Glass Composite 0.030". 113

28. Comparison of the Three-Point-Bend Test Load/Deflection [L/D] and
Approximated Flexural Stress/Strain [S/S] Diagrams of Tru-Chrome® 0.020",
Tru-Chrome® 0.018", Tru-Chrome® 0.016", and Tru-Chrome®0.014" --
(a) [L/D] Diagrams and
(b) Approximated Flexural [S/S] Diagrams. 114

29. Comparison of the Three-Point-Bend Test Load/Deflection [L/D] and
Approximated Flexural Stress/Strain [S/S] Diagrams of Tru-Chrome® 0.018",
A. J. Wilcox Australian Regular 0.018", and A. J Wilcox Australian Special+
0.018" --
(a) [L/D] Diagrams and
(b) Approximated [S/S] Diagrams. 115

LIST OF FIGURES continued

Figure Page

30. Comparison of the Three-Point-Bend Test Load/Deflection [L/D] and Approximated Flexural Stress/Strain [S/S] Diagrams of Tru-Chrome® 0.018", Blue Elgiloy® 0.018", and Red Elgiloy® 0.018" --
(a) [L/D] Diagrams and
(b) Approximated [S/S] Diagrams. 116

31. Comparison of the Three-Point-Bend Test Load/Deflection [L/D] and Approximated Flexural Stress/Strain [S/S] Diagrams of Tru-Chrome® 0.018", Titanal® 0.018" and Titanal® XR 0.018" --
(a) [L/D] Diagrams and
(b) Approximated [S/S] Diagrams. 117

32. Comparison of the Three-Point-Bend Test Load/Deflection [L/D] and Approximated Flexural Stress/Strain [S/S] Diagrams of Tru-Chrome® 0.018", Neo-Sentalloy® 0.018" x 0.025", Sentalloy® Light 0.018", Sentalloy® Medium 0.018", and Sentalloy® Heavy 0.018" --
(a) [L/D] Diagrams and
(b) Approximated [S/S] Diagrams. 118

33. Comparison of the Three-Point-Bend Test Load/Deflection [L/D] and Approximated Flexural Stress/Strain [S/S] Diagrams of Tru-Chrome® 0.018", TMA® 0.018", NiTi™ 0.018", Tripleflex™ 0.0195", and Respond® 0.0175" --
(a) [L/D] Diagrams and
(b) Approximated Flexural [S/S] Diagrams. 119

LIST OF FIGURES continued

Figure Page

34. Comparison of the Three-Point-Bend Test Load/Deflection [L/D] and
Approximated Flexural Stress/Strain [S/S] Diagrams of Tru-Chrome® 0.018",
Tripleflex™ 0.0195", MX-501 (PEEK) 0.0236" Respond® 0.0175"
0.0175", WP-320 (PET) Polyester 0.0157", WOX-3 (PEEK) 0.0157"
WP-89 (PET) Polyester 0.0138", Optiflex™ 0.020", WN-101 Nylon 6/6
0.014" --
(a) [L/D] Diagrams and
(b) Approximated Flexural [S/S] Diagrams. 120

35. Comparison of the Three-Point-Bend Test Load/Deflection [L/D] and
Approximated Flexural Stress/Strain [S/S] Diagrams of Tripleflex™
0.0195", MX-501 (PEEK) 0.0236", Respond® 0.0175",
WP-320 (PET) Polyester 0.0157", WOX-3 (PEEK) 0.0157",
WP-89 (PET) Polyester 0.0138", Optiflex™ 0.020", WN-101 Nylon 6/6
0.014" --
(a) [L/D] Diagrams and
(b) Approximated Flexural [S/S] Diagrams. 121

36. Comparison of the Three-Point-Bend Test Load/Deflection [L/D] and
Approximated Flexural Stress/Strain [S/S] Diagrams of Tru-Chrome®
0.018", Glastic® Fiber Glass Composite 0.030", and Optiflex™
Fiber Glass Composite,0.020" --
(a) [L/D] Diagrams and
(b) Approximated Flexural [S/S] Diagrams. 122

LIST OF FIGURES continued

Figure Page

37. Three-point-Bend Test Load/Deflection [L/D] and
Approximated Flexural Stress/Strain [S/S] Diagrams for
Individual Materials --
(a) [L/D] Diagram of Tru-Chrome® 0.020",
(b) Approximated Flexural [S/S] Diagram of Tru-Chrome® 0.020",
(c) [L/D] Diagram of Tru-Chrome® 0.018", and
(d) Approximated Flexural [S/S] Diagram ofTru-Chrome 0.018". 123

38. Three-point-Bend Test Load/Deflection [L/D] and
Approximated Flexural Stress/Strain [S/S] Diagrams for
Individual Materials --
(a) [L/D] Diagram of Tru-Chrome® 0.016",
(b) Approximated Flexural [S/S] Diagram of Tru-Chrome® 0.016",
(c) [L/D] Diagram of Tru-Chrome® 0.014", and
(d) Approximated Flexural [S/S] Diagram of Tru-Chrome® 0.014". 124

39. Three-point-Bend Test Load/Deflection [L/D] and
Approximated Flexural Stress/Strain [S/S] Diagrams for
Individual Materials --
(a) [L/D] Diagram of A. J. Wilcox Australian Regular 0.018",
(b) Approximated Flexural [S/S] Diagram of A. J. Wilcox Australian
Regular 0.018",
(c) [L/D] Diagram of A. J. Wilcox Australian Special+ 0.018", and
(d) Approximated Flexural [S/S] Diagram of A. J. Wilcox Australian
Special+ 0.018". 125

LIST OF FIGURES continued

Figure Page

40. Three-point-Bend Test Load/Deflection [L/D] and
Approximated Flexural Stress/Strain [S/S] Diagrams for
Individual Materials --
(a) [L/D] Diagram of Blue Elgiloy® 0.018",
(b) Approximated Flexural [S/S] Diagram of Blue Elgiloy® 0.018",
(c) [L/D] Diagram of Red Elgiloy® 0.018", and
(d) Approximated Flexural [S/S] Diagram of Red Elgiloy® 0.018". 126

41. Three-point-Bend Test Load/Deflection [L/D] and
Approximate Flexural Stress/Strain [S/S] Diagrams for
Individual Materials --
(a) [L/D] Diagram of TMA® 0.018",
(b) Approximate Flexural [S/S] Diagram of TMA® 0.018",
(c) [L/D] Diagram of NiTi™ 0.018", and
(d) Approximate Flexural [S/S] Diagram of NiTi™ 0.018". 127

42. Three-point-Bend Test Load/Deflection [L/D] and
Approximate Flexural Stress/Strain [S/S] Diagrams for
Individual Materials --
(a) [L/D] Diagram of TMA® 0.018",
(b) Approximate Flexural [S/S] Diagram of TMA® 0.018",
(c) [L/D] Diagram of NiTi™ 0.018", and
(d) Approximate Flexural [S/S] Diagram of NiTi™ 0.018". 128

Figure Page

43. Three-point-Bend Test Load/Deflection [L/D] and
Approximate Flexural Stress/Strain [S/S] Diagrams for
Individual Materials --
(a) [L/D] Diagram of Titanal® 0.018",
(b) Approximate Flexural [S/S] Diagram of Titanal® 0.018",
(c) [L/D] Diagram of Titanal® XR 0.018", and
(d) Approximate Flexural [S/S] Diagram of Titanal® XR 0.018". 129

44. Three-point-Bend Test Load/Deflection [L/D] and
Approximate Flexural Stress/Strain [S/S] Diagrams for
Individual Materials --
(a) [L/D] Diagram of Neo-Sentalloy® 0.018" x 0.025",
(b) Approximate Flexural [S/S] Diagram of Neo-Sentalloy® 0.018" x 0.025",
(c) [L/D] Diagram of Sentalloy® Light 0.018", and
(d) Approximate Flexural [S/S] Diagram of Sentalloy® Light 0.018". 130

45. Three-point-Bend Test Load/Deflection [L/D] and
Approximate Flexural Stress/Strain [S/S] Diagrams for
Individual Materials --
(a) [L/D] Diagram of Sentalloy® Medium 0.018",
(b) Approximate Flexural [S/S] Diagram of Sentalloy® Medium 0.018",
(c) [L/D] Diagram of Sentalloy® Heavy 0.018", and
(d) Approximate Flexural [S/S] Diagram of Sentalloy® Heavy 0.018". 131

Figure Page

46. Three-point-Bend Test Load/Deflection [L/D] and
Approximate Flexural Stress/Strain [S/S] Diagrams for
Individual Materials --
(a) [L/D] Diagram of MX-501 (PEEK) Monofilament 0.0236",
(b) Approximate Flexural [S/S] Diagram of MX-501 (PEEK) Monofilament 0.0236",
(c) [L/D] Diagram of WOX-3 (PEEK) Monofilament 0.0157", and
(d) Approximate Flexural [S/S] Diagram of WOX-3 (PEEK)
Monofilament 0.0157". 132

47. Three-point-Bend Test Load/Deflection [L/D] and
Approximate Flexural Stress/Strain [S/S] Diagrams for
Individual Materials --
(a) [L/D] Diagram of WP-89 (PET) Polyester Monofilament 0.0138",
(b) Approximate Flexural [S/S] Diagram of WP-89 (PET)
Polyester Monofilament 0.0138",
(c) [L/D] Diagram of WP-320 (PET) Polyester Monofilament
0.0157", and
(d) Approximate Flexural [S/S] Diagram of WP-320 (PET)
Polyester Monofilament 0.0157". 133

48. Three-point-Bend Test Load/Deflection [L/D] and
Approximate Flexural Stress/Strain [S/S] Diagrams for
Individual Materials --
(a) [L/D] Diagram of WN-101 Nylon 6/6 Monofilament 0.014",
(b) Approximate Flexural [S/S] Diagram
of WN-101 Nylon 6/6 Monofilament 0.014",
(c) [L/D] Diagram of Optiflex™ Fiber Glass Compsite 0.020", and
(d) Approximate Flexural [S/S] Diagram of Optiflex™
Fiber Glass Composite 0.020". 134

LIST OF FIGURES continued

Figure Page

49. Three-point-Bend Test Load/Deflection [L/D] and
Approximate Flexural Stress/Strain [S/S] Diagrams for
Individual Materials --
(a) [L/D] Diagram of Glastic® Fiber Glass Composite 0.030", and
(b) Approximate Flexural [S/S] Diagram of Glastic®
Fiber Glass Compsite 0.030". 135

INTRODUCTION

The public demand for a more esthetic fixed orthodontic has become obvious by the popularity of the various esthetic brackets introduced to orthodontics over the last several years. While these esthetic brackets, which are generally clear in color, have become commonplace, no complementary esthetic orthodontic archwires have been accepted in to the marketplace to a significant extent due to lack of development.

The objective of this study was to obtain and test esthetic materials that were available from suppliers and manufacturers in configurations similar to the dimensions of commonly used orthodontic arch wires. Esthetic materials were selected on the basis that their mechanical properties might approximate those of a specific type of metal wire, and that these esthetic materials could possibly be used to produce a wire that is clear or tooth colored.

Before the mechanical properties of the new esthetic materials could be tested and compared to those of the various commonly used metal alloy wires, a reliable test protocol had to be developed. In addition, it had to be determined which mechanical properties were important to investigated in order to estimate the clinical efficacy of the wires under consideration.

A review of the orthodontic literature indicated that several different test methods had been developed and favored by different investigators. Their had been some debate as to whether defining the mechanical properties of a wire in terms of the apparent or effective

mechanical properties was more important to the clinician then reporting the actual material properties of the wire (Nikolia *et al.*, 1988). Since this study dealt with the selection of new materials on the basis of their inherent material mechanical properties, rather then how the would respond in various configurations (*e.g.*, multistranded) or their apparent properties, testing protocols were established which had the capability of determination of actual material properties. In order to test for actual material properties, certain restrictions were placed of the manner of testing which allowed for the implementation of basic bending and tensile fundamental formulae.

Since the geometry of loading in the tensile test allows for the simplest determination of actual material properties, it was considered a necessary test and included herein. A three-point-bend test was designed in order to make a assessment of the flexural properties of the esthetic wires. Defining the flexural properties was important as this type of deformation simulates the flexural type of deformation that wire undergo clinically.

Generally, orthodontic investigators have reported the tensile modulus of elasticity (E_t), the flexural modulus of elasticity (E_f), along with respective yield strengths at various arbitrary offsets, in tensile and/or various bend tests, in order to define to relevant mechanical properties of the wires tested. The modulus of elasticity (E) gives insight as to the relative stiffness a wire and the yield strength (YS), which is an arbitrary parameter (dependent on where the investigator would like to establish his standardized measurement), basically defines a point were the wire has exceeded its elastic range and has began to develope a permanent deformation when exposed to a particular load.

Once the test protocols were established, the spectrum of commonly used metal orthodontic wires were tested in order to verify the test methods and establish a standard of comparison for the esthetic materials that were obtain and considered suitable for testing. Decisions were then made as to whether the esthetic materials tested had potential to produce clinically effective esthetic arch wires and which mechanical properties needed further investigation.

LITERATURE REVIEW

The Need for Esthetic Arch Wires

Advances in the esthetic quality of fixed orthodontic appliances have been dramatic with the introduction of clear orthodontic brackets in to the market. All major orthodontic supply companies now offer some sort of esthetic bracket whether it be ceramic or plastic (*Allure, **Gem Sapphire,***Quasar, +Slikon, ++Starfire). The obvious marketability of these appliances have led all major suppliers to develop esthetic bracket product lines. Unfortunately, complementary esthetic arch wire have not yet successfully entered the market place to a great extent. The only esthetic orthodontic arch wires that are now on the market are the +++teflon-coated "White" stainless steel wire, *Optiflex™, a clear synthetic initial aligning wire, made of fiber-optic material which is fiber glass in a nylon matrix, and *Spectra-Sentalloy®, which is a nickel-titanium wire with an ionized titanium nitrate surface that gives the wire a whitish color. Although the first two of these new wire types are esthetic, their clinical efficacy is limited by virtue of their structure or composition. The diameter of the stainless steel in the teflon -coated wires must be reduced in order to provide room for the teflon coating and while

---

*GAC International, Commack, N.Y.

**Ormco, Division of Sybron Corporation, Glendora, Calif.

***Rocky Mountain Orthodontics, Denver, Col.

+American Orthodontics, Sheboygan, Wis.

++Unitex Corporation, Monrovia, Calif.

+++Lee Pharmaceuticals, S. El Monte, Calif.

the Optiflex™ wire is very esthetic and does have some application as an initial aligning wire, it maybe too brittle for general initial aligning purposes. The third wire, Spectra-Sentalloy®, is more esthetic than the untreated metal alloy wires, and does offer the ideal mechanical properties of nickel-titanium, however, it still has an opaque appearance (coincidentally, wire friction and nickel leaching is reduced by treating the surface of the Spectra-Sentalloy® wire).

The efforts of orthodontic supply companies to market a maximally esthetic appliance is reinforced by some recent investigations that have concentrated on determining patients perspectives on seeking treatment and their concerns about the appearance of the appliance. Gosney (1985) in a survey of children from 8 to 17 years old, reported that 23% of the patient in a survey experience anxiety about the visibility of their fixed appliances. Of the patients surveyed 84% said they were teased about their fixed appliances, and 12% indicated that this teasing was a concern. Gosney (1985) also suggested that general anxiety over fixed appliances wear increased with age. Interestingly, 73% of the patients surveyed who said they suffered "lots" of worry over appliance visibility or discomfort would still be willing to undergo treatment if so advised by their dentist. It can be inferred from this data that many patients may undergo orthodontic treatment and still have an underlying anxiety about the visibility of their appliances.

In a survey of adults' attitudes toward orthodontic therapy, Tayer (1981) found that 74% of those survey had indicated they had initial doubts and feeling of hesitation about beginning treatment. One of the two most cited reasons for hesitation was the question of peer reaction. Tayer (1981) included some quotations in his article of people he surveyed to

illustrate some of the concerns that patients experienced before deciding to start treatment with fixed appliances: "I just didn't want them because I thought they looked terrible on other people", "I was concerned about appearances...", "...I was afraid of the way people would respond to them...", and "I feared people would focus on my mouth and they would turn off...". The foregoing literature makes a strong case for development of a fixed orthodontic appliance that is as esthetic as possible, if not virtually invisible. The popularity of esthetic brackets with the general public has encouraged their widespread use even in the light of some technical disadvantages such as increased chair time due to bracket failure, enamel wear, and increased appliance cost. The demand for an esthetic appliance must be great in order for patients to endure the negative aspects of the state-of-the-art esthetic brackets.

As the quality and clinical compatibility of the esthetic orthodontic brackets improves, so will the need for development of complementary esthetic orthodontic arch wires. It is now necessary to elevate the esthetic potential of the orthodontic arch wire by introducing new materials inasmuch was the case of the introduction of nickel-titanium, titanium-molybdenum, and multistranded stainless steel wires to the optimization of the clinical mechanical efficacy of the modern metal arch wires.

An Assessment of Various Preclinical Testing Protocols for the Mechanical Properties of New Materials in Orthodontic Wires

The recent literature on the testing of the mechanical properties of orthodontic wires demonstrates that several authors have favored different bend test techniques depending on

which factors they felt were important to investigate. Goldberg and Burstone (1979), Drake *et al*. (1982), and Asgharnia and Brantley (1986) used a cantilever bend test method which is outlined by the American Dental Association Specification No. 32, and was design directly from pure bending model theoretical formulae and therefore has limitations on the manner of loading and test geometry. Kusy and Dilley (1984) developed a three-point-bend test which uses standard specimen supports and maintains the assumptions made for a pure bending models and the accompanying bend test formulae. The cantilever and the three-point-bend test are derived from essentially the same hypothesis, and are equally credible from a theoretical perspective as long as testing conditions do not vary from fundamental assumptions. Miura *et al*. (1986) and Nikolia *et al*. (1988) favored a three-point-bend test which used brackets or bracket-like supports to hold the wire during the bend test to simulate intraoral conditions. Ligation of the wire to bracket-like supports or other types of supports that tend to restrict the free movement of the wire during the bend test, and are likely to cause other phenomenon, such as frictional and shear components, that cannot be explained by theoretical formulae developed for pure bending situations. One of the conditions of a pure bending model is that the specimen rest freely on the test supports. Ashgarnia and Brantley (1986) and Miura *et al*. (1986) reported that the cantilever bend test deviated from theoretical bending assumptions, especially when concerned with very flexible wires, because the test apparatus tends to bend the wire in a skewed manner, rather than as an even arc which is provide for by the assumptions of the pure bending model. They discussed that this occurs because a moment is only applied to one end of the wire and the other end of the wire which

is fixed to the bending apparatus tends to bend at a smaller radius.

The Council on Dental Materials and Devices of the American Dental Association published Specification No. 32 for Orthodontic Wires Not Containing Precious Metals in December 1977, which established a standardized cantilever test protocol, however, many investigators comparing the mechanical properties of new metal alloy wires to tradition stainless steel wires have chosen alternative testing techniques for their studies (Kusy and Dilley, 1984; Ingram *et al.*, 1986; Nikolai *et al.*, 1988). The investigators reasons for not using the ADA Specification No. 32 cantilever test include that they felt there was significant departure from ideal bending mechanics, they preferred to design a test that simulates actual clinical bending conditions to a greater extent, or they felt their test protocols were more convenient. ADA Specification No. 32 also includes directives on classification, packaging, marketing, in addition to the testing of orthodontic wires. The specification provides bending properties of a wire by means of bending moments and angular deflections with the use of free-end cantilever specimen that is tested on a *stiffness tester or **torque meter.

Nikolai *et al.* (1988) explained why he judged the flexural (elastic-bending) test protocol of the ADA Specification No. 32 to be inadequate. He refuted the validity of the protocol of the ADA Specification No. 32 flexural test, which uses an in-plane couple loading at one end of a cantilever wire, on the basis of what he considered three erroneous elements in the specification test protocol.

---

*Tinius Olsen Testing Machine Co.,Willow Grove, Pa.

**Power Inc., Skokie, Ill.

First, he discussed that the protocol was incompatible with highly flexible wires that came on the market after the specification was developed such as titanium alloy and multistranded stainless steel wires. Second, he pointed out that various assumptions made in the derivation of theoretical formulae were in error for this particular application. Third, he felt that clinical interpretation of the data was limited because the specification test involved the determination of actual material mechanical properties rather than structural (apparent or effective) properties which are dependent on shape and size of the wire.

At the time when the ADA Specification No. 32 was introduced, relatively stiff and moderately resilient materials such as stainless steel and cobalt-chromium-nickel were commonly used in standard arch wire sizes. Generally, these wires were of larger cross sections then the nickel-titanium alloy and multistranded wires of greater flexibility that are used today. State-of-the-art materials tended to influence the selection of material test parameters such as the selection of the specimen span of 1 inch (25.4 mm) and the yield strength curve arbitrary offset of 0.05 radians (2.9 degrees). While trying to obtain yield strength data on the new wires of smaller diameters and greater flexibility, researchers found that large elastic defections occurred prior to lateral-buckling failures (Nikolai *et al.*, 1988). Nikolia *et al.* (1988), further discussed that, erroneous determinations of flexural modulus of flexural elasticity (E_f) could result when the applied couple of the torque meter provided angular deformation to these highly flexible cantilevered wires and caused them to undergo large deflections before the wire takes a permanent set. To minimize the amount of wire deflection while testing these highly flexible wires, researchers began to experiment by using

shorter test spans of these materials, and consequently yielding variable mixed results as test span lengths became unstandardized.

Large deflection of the highly flexible wires in the elastic range were not encompassed in assumptions made in the simplification of the original differential equation that ultimately is the simplified beam-deformation formulae used in the ADA Specification No. 32. The assumption is made that the length of the specimen is long in comparison to the amount of deflection that will occur. Relating to data taken during the ADA Specification No. 32 test, any data in which the maximum specimen deflection exceeds 10% of the specimen length or 0.1 inch (2.5 mm) should be excluded from the elastic-modulus determination (Nikolai *et al.*, 1988). Knowing the mechanical properties of the highly flexible wire types such as nickel-titanium, deflections of greater than 10% are likely to occur during bend testing and this will produce errors in bend test data because of deviations from the theoretical assumptions in the development of the specification formula. This will lead to some inherent errors in flexural modulus of elasticity (E_f) determination under these conditions. As seen in actual clinical applications, the use of leveling orthodontic arch wires often requires activations of greater then 10% of the respective interbracket distance. In Addition, as related to the testing of newer multistranded wires, the structural beam theory used in Specification No. 32 is derived from specimens having solid cross sections (Nikolai *et al.*, 1988). Although the cross section can be corrected for the presence of voids (Kusy and Dilley, 1984), computations do not account for stiffness resulting from the strand configuration of the multistranded wire (Nikolai *et al.*, 1988).

Yoshikawa *et al.* (1981), working in association with Burstone realized that the flexural modulus of elasticity (E_f) equation used in Specification No. 32 for a known moment at the fixed end was only technically correct for long beams which are not greatly deflected and is not accurate for small beams that undergo large deflection. With this in mind, they formulated modifications that would be necessary to produce accurate data for their testing purposes. Clinically, orthodontic wires undergo large deflections and investigators have tested wires under conditions of large deflections. Modifications to the derivation of the flexure modulus of elasticity (E_f) must be made in order to produce accurate data. This became obvious when it was found that the flexural modulus of elasticity (E_f) of standard orthodontic stainless steel wires varied both with the specimen span length and the amount of deflection. This is contrary to the theoretical definition of the modulus of elasticity which is independent of specimen geometry and amount of deflection if maintained in the elastic range. Yoshikawa *et al.* (1981), described two analytical techniques for providing a corrected measurement of the flexure modulus in free-end cantilever bending for small-diameter wires over relatively large deflections. One method involved a plot of the apparent modulus vs. deflection and an extrapolation back to zero to obtain a corrected flexure modulus. The second method involved iterative calculations of the flexure modulus that were corrected for span length and the applied force vector during testing. These modifications to the original cantilever beam theory provided consistent values for the flexural modulus of elasticity (E_f) that were independent of the cantilever span length, cross section, and wire deflection. Uncorrected values of the flexure modulus of elasticity were found to be within 11 % of the average

size, could determine the force applied to a tooth for a particular wire and amount activation by multiplying the amount of actual activation to render engagement of the wire (distance) by the transverse stiffness (similar to the modulus of elasticity (E) but in terms of force/distance) at the activation site, particularly with the assumption of the linear elastic behavior. Nikolai *et al.* (1988) felt that the structural properties (apparent mechanical properties) of the wires would differ from the actual mechanical properties of the material the wire is made of, because formulae derived from structural bending theory for determining mechanical properties are dependent on wire material, cross-sectional size and shape, and length. He felt that by directly determining the structural properties (apparent mechanical properties) of the arch wire in a five-point-bend test which closely simulates actual clinical use, even with the admission of significant frictional influences from the supports and the dependency on the support span (bracket) width, a more useful protocol could be presented. Nikolai (1989) in acceptance of the nonideal bending conditions imposed by his bending fixture apparatus, and by other currently used bend test techniques, was in the process of modifying the ideal bend test formula by adding a multiplication factor to the theoretical equations to account for such inherent departures from the ideal bending assumptions such as those imposed by various loading and support formats and mesiodistal bracket widths.

Miura *et al.* (1986) used a three-point bend test with single wing brackets as wire supports (technically more similar to a five-point-bend test since there are two points of contact in each support bracket). He felt that a "three-point bend test" of this type of design would be necessary to clarify the relationship between the loading and deflection by

determining the force being delivered at a site similar to that which occurs in actual orthodontic tooth movement. A test fixture of this type would imposes several departures from geometric assumptions made in the development of pure bending theory (Byars and Snyder, 1969) such as unaccounted shear force and frictional factors. Miura *et al.* (1986) focused on load-deflection behavior for the various wires sizes of the arch wires he tested rather than determining the actual material properties of the wires.

Asgharnia and Brantley (1986) in concluding their comparison of cantilever bending and tension tests of orthodontic wires, recommended that due to the shortcomings of the cantilever ADA Specification No. 32 cantilever test, such as the uneven bending arc, the three-point and four-point bending test such as those reported by Kusy and Dilley (1984), who were particularly careful in designing bending tests to accurately determine actual mechanical properties rather that apparent properties, appeared promising and warranted further consideration to act as a possible standard for the measurement of mechanical properties of orthodontic archwires. Because there has been so much variation in bending test protocols and presented data, several authors have recommended reporting the mechanical properties of archwires in terms ratios with a selected standard wire, thus eliminating test method bias (Burstone, 1981; Nikolai *et al.*, 1988; Brantley, 1990).

Orthodontic wires can be characterized in terms of many material mechanical properties. Several basic material properties which are clinically significant parameters, useful in appliance design, and measurable by standardized laboratory techniques have become popular with a number of investigators. These properties include the tensile and/or the

flexural modulus of elasticity (E_t and/or E_f), (Goldberg and Burstone, 1979; Drake *et al.*, 1982; Kusy and Dilley, 1984; Asgharnia and Brantley, 1986; Kusy and Stush, 1987); the yield strength (YS), (Goldberg and Burstone, 1979; Drake *et al.*, 1982; Asgharnia and Brantley, 1986; Kusy and Stush, 1987); springback which relates to the ratio of yield strength to the modulus of elasticity of the material (YS/E), (Goldberg and Burstone, 1979; Drake *et al.*, 1982); the spring rate and the bending moment (Andreasen and Morrow,1978; Goldberg and Burstone, 1979); and the modulus of resilience (M_r) or stored energy (Andreasen and Morrow, 1978; Drake *et al.*, 1982). Generally, these orthodontic researchers have derived this information from load-deflection data by means of constructing plots which are similar to stress-strain diagrams, however these plots are not independent of specimen geometry. Test methods vary among investigators which include use of cantilever bend tests with the Tinius Olsen stiffness tester (Andreasen and Morrow, 1978; Goldberg and Burstone, 1979), conventional tensile tests with an Instron universal testing machine (Goldberg and Burstone, 1979; Drake *et al.*, 1982, Miura *et al.*, 1986), and three-point (Kusy and Dilley, 1984; Miura *et al.*, 1986), four-point (Kusy and Dilley, 1984) or five-point bend tests (Nikolai *et al.*, 1988).

As new materials entered the orthodontic wire market, such as multistranded stainless steel, Cobalt-chromium, nickel-titanium, and beta-titanium, stainless steel wires became regarded as the standard for comparison for these new materials (Andreasen and Morrow, 1978; Goldberg and Burstone, 1979; Drake *et al.*, 1982, Kusy and Dilley, 1984; Asgharnia and Brantley, 1986). Although author's values for moduli of elasticity (E) and yield strengths (YS) of the above materials are generally similar, there is some variation in values that have

been reported (Kaplia and Sachdeva, 1989). Table I lists modulus of elasticity (E) and yield strength (YS) values with respect to various wire types, testing method, and investigators. The variability in this data may be attributed to material variability, type of test performed whether it was free-end cantilever, three-point, four-point, or five-point bending, and additionally if the test was done in tension or bending. Several investigators found that, while testing wire specimen at varied span lengths during bend test, the span length significantly effected the reported flexural modulus of elasticity (E_f). Kusy and Dilley (1984) found that the flexural modulus of elasticity (E_f) increased with decreasing span length. Brantley *et al.* (1978), Brantley and Myers (1979) and Yoshikawa *et al.* (1981) found that the reported flexural modulus of elasticity (E_f) increased with increased span length. Brantely and Myers (1978) stated that the test span dependence of the flexural yield strength (FYS) is consistent with the pure bending model of deformation while the test span dependence of the flexural modulus of elasticity (E_f) makes it evident that there is deviation in the actual loading conditions from the idealized bending model.

Metallurgical references have reported the modulus of elasticity (E) for stainless steel in the range of 27.8 to 30.2x10^6 psi, while the dental literature has reported a broader range of values for stainless steel wires in the range of 18.3 to 38.0x10^6 psi (Kusy and Dilley, 1984). Kusy and Dilley (1984) suggested that the smallness of the size of the specimen used in orthodontic wire testing are just too small for most conventional equipment, established experimental procedures, and /or theoretical approaches to reconcile. It was also sighted that most previous studies did not account for systematic errors such as machine deflection, the

use of appropriate machine sensitivities, excessive wire deflections, changes in the loading state, and specimen geometry.

The majority of orthodontic researchers have reported values of the modulus of elasticity (E) for stainless steel used to ultimately produce orthodontic arch wires is some what lower that standard metallurgical references. Several materials engineers including Brantley *et al.* (1978) and Goldberg *et al.* (1977) who have worked in association with orthodontist researchers, have published studies that demonstrate that the consistently low values of the modulus of elasticity for stainless steel orthodontic wires which have been reported in some of the recent orthodontic literature may not be in error but reflect the actual physical properties of the steel used in orthodontic wire. Goldberg *et al.* (1977) by means of microstructural analysis and methods for determining the preferred crystallographic orientation with a photographic x-ray technique on as-received and heat-treated stainless steel wire, attempted to demonstrate that this apparently reduced modulus of elasticity of orthodontic wire was actually phenomenon caused by the cold drawing process, and not experimental error. Although they were unable to identify the specific factors that lower the reported values of the modulus of elasticity, stress-induced changes in microstructure, residual strains, and crystallographic texturing were suggested as contributory. Brantley *et al.* (1978) sighted previous metallurgical investigators who established values of the modulus of elasticity for fully annealed (softened) austenitic stainless steel at approximately 29 to 30×10^6 psi and after cold working, a decreased modulus was established at a lower limit of approximately 22 to 23×10^6 psi. There is considerable inconsistency in the reported values

for the modulus of elasticity (E) particularly for stainless steel, whether the variation in reported values is a result of physical properties reflected as a result of formation of the wire or experimental error is still the subject of debate among investigators. The exact value for the modulus of elasticity for the stainless steel used to make arch wires has been debated to a great extent because stainless steel has become the primary standard of comparison for all other materials used to make orthodontic arch wires. By summarizing the values of the modulus of elasticity (E) and yield strength (YS) for the various metal alloy wires (Table I), it is demonstrated that while exact agreement of values is not evident, reported values of the various metal alloy wire types are within ranges which allows for the unique identification of the mechanical properties of the respective types of metal alloy wires.

Much mechanical property data has now been compiled on all the commonly used types of metal alloy wires including Cobalt-chromium, nickel-titanium, beta-titanium, and multistranded stainless steel (Kapila and Sachdeva, 1989). These metal alloy wires, in addition to stainless steel, are suitable standards of comparison for orthodontic wires of newer materials. Investigators have generally tested their standard materials by means of their own technique, rather than relying strictly on reference standards. Establishing one's own standard values during testing allows the investigator to verify the accuracy of his apparatus by comparing his data to other published standards and as new materials are tested under the exact same conditions, a more direct comparison of the data is provided. With data on the mechanical properties on such a variety of wires, there is a good basis for comparison to any new material that may approximate the characteristics of any of the

relatively new metal alloys in addition to stainless steel.

Understanding the Material Mechanical Properties of Orthodontic Wire

In the study of metals it is customary to plot diagrams (Figure 1) where the relationship between stress, σ, and strain, ε, for a particular material is reported (Popov, 1963). Generally the abscissa (horizontal) scale is for the strain, ε, and the ordinate (vertical) scale is for the stress, σ. In typical tension tests, the strain is the change in length divided by the instantaneous value of length.

$$\varepsilon = \int_{L_o}^{L_f} dL/L = \ln(L_f/L_o)$$

where L_F=the gage length at fracture, in (mm)

L_o=the initial gage length, in (mm)

ε=strain, elongation per unit length, in/ in (mm/mm)

The stress, σ, is computed by dividing the force applied to the specimen by the actual cross sectional area of the specimen at the same instant. True stress-strain diagrams account for this incremental change in specimen cross sectional are during elongation. Since in the study of orthodontic wires the diameters are initially so small, no attempt is made to find the incremental change in diameter of the wire as elongation of the specimen proceeds in tensile testing due to difficulty in measurement (Designation: A370-88, Standard Test Methods and Definitions for Mechanical Testing of Steel Products, American Society of Testing and Materials, 1988). Assessment of cross-sectional area during the tensile elongation does

influence the stress-strain curve but not to a significant extent in elastic ranges of the stress-strain plot. Stress is given in units of force such as pounds-force per square inch (lbf/in^2) or Newtons per meter squared (N/m^2).

Orthodontic researchers (Andreasen and Morrow, 1978; Drake *et al.*, 1982; Goldberg and Burstone, 1982; Asgharnia and Brantley, 1986; Kusy and Stush, 1987) have modified the original concept of the stress-strain diagram where substitutions are made where instead of the ordinate being stress, it is given in terms of bending moment (lbf x ft, N x m) or force (lbf, N) and instead of the abscissa being strain, it is given in terms of angular deflection (degrees) or linear activation (in, mm), respectively. The plots of bending test data are given in parameters that are useful to the investigator and clinicians since it is practical to recognized deflections or activations of wire in terms of actual angular or linear measurements rather than in terms of in/in (mm/mm) units. In addition, the data of these load-deflection plots are not independent of the area of the specimen, and different curves are produced for each wire size rather than a single curve as seen for a given material as on stress-strain diagrams. Load-deflection diagrams make it possible to observe the variable behavior of a given material as the wire cross-section is varied. Since the clinician has a limited number of wire cross-sectional sizes to choose from, it is convenient to look at load-deflection diagrams since each wire size will have a different curve, because these diagrams are not independent of wire cross-section. That is to say that the load-deflection curve of a 0.014" stainless steel wire will have a lower load for a given deflection than a 0.016" stainless steel wire, and so on as compared to 0.018" and then 0.020" stainless steel wires. However, from the perspective

of an investigator who is considering new materials and varied cross-sectional shapes and sizes in new arch wire design, the traditional stress-strain diagram, since there is only one curve per material, may be a more convenient source of information since it is independent of wire geometry. The investigator can select potential arch wire design of any cross sectional shape and plug it in to the stress-strain data of a given material to model its response to variable loads.

Hooke's Law, although being an idealization and a generality, states that for nearly all materials, the application of a force results in a linear deflection, or in other words, for a certain distance from the origin, the experimental values of stress vs. strain data lie on an essentially straight line (Popov, 1963). The modulus of elasticity (E) or Young's modulus, is graphically interpreted as the slope (stress-strain) of a straight line from the origin to a rather vague point on the stress-strain diagram known as the proportional limit. The proportional limit is a vague point in terms of actual graphical interpretation, however theoretically it is the point where Hooke's Law no longer applies, that is where linear behavior ends on the stress-stain diagram. As is the case with mild steel, there is a portion of the stress-strain curve which plateaus out (line ab on Figure 2) after the proportional limit has been reached. The stress associated with this plateau is known as the yield point (point A on Figure 2). The yield point reflects a large amount of deformation at a constant stress. Most materials, particularly brittle ones, do not express this yielding phenomenon. As the case with most materials the elastic limit is so near to the proportional limit that the two points are taken as one. Most materials do not express a well-defined yield point, so one is arbitrarily defined by using the

offset method. In engineering purposes, it is customary to select a 0.2% offset line in terms of strain. This 0.2% off-set strain line is drawn parallel to the straight-line (linear) portion of the original stress-strain diagram (Popov, 1963). The point of intersection of this arbitrary line with the original stress-strain curve is defined as the yield point of the material at a 0.2% offset (point "A" on Figure 3). The stress at this point is known as the yield strength (YS) at the 0.2% offset. Practically speaking this yield strength (YS) corresponds to a point were the elastic limit of the material is reached and plastic behavior begins, although theoretically this phenomenon actually occurs at the elastic limit which is usually very close to the graphically covert proportional limit. Technically, the material behaves elastically when it is able to completely regain its original dimension upon removal of the applied force. When a stress eventually causes a permanent deformation, the elastic limit of a material is exceeded and plastic deformation results, the material does not completely regain its original dimension. Another significant point is the ultimate strength (point "B" on Figure 2) of a material or were failure of the material occurs particularly in tensile tests, this rarely occurs during bend testing for flexible materials because buckling occurs first in many materials that are not very brittle and the specimen slips down between the test span supports before breakage of the specimen can occur. In bend tests the ultimate bending moment refers to the point were the maximal force develops (at the highest obtained point on the curve; Burstone and Goldberg, 1983) during the bend test, however, this point is usually not associated with specimen breakage.

The ratio of yield strength (YS) to the modulus of elasticity (E) is related to the springback

(Kapila and Sachdeva, 1989). Springback has also be referred to as maximum elastic deformation, maximum flexibility, range of activation, range of defection, or working range. If the springback is comparatively high, larger activations of the wire are possible without permanent deformation and there is a resultant increase in the working time of the appliance. Nickel-titanium has a higher springback that stainless steel.

The spring rate of a material is defined as the change in load divided by the change in deflection (Andreasen and Morrow, 1978). This can be significant when a clinician is seeking a specific depth of bracket engagement. A wire such as nickel-titanium will produce a much smaller change in force with respect to a given amount of deflection, when compared to stainless steel. This is do to the fact that nickel-titanium has a much lower stress-strain curve slope than stainless steel. The force change for the nickel-titanium wire is much less than the force change of the stainless steel wire for the same chosen deflection. Since the ratio of change in force divided by the change in deflection is lower for nickel-titanium wire, it has a lower spring rate and will produce a lower, more consistent, and continuous force on the teeth. On the other hand, the spring rate for stainless steel is greater then that for nickel-titanium and would exhibit a more drastic force variation (because the slope of its stress-strain curve is greater) as the wire is deflected across a given distance to engage into a bracket slot.

The bending moment (kg-cm or lb-in) as applied to torsion bend tests (Andreasen and Morrow, 1978; Burstone *et al.*, 1985) is the load placed at the free end of a cantilevered specimen in order to produce a angular couple and a resulting deflection. Generally, the

bending moment is, at any section of a beam, the algebraic sum of the external forces acting on the beam at one end of the section (Griffel, 1966).

The stored energy or modulus of resilience (M_r) is the energy available to move teeth. (Andreasen and Morrow, 1978). The stored energy is the area under the load-deflection curve after the amount of springback in the wire at this point is taken into account.

Burstone and Goldberg (1983) in their free-end cantilever bend tests, described three maximum bending moments in the laboratory analysis of orthodontic wire that can be associated with three different springbacks. The bending moment at the elastic limit, M_e (usually that from tensile data); the bending moment at a point were yield is just noticeable at an arbitrary offset, M_y, and corresponds to the yield strength (YS); and the bending moment were the moment is the overall maximum or ultimate, M_{ult}, and considerable deformation has taken place; were considered. Although the yield strength (YS) at an arbitrary offset near the proportional limit has been recorded by the majority of investigators, (Andreasen and Morrow, 1978; Drake *et al.*, 1982; Kusy and Dilley, 1984) and the ADA specification No. 32 has directives on reporting yield Strength (YS) at prescribed yield point offset near the proportional limit for materials, Burstone and Goldberg (1983) demonstrated that the ultimate bending moment, M_{ult}, and its associated ultimate strength is a more clinically significant parameter than the bending moment, M_y, and yield strength (YS) at the arbitrary yield point. They explained that the ultimate strength occurs were the overall moment is maximal and more importantly a significant amount of permanent deformation has transpired, therefore simulating the actual clinical utilization of orthodontic wire more accurately. As can be

observed clinically, wires are used in applications such as bracket engagement where the elastic limit is exceeded and some deformation occurs at the time of placement of the wire. Since a fair amount of plastic deformation (permanent set) was taking place, the use of the yield strength (YS) at bending moment, M_y, for the calculation of force magnitude in an appliance can give errors in predicting the actual forces delivered. For this reason Burstone and Goldberg (1983) have advocated the use of the ultimate bending moment, M_{ult}, for predicting force magnitude delivery in appliances. What may appear to be a surprising phenomenon, is that while the deflection that occurs with the ultimate bending moment, M_{ult}, is well out of the elastic range, the springback SB_{ult} associate with the ultimate bending moment, M_{ult}, is greater than the springbacks SB_e and springback SB_y as associated with the moment at the elastic limit, M_e, and the moment at the yield point, M_y, respectively . This is due to the fact that, since the amount of wire activation is greater when the wire is in its maximal bending moment range, although some springback potential is lost, because the initial activation was somewhat greater, the overall springback will still be greater than when a small activation that is maintain in the elastic range delivers a smaller but totally restorable springback with is wholly in the elastic range. This point is interesting because the ultimate springback, SB_{ult}, reflects components of elastic and plastic bending phenomenon of the wire, which likely occurs in actual clinical application of the wire. The forgoing discussion demonstrates that and arch wire can produce considerable forces although it has been deflected out of what is consider the elastic range of the material.

Bend Test Theory and the Assumption that Limits Its Application

In order to develope an equation to determine values of the flexural modulus of elasticity (E_f), it is necessary to understand the theory of bending. The case of a symmetrical sectioned beam such as an orthodontic wire will be developed for a pure bending model. As known, a beam that is subjected to a transverse load will bend. In such a case the effects of twisting and buckling, that may be present, in combination with the bending may present an overwhelmingly complicated problem.

If the bending effects of the beams are to be studied alone, then certain restrictions must be placed on the geometry of the beam and on the manner of loading (Griffel, 1967; Byars and Snyder, 1969): (1) The beam be made of a homogeneous material that has the same modulus of elasticity in tension and compression. (2) The beam be straight, or if curved, its length must be 10 times the depth of curvature. (3) It has a uniform cross section. (4) The beam's cross section has a longitudinal plane of symmetry. (5) The beam is long in proportion to its thickness. (6) The maximum stress does not exceed the proportional limit. (7) The resultant of the applied load lies in the plane of symmetry. The preceding assumptions will eliminate the possibility that the beam will twist. Another assumption will be that for the given geometry, the primary mode of beam failure will be bending rather than buckling. So that bending effects can be studied alone, loading will be restricted so that resultant normal and shear forces on any section perpendicular to the longitudinal axis of the beam will be zero. Normal force is the component of force directed perpendicular to the plane of the applied load, it can be in terms of tensile or compressive force in longitudinal axis

of the beam. Shear force is the component of force tangential to the plane at which the load is placed. A zero shear force implies that the bending moment is the same at all locations on the beam, so the beam can be thought of as being loaded by only pure couples applied at the plane of symmetry at each end of the beam. In this type of pure bending the plane of symmetry becomes the plane of bending. Several conclusions about the longitudinal deformation of the beam must be made (Byar and Snyder, 1969). First, the plane sections originally perpendicular to the long axis of the beam, must remain as a planes and perpendicular to the long axis after bending . That is to say that the planer cross sections are truly still planes and do not become curved or warped after bend. Second, once the beam is deformed, these cross sectional plane must have a common intersection. In other words any line parallel to the longitudinal axis of the beam prior to bending will become an arc of a circle after deformation. As the beam is influenced by the couples, the upper fibers of the beam are shortened, compressed, while the lower fibers of the beam are elongated. There is one surface in the beam of particular interest where the fibers undergo no compression or elongation. This longitudinal surface is known as the neutral surface. A beam of symmetrical cross section under pure bending has is neutral surface perpendicular to the longitudinal plane of bending. The intersection of the neutral surface with the longitudinal place of bending is the neutral axis (Byars and Synder, 1969). Significant to the development the pure bending model is that the radius of curvature of the beam is constant for the entire length of the beam, and that the longitudinal axial strain in any plane of the beam is proportional to its distance from the neutral surface over the entire length of the beam. Transverse deformation

or deformation perpendicular to the longitudinal plane of symmetry will have to be considered negligible in order to assume that the longitudinal axial stress throughout the length and thickness of the beam is proportional to the distance from the neutral surface (Byars and Synder, 1969). Due to Poisson's effect, the beams actually undergo a double curvature. The curvature due to Poisson's effect, the transverse deformation or deformations perpendicular to the longitudinal plane of synmmetry, will be considered negligible and it will be assumed that the longitudinal axial strain throughout the length and thickness of the beam is in proportion to the distance from the neutral surface. This stipulation is necessary because longitudinal bending is valid only for plane of symmetry bending.

The presence of shear forces that result in shear stresses and shear deformations would tend to invalidate some of the previous assumptions about the geometry of bending. Plane sections would no longer remain as planes after bending and extremely complicated bending geometries would result. Advantageously, for a beam whose length is large in comparison to it's diameter or width as the case with orthodontic wire, the shear force effect can be considered very small, negligible and the assumption of pure bending with longitudinal axial strain can be retained.

In terms of theoretical assumptions and bending geometry, Kusy and Dilley (1984) reported that a four-point bend test may have advantages over a three-point bend test in that, in the four-point bend test there is pure bending between the inner supports, and there is no shear component in this region of bending. This fact is consistent with the forgoing development of the pure bending model, that pure bending is more likely to occur between

the inner supports of a four-point-bend test than between the supports of a three-point-bend test. Theoretically, pure bending would be less likely in the three-point-bend test by virtue of the centrally load beam which would be more susceptible to shear forces. In addition, that because there is a uniform stress and strain field along the beam surface, there is no stress concentration (that can cause buckling) near the points of loading. Finally, with the beam under a more uniform stress the results would be more representative of the bulk properties of the beam. However, even in the light of these theoretical advantages to the four-point bend test, Kusy and Dilley (1984) found that the results with the four-point bending apparatus were more variable and less reproducible that those of the three-point bend test. The causes of such variations in data could possibly be due to minute misalignments in test apparatus, different wire geometries, or inaccurate beam formulae.

As demonstrated by the forgoing discussion there are may assumptions and consideration that are necessary in the development of an equation to give the value of theoretically meaningful flexural modulus of elasticity (E_f). The modulus of elasticity (E) is in actuality the slope on the initial linear (elastic) portion of the uniaxial stress-strain curve (Byars and Synder, 1969). Of particular significance is that this derivation applies to a uniaxial stress-strain curve, as was the case for pure bending with restrictions on the manner of loading and bending geometry.

Authors other than Kusy and Dilley (1984) found that not only does the flexural modulus of elasticity (E_f) vary with test type but with the span of the specimen used. The flexural modulus of elasticity (E_f) has been show to increase with the length of the specimen (Brantley

et al., 1978; Brantley and Myers, 1979; and Yoshikawa *et al.*, 1981). In addition, for some materials such as polymers the undergoing stress-strain testing, the modulus of elasticity (E) will be dependent on the speed of testing or the rate at which the strain occurs. A more rapid application of stress will be reflected in a higher modulus of elasticity (E) particularly in polymers (Nielsen, 1974).

Although the modulus of elasticity (E) is theoretically the same in tension and compression for most materials (Byars and Snyder, 1969), the variation of material strength in tension and compression results from differences in physical phenomenon of bending and tension. This is why tests done it tension always yield different data for strength of materials than tests done in bending for the same material, because bending (flexural) strengths tend to be greater than tensile strengths (Nielsen, 1974). Tensile properties, particularly in brittle materials, are dependent on flaws and submicroscopic cracks in the material as it is stretched. Conversely, as a material is subjected to compression, cracks tend to close rather than open. A compression test would tend to be more characteristic of a pure material and a tensile test would tend to be more characteristic of the flaws in a material. Therefore the strength of a material is considerably greater in compression than in tension (Broutman and Krock, 1967; Nielsen, 1974). Actually, a specimen in a bending (flexural) test is partially under compression and partially under tension while a specimen in a tensile test is subjected to more pure tensile stress. Although the stress phenomenon is simplified in the tensile test and easier to model mathematically, the bending tests do have the advantage of practical clinical interpretation over the traditional tensile test.

Tensile Test Theory: Its Simplified Assumptions in Comparison with the Various Bend Tests

As is the case with the various bend tests, the tensile test also has restrictions on the test geometry. Do to the nature of the geometry of the tensile test, assumptions are fewer. Restrictions on the tensile test geometry include: (1) the material of the body be homogeneous and isotropic, (2) the line of action of the resultant externally applied forces must be coincident with the longitudinal centroidal axis of the member, or in other words the specimen must undergo centroidal loading, (3) the region between cross sections that are perpendicular to the centroidal axis have a uniform stress that is accompanied by a uniform strain throughout each length of fiber, that is parallel cross sections of the member that are perpendicular to the centroidal axis must remain parallel to each other during loading (Byars and Snyder, 1969). If the requirement of the uniform stress distribution is to be meet, that is parallel sections stay parallel, than these ideal conditions can be nearly meet if the longitudinal dimension of the body is relatively large in comparison to the transverse dimension of the body so that the localized effects of the applied load will disappear in sections a sufficient distant from the point of application.

Information about the physical properties of a material from the tensile test can be compared to that which the various bend tests yield in order to examine the accuracy of assumptions made about the bending geometry in the use of such simplified equations as that to determine such values of the flexural modulus of elasticity (E_f). The tensile modulus of elasticity (E_t) as determined by the ideal tensile test requires only that the slope of the linear potion of the stress-strain diagram. The flexural modulus of elasticity (E_f) as determined by

the various bending tests requires that an addition factor, the moment of inertia (I), of the specimen be taken into consideration. The three-dimensional characteristics of the specimen influence the calculation of the flexural modulus of elasticity (E_f) in the ideal bending tests.

Possible Esthetic Substitutes for Metal Alloy Orthodontic Arch Wires

Plastics, or in other words, polymer materials, have great variability in providing products of high esthetic potential. Because dyes and pigments can be incorporated directly into the polymer resins, it is possible to produce an item in an unlimited range of colors both simply and economically (MacDermott, 1984). The amorphous polymers, those that have random molecular arrangement, tend to transmit light easily, and are thus transparent. The crystalline polymers, due to an ordered structural arrangement of the molecules, tend to reflect most incident light and are thus opaque (MacDermott, 1974).

Although there is considerable diversity in the physical properties of various polymers and composite-polymers, plastics as a class are generally lower in strength and stiffness than metals (O'Toole, 1989). The development of composite materials, that is the reinforcement of polymers with fiber glass or other minerals, has dramatically increased the strength to stiffness ratio of polymer products to one that is approaching that of die cast metals (MacDermott, 1974). The proportion of a polymer that is crystalline not only effects the appearance of the material, but also effects the modulus of elasticity and the melting point. The greater the proportion of crystalline material in the polymer, the higher the modulus of elasticity and the higher melting point (Powell, 1983). Tensile strength, solubility, and

hardness are also associated with the degree of crystallinity in the polymer (Seymour, 1987). The degree of crystallinity and the morphology of the crystalline materials have great effects on the mechanical properties of polymers, and since these factors have a large range of variability, the mechanical properties of crystalline polymers take on a bewildering array of possibilities (Neilsen, 1974).

The entire family of polymer materials, whether organic or inorganic, are comprised of extremely large molecules, macromolecules. Atoms in the polymer chain are held together by covalent bonds (Seymour, 1987). Conversely in metals, the metal cations (+ charge) are held together by a loosely held cloud of valence electrons (- charge). These fluid electrons distributed about the cluster of spherical cations in metals give rise to such metallic properties as luster, electrical conduction, malleability, and ductility. On the other hand, the covalently bonded electrons of non-metallic compounds such as organic polymers function to provide transparency, low specific gravity, low conductivity, and resistance to corrosion in these materials (Seymour, 1987).

The molecular structure of polymers consists of long chains of carbon-carbon bonds. Some polymers are linear such as the hydrocarbon polymer, linear polyethylene (LDPE). A single macromolecule of linear polyethylene (LDPE) consists of more than 100 carbon-carbon bonds. Polymers can be linear or branched. Branched polymers have some repeating monomer units of the polymer molecule covalently bonded adjacent to the length of the polymer chain or backbone. Pendant groups are those monomer repeating units that have some other type of atom other than hydrogen bonded off of the carbon atoms in the polymer

chain. Polyvinyl alcohol (PVA), polyacrylic acid (PAA), polyvinyl chloride (PVC), polystyrene (PS), polypropylene (PP), and polyacrlonitrile (PAN), are comprised of pendant groups having the respective functional groups OH, COOH, CL, C_6H_5, CH_3, and CN replacing a hydrogen atom on every other carbon atom in the chain (Seymour, 1987). Not only do the physical properties of the polymer vary with the type of pendant group, but also the stereospecificity of these pendant groups about the polymer backbone. Polymer chains may also be crosslinked and present as a continuous network or mesh of covalently bonded atoms. Copolymers are those polymers where more than one type repeating monomer unit is present in the macromolecule. For example, a polymer can have repeating monomer units of ethylene and vinyl alcohol in the macromolecular chain. These copolymer units can be in random or alternating arrangement on the macromolecule chain. The properties of the resulting copolymer will be different from either repeating unit its composition. Other factors such as intermolecular forces, Van Der Waals, and chain entanglement have influence on the physical properties of polymers (Seymour, 1987).

Polymers may be classified as elastomers (rubbers), plastics, and fibers depending on the strength of the intermolecular forces (Seymour, 1987). There is considerable overlap in these broad classifications. Rigid plastics and fibers have the characteristic of high moduli of elasticity, while elastomers have large reversible elongations when a stress is applied. A rigid plastic exhibits a plateau above the yield point on a stress-strain diagram, which in the family of polymers is most similar to that of some metals (Figure 4). Since plastics are viscoelastic, that is, they are complex aggregates of many different elastic and fluid elements, their

physical properties are intermediate between crystalline metals and very viscous fluids. When a plastic is loaded, they are subjected to many variables that do not generally affect metals (O'Toole, 1989).

Stress-strain curves for plastics vary substantially with the rate of loading and relatively small changes in temperature. Plastics do not have proportional limits as metals, and in theory and practice their stress-strain diagram are curvilinear at ordinary loading rates and use-temperatures. Some rigid plastics have small linear ranges on stress-strain diagrams at room temperature. This linear range is substantial for some highly filled (composite) and rigid thermoset plastic materials, although this stress-strain phenomenon is still dependent on test conditions. Yield points for plastics are not sharply define or do not exist, and as a result this quantity is a very uncertain criteria for product design. Although plastics can be made to rupture in tension, many plastics will not rupture during bending and compression tests. Because of this, stress-strain testing of plastics frequently can not furnish usable data for maximal loads in bending or compression (O'Toole, 1989). Since traditional stress-strain tests are done during short time spans, they do not take in to account the time dependent viscoelastic properties of plastics. The long term behavior of plastics must be evaluated by creep tests where deformation and rupture are measured as functions of time under static tensile, flexural, or compressive loads (O'Toole, 1989). Typical stress-strain data tends to grossly overestimate the properties of plastics since time dependent changes are not taken into consideration. The elastic limit of plastics is also dependent on time and temperature. Since the design equations for metals are base on elasticity and presume elastic constants,

such as tensile modulus, the viscoelastic nature of plastics is not well demonstrated with these equations. In order to use these equations with viscoelastic materials, it is necessary to modify viscoelastic or creep data by means of curve plotting or equations (O'Toole, 1989). Traditional stress-strain data may be useful in obtaining a general or rough estimation of the level of strength and rigidity that a given plastic has compared to other plastics (O'Toole, 1989). Ultimate product design requires that the creep properties of a given polymer be well understood. The fatigue characteristics of the polymer also need to be known before the product design can be completed.

TABLE I

The Mechanical Properties of Metal Arch Wires as Reported in the Orthodontic Literature

Wire Type and Composition	Reference	Test Type	Modulus of Elasticity (E)	Yield Strength (YS)
			$x10^3$ psi ($x10^9$ N/m^2)	$x10^3$ psi ($x10^9$ N/m^2)
Stainless Steel 71% Fe, 18% Cr, 8% Ni, <0.2% C	Goldberg and Burstone, 1982	Tensile	275(1.89)	25,000(172.4)
	Asgharnia and Brantley, 1986	Tensile	188(1.30)	24,400(168.3)
		Bending	287(1.98)	30,800(212.4)
	Kusy et al., 1989	E: Bending	226(1.56)	28,000(193.0)
		YS: Tensile		
Cobalt-Chromium-Nickel 40% Co, 20% Cr, 15% Ni, 15% Fe, 7% Mo, 2% Mn	Golberg and Burstone, 1982	Tensile	319(2.20)	29,000(200.0)
	Asgharnia and Brantely, 1986	Tensile	130(0.90)	25,000(172.4)
		Bending	210(1.45)	31,000(213.8)
	(Blue Elgiloy)			
Nickel-Titanium 52% Ni, 45% Tl, 3% Co	Drake et al., 1982	Tensile	45(0.31)	4,300(29.7)
		Bending	65(0.45)	4,300(29.7)
	Asgharnia and Brantley, 1986	Tensile	49(0.34)	5,000(34.5)
		Bending	82(0.56)	7,000(48.3)
	Kusy and Stush, 1987	E: Bending	86(0.59)*	6,440(44.4)*
		YS: Tensile	69(0.48)**	4,850(33.4)**
Beta-Titanium Molybdenum 79% Ti, 11% Mo, 6% Zr, 4% Sn	Drake et al., 1982	Tensile	125(0.86)	9,960(68.7)
		Bending	141(0.97)	8,370(57.7)
	Goldberg and Burstone, 1982	Tensile	170(1.17)	9,400(64.8)
	Asgharnia and Brantley, 1986	Tensile	95(0.45)	9,400(64.8)
		Bending	165(1.14)	12,500(86.2)
	Kusy and Stush, 1987	E: Bending	105(0.72)	10,500(72.4)
		YS: Tensile		
Multistranded Stainless Steel				
3-Stranded, 0.0195" (Hi-T Twist Flex, Unitek)	Goldberg et al., 1983	Bending	------	^3,820(26.3)
6-Stranded, 0.0175" (Respond, Ormco)	Goldberg et al., 1983	Bending	------	^1,720(11.9)
9-Standed, 0.016" x 0.022" (D-rect, Ormco)	Goldberg et al., 1983	Bending	------	^^1,260(8.6)
			------	^^^890(6.1)

*Round Wires.

**Square and rectangular wires.

^Apparent properties.

^^Apparent properties, loaded parallel to smaller cross-sectional dimension.

^^^Apparent properties, loaded parallel to larger cross-sectional dimension.

FIGURE 1
A Typical Tensile Test Stress-Strain Diagram for a 0.018" Stainless Steel Orthodontic Arch Wire (Tru-Chrome®).

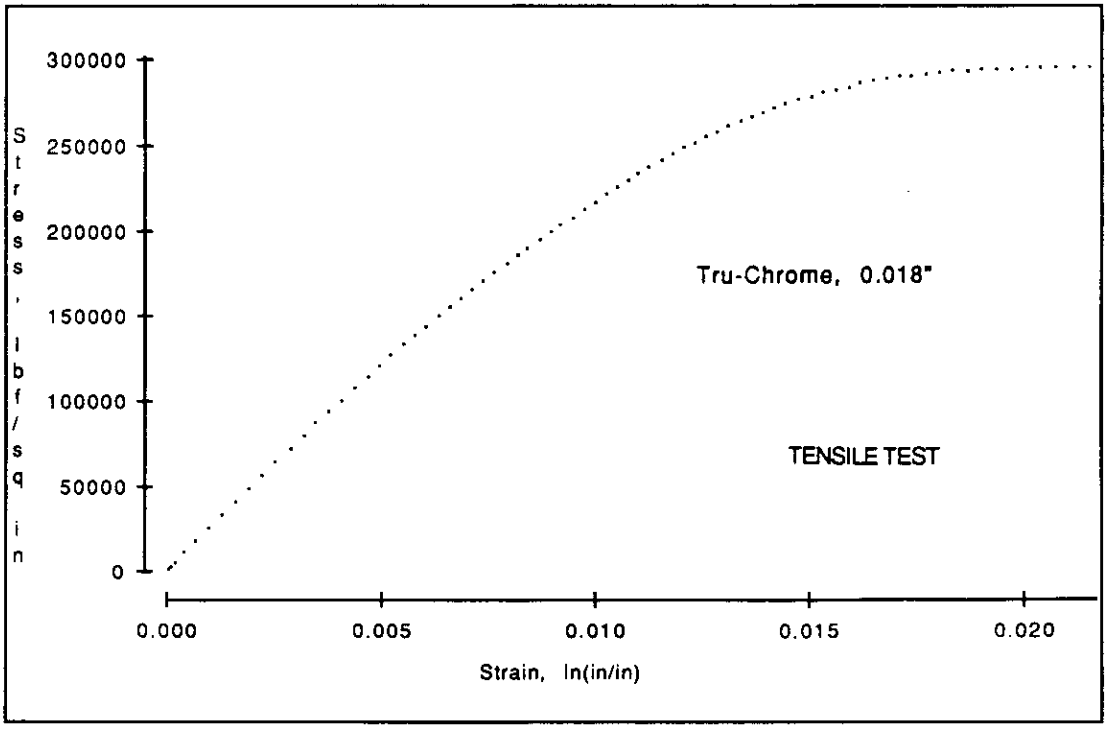


FIGURE 2
A Stress-Strain Diagram for a Mild Steel Which Demonstrates the Proportional Limit, the Actual Yield Point (Strength), and Ultimate Strength.

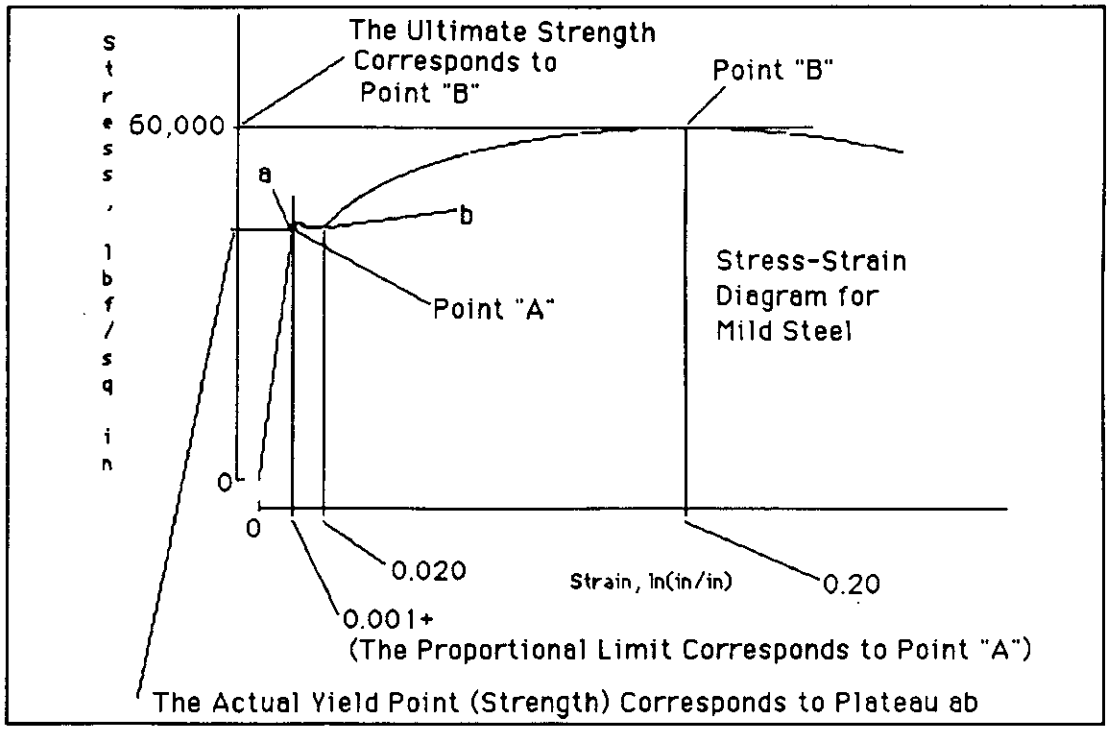


FIGURE 3
A Demonstration of the 0.2% Yield Strength Offset Method

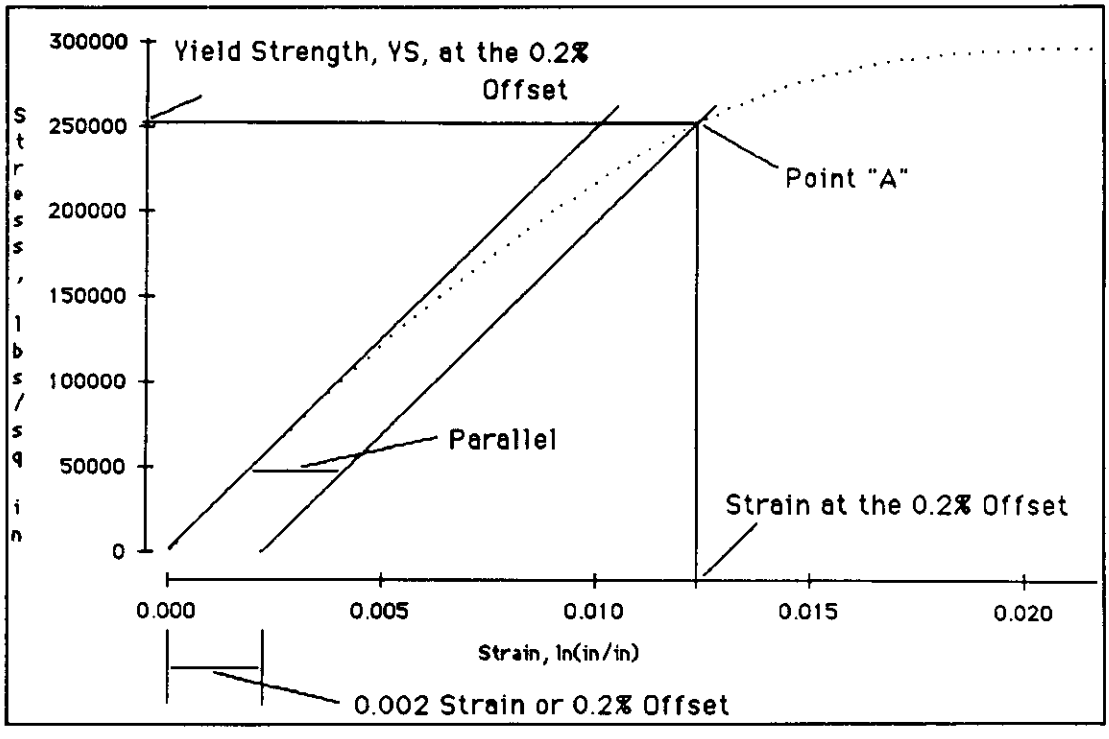
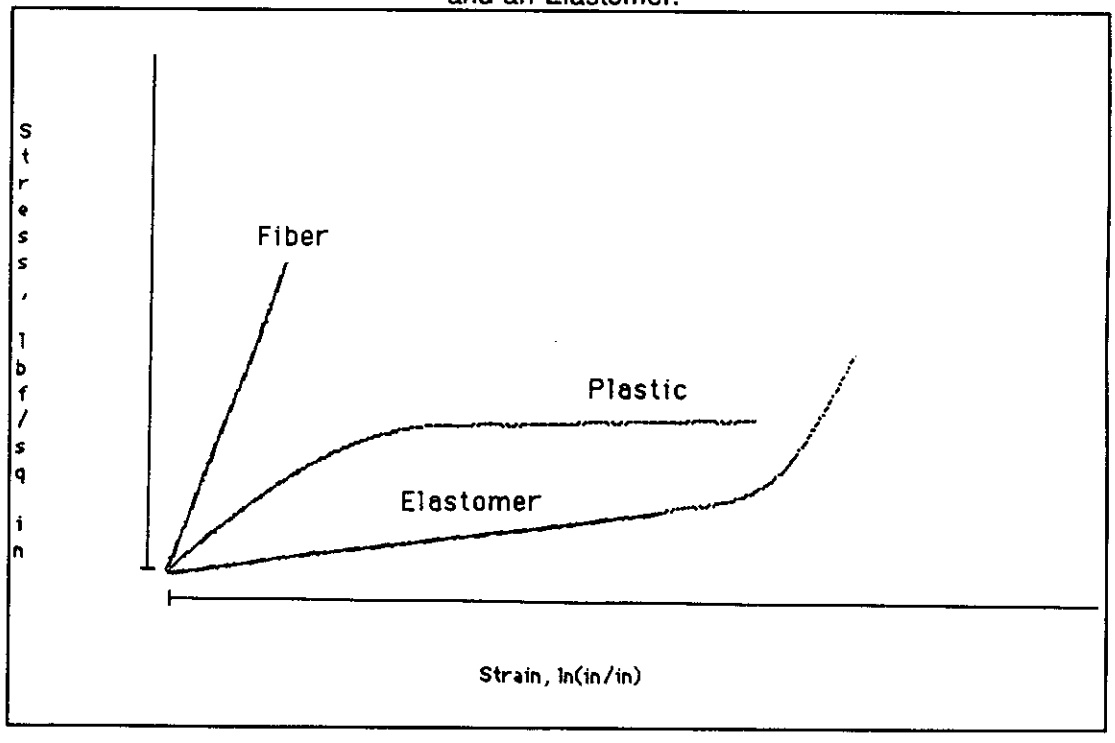


FIGURE 4
An Example of Typical Stress-Strain Curves for a Fiber, a Plastic, and an Elastomer.



STATEMENT OF THESIS

The objectives of this investigation are:

(1) To obtain clear or tooth colored materials that are available from suppliers and/or manufactures in dimensions similar to orthodontic arch wire.

(2) To design a test protocol and the necessary testing apparatus to test the mechanical properties of materials that are in wire form.

(3) To test various commonly used metal-alloy wire so the accuracy of the test method can be verified and a standard of comparison established for the esthetic materials that are to be test.

(4) To test esthetic materials as they are received and considered suitable for testing, and finally make determinations about their possible clinical efficacy as orthodontic arch wires.

MATERIALS AND METHODS

Materials

The Search for Esthetic Materials

The search for esthetic materials that could be used to form orthodontic archwires involved contacting numerous polymer and polymer-composite manufactures and suppliers. A directory of supplier and manufactures such as the *Modern Plastics Encyclopedia (1990) was used to provided a current listing of phone numbers and addresses of all polymer and polymer-composite suppliers and manufactures. The Modern Plastics Encyclopedia also contained material property summaries of a vast numbers of polymeric materials. Suppliers and Manufactures were listed in the Modern Plastics Encyclopedia according to the of type and/or form of the materials that they supplied.

Generally inquiries to companies were first met by sale personnel and then the specific inquires were forwarded to the companies technical personnel if they felt that their products had any potential. Although the number of polymers and composite materials that could possibly be tested was overwhelming, only a small percentage of the companies contacted where able to supply these materials in wire form in the dimensions the 0.014 " to 0.022" diameter range or somewhat near this range. Only materials that were already in wire form in the specific dimensions of orthodontic archwires were considered for testing in this study, as developing protocol for actually forming arch wire from raw materials was not an objective of

*McGraw-Hill, Hightstown, N.J.

the study. Although many large material suppliers had many raw material that had material properties in favorable ranges in forms such as beads, they could not provide a means of forming wires in the necessary dimensions. In additrion, when technical personnel were made aware of the small geometric configurations needed for the wires they often cited difficulties in the formation process or possible inabilities to locate a means of forming the materials into the requested diameters while discussing their raw material products. About 90 phone calls were made to total of approximately 37 companies it reference to obtaining information about there products and ultimately requesting samples when materials were available in suitable dimensions. Four companies responded by sending a total of 8 different esthetic material samples, 6 of which were selected for testing.

Commonly Used Metal Alloy arch wires That were Tested in Order to Verify the Test Protocol and Become a Standard of Comparison for Esthetic Materials

In order to establish a comparative spectrum of material mechanical properties of commonly used metal alloy wires types, major orthodontic supply companies were asked to donate some commonly marketed products. Metal alloy wires that were received and selected for testing are organized in Table II. Wires were received directly from the suppliers: in Standard 14" straight lengths of Tru-chrome® and Triple-Flex™, standard 10" straight lengths of Regular and Special Plus A.J. Wilcox Australian wire, standard 7&1/4" straight lengths of Titanal® and Titanal® XR, and all other wires were receive in preformed arches (see Table II for names of wire supply companies). Tru-Chrome® round wires in sizes of

0.014", 0.016", 0.018", 0.020" were tested to determine if the results of the tensile and bend tests were independent or influenced by diameter size. Theoretically, results should be independent of wire size if a good testing model for the actual mechanical properties of the wire material had been developed. A wire diameter of 0.018" was selected for the testing size all other metal wires. If 0.018" was not available at the time of testing for a particular type of wire the nearest size to 0.018" was used. Round wire with a 018" diameter is commonly used wire size in the clinical practice of orthodontics. All metal wire specimens, for a particular material, were taken from the same package for both the tensile and bend tests to ensure that they were from the same lot number. The actual diameters of all wires were measured with a micrometer to an accuracy of ± 0.0001" prior to testing.

Esthetic Materials Received from Suppliers that were in Wire Form and Were Considered Suitable for Testing

As specimens of various materials were received from the suppliers, they were selected for testing on the basis of being received in wire form and there potential to be used to produce esthetic orthodontic arch wires in the proper sizes. Esthetic archwire materials that were received and considered suitable for testing are organized with some information about their composition in Table III. All esthetic materials that were tested were in the shape of round wire. Esthetic wires were received directly from the suppliers in standard 6" straight lengths of Optiflex™, standard 8" lengths of Glastic®, and all other specimens were received on 100ft. wound spools (see Table III for the names of suppliers). Generally, where possible

esthetic wire diameters were selected in the clinical orthodontic working diameter range of 0.014" to 0.020". All esthetic wire specimens, for a particular material, were taken from the same package or spool for both the tensile and bend tests to ensure they were from the same lot number. The actual diameter of all wires were measured with a micrometer to an accuracy of ± 0.0001" prior to testing.

Methods

Three replicates of each of the test conditions summarized in Tables II and III were preformed on (1) a uniaxial tensile test to material failure and (2) a three-point-bend test up to the occurrence of the maximal bend stress or obvious specimen slippage. Values for the tensile modulus of elasticity (E_t), the yield strength at the 0.2% offset and the corresponding stain at the 0.2% offset, were reported from the tensile data. The values for the flexural modulus of elasticity (E_f), and with use of the approximated flexural stress-strain diargams, the yield strength at the 0.2% offset, the corresponding strain at the 0.2% offset, the load corresponding to the 0.2% strain offset, and the deflection corresponding to the 0.2% strain offset, were reported from bend test data. Representative stress-strain diagrams for tensile data, approximated flexural stress-strain diagrams for bend test data and load-deflection diagrams which allowed for consideration in terms of clinically obvious parameters for bend test data were reported. No wires were heat treated and all tests were preformed at room temperature, approximately 81°F (27°C).

Protocol for Tensile Test:

The *Instron Model 1125 Universal Testing Machine was used for all trials. A **1000 lbs Instron Reversible Load Cell was used to detect changes in load (see Figures 5 and 6). The load cell was calibrated with standard weights at zero, mid-range and full scale. The load cell had variable full scale calibration ranges (sensitivity) of 1000, 500, 200, 100, 50 and 20 lbs. The full scale calibration range was selected for each material so that the ultimate tensile strength would occur in approximately the middle or upper third of the graph. This was done so that the sensitivity of the load cell was maximized for each specimen type. The average error over each of the full scale calibration load ranges used, 200, 100 , 50, and 20 lbs, were ± 0.0116 lbs (± 5.3 g), ± 0.023 lbs (± 10.4 g), ± 0.028 lbs (± 12.7 g), and ± 0.0129 lbs (± 5.9 g), respectively. The graph drawn from the chart recorder of the Instron Universal Testing Machine that was produced during each test was only used to assist the operator in observing the progression of each experiment and to aid the operator in selecting the appropriate load cell full scale calibration range (sensitivity). Actual data used in determination of the modulus of elasticity (E) and Yield strength (YS) at 0.2% offset and the corresponding strain at the 0.2% offset was determined from data accumulated by means of a *** Macintosh® IIx Computer and the ^Analog Connection Quicklog™ Laboratory and Factory Data Acquisition Program. Data was stored by means of a Macintosh® IIx Computer with

---

*Model 1125 Instron Universal Testing Machine, Instron Corp., Canton, Mass.

**Catalog #2511-301, 1,000 lbs Reversible load cell, Ibid.

***Apple Computer, Inc., Rolling Meadows, Ill.

^Strawberry Tree Computers, Inc., Sunnyvale, Calif.

data worksheets by means of the *Microsoft® Excel Program. Data received from the Instron Strain Data Unit was provided to the data acquisition system in terms of 0 to 10 volts. This information was converted to stress and strain units. Thus 0 lbf corresponded to 0 volts and the full scale load for a given sensitivity setting corresponded to 10 volts. One data point was selected every 1 second by the data acquisition system (the rate of data point selection was variable. This rate was chosen because it allowed for ample data points to be collected in the linear region of the plot to draw a significantly linear line).

The elongation of the specimen, which was used to calculate the strain was detected by a light weight 1" gage length **Instron Extensometer which had a 10% travel or 10% maximum strain (see Figures 5, 6, 7, and 8). The specimen clips of the extensometer had to be modified to accommodate the small diameter of the wires. Since the notch on the plastic part of the clip was designed for larger specimen, the wires would slip through this notch. The plastic fitting in the spring loaded clip was rotated 90°, and a new very small notch (approximately 0.010") was made in each clip to facilitate the clamping of the extensometer to the specimen (Burstone, 1977). The extensometer was calibrated before testing by use of an ***Instron High Magnification Fixture Extensometer Calibrator (see Figure 5). The extensometer was calibrated and the appropriate strain magnification ratio was selected so that the specimen would fail (break) before the maximum strain range had been exceeded. A

---

*Microsoft Corporation,Redmond,Wa.

**Catalog #2630-001 Extensometer, Instron Corp., Canton, Mass.

***Catalog #2602-001, High Mag. Calibration Fixture, Ibid.

strain magnification ratio setting of 400:1 on the Instron Strain Data Unit or a full scale extension of 0.05" was used for all stainless steel type wires (not including multistranded stainless steel) as they did not exceed 0.05" of elongation during the test. All other materials used a strain magnification ratio setting on the Instron Strain Data Unit of 200:1 or a full scale extension of 0.1". If a specimen exceeded 0.1" of elongation during the test prior to failure, the crosshead was stopped, and the extensometer was recompressed to the 0.0" position and the crosshead was started from that point again. This procedure was repeated until the specimen failed (broke) if necessary. Rezeroing the extensometer was necessary with some material because the exceeded the 0.1" full scale elongation limit of the extensometer prior to failure. Instron extensometers are available that could provide up to 100% elongation or 1", however, only an extensometer with a 10% or 0.1" travel was available for use. The linear portion of all material tested was always with in the 10% or 0.1" elongation range so any errors produced in the rezeroing process were not of significant to relevant data. The average error in recording the elongation for the full scale strain calibrations (sensitivity) used, 0.05" (strain magnification ratio of 400:1) and 0.1" (strain magnification ratio of 200:1), was $\pm$ 2.9×10^{-5} in ($\pm$ 7.4×10^{-4} mm) and $\pm$ 3.6×10^{-6} in ($\pm$ 9.1×10^{-5} mm), respectively.

The data received in terms of voltage was converted with the following formulae to ultimately provide a unit corrected stress-strain plot. The ordinate (vertical axis) of the plot or stress, σ, was defined by the following equation,

$$\sigma = a^{*}V_{\sigma}/A$$

where σ= stress, the converted ordinate data, psi

a= data acquisition conversion factor, lbs/volts

V_σ = voltage from meter detecting load, volts

A= cross sectional area of wire being tested, in^2

The abscissa (horizontal axis) of a stress-strain curve or strain, ε, is given by

$$\varepsilon=\ln(L/L_o)$$

where L=the characteristic gage length ,in

L_o= the original gage length, in

and,

$$\varepsilon=\ln[(L_o + V_\varepsilon{}^*b)/L_o]$$

or for convenience,

$$\varepsilon=\ln[1+V_\varepsilon{}^*b/L_o]$$

where ε=strain, the converted abscissa data, in/in

b=the date acquisition conversion factor, in/lbs

V_ε=voltage from meter detecting change in length, volts

L_o=original gage length, in

A pair *Instron 1000 lbs capacity screw action tensile test grips were modified to permit testing of small diameter wire specimens (see Figures 5 and 6). The lower grip as originally received from the plant in attached to the Instron tensile grip housing by a loosely fitting pin in a slot that allowed slight upward movement of the lower grip until the pin was engaged. Since

---

*Catalog #2710-003, 1,000 lbs Screw Action Grips, Instron Corp., Canton, Mass.

the weight of the lower grip was about 10 lbs, when ever a load developed that exceeded 10 lbs, the lower grip would be lifted by the specimen in tension and produce a "bump" (artifact) on the stress-strain curve until the pin was engaged. This made interpretation of the initial linear portion of the curve more difficult. Because of this the lower grip was modified with a jam-nut which would secure the lower grip and not permit any upward movement during the test. The upper grip was attached to the load cell by means of a multidirectional, self-centering (universal) hinge which insured uniaxial loading of the clamped specimen. As any serrations on the grip face would cause deformation and/or cutting of the wire surface during tightening of the grips and subsequently during applying loads during tensile testing. Four "Instron 2" smooth flat type grip faces were used to hold the specimen during testing (see Figures 7 and 8). The grip faces allowed for a maximum of 2" of wire specimen to be compressed between each grip. In order to prevent slippage of the specimen in the grips, four pieces of 400-grit emery paper that were cut to the size of the grip-face . Two pieces of the emery paper were held back-to-back, in effect acting as double sided emery paper, and one of these units was placed against the each grip face. The specimen was then tightened between the emery paper and grips on either side. No specimen slippage was observed using this gripping technique. The titanium-molybdenum and nickel-titaniums (except the Titanal®) wires from preformed arch wires had more slippage with the emery paper and did not appear to slip when emery paper was not used. Because these wires were relatively soft,

---

*Catalog #2702-024 Smooth Surface Grip Faces, Instron Corp., Canton, Mass.

the ends of the wire in the grips became slightly compressed upon clamping, however, this did not predispose these particular specimens to have failure within the grips. The 400-grit emery paper was used with all other specimens in order to stop slippage in the grips. The relatively hard (stainless steel, multistranded stainless steel) or relatively soft (polymers) required the use of emery paper to avoid slippage. The Titanal® wires appeared to be a more brittle brand of nickel-titanium and better clamping results occurred when emery paper was used.

The intergrip distance was set on the machine to allow 1 & 3/8" between the grips before the specimen gripping procedure and the test began. The wire (and emery paper if indicated) was first tightened in the upper grip with a torque wrench to 90 to 140 lbf x ft (122 to 189 N x m). The upper clamp was then pinned in to the multi-direction hinge which was attached to the load cell. The load meter was then zeroed out by means of the load cell balance control (the load cell balance control was not adjusted again after this point in each test as this would throw-off the zero value of load). The lower grip was then installed in the bottom grip housing of the Instron machine test frame and the jam-nut was secured. The wire (and emery paper if indicated) was tightened in the lower grip with a torque wrench to 90 to 140 lbf x ft (122 to 189 N x m). Great care was taken not to introduced any tension or compression on the wire while tightening the lower grip. Slight slack or compression was taken out of the specimen by using the manual crosshead control at this time, however, the load meter was observed while doing this so no load was added to the specimen. The extensometer was then carefully placed on the specimen and the specimen was again checked and adjusted for

slack or compression with the manual crosshead control. The acquisition system was initiated on the computer just prior to starting the Instron cross-head motion.

Wires generally failed at the juncture of the wire where it entered the specimen grip or often somewhere in the gage length, depending on the particular type of specimen. Failures at the edge of the grip would be expected do to the stress concentrations in this area do to the dramatic change in area between the wire and the grip face. Because the primary interest of the study is with elastic and initial permanent deformation regions of the wire, the variable location of the wire failure was not of major concern since determination of the ultimate tensile strength was considered to be less important in normal clinical applications (ultimate yield strength data did appear to be regular however). Although the gage length was only slightly less that the initial distance between the grips, do to the restricted available straight lengths of some of the specimen taken from preformed arch wires, the extensometer, when placed on the wire specimen, was always centrally positioned between the tensile test grips, so the extensometer would consistently measure the strain near the center of the specimen as the strain may vary at different location on the specimen.

Several of the metal-alloy specimens tested were only available in preformed arch wires. The smallest of these preformed arches only had an approximate straight section of arch wire of as little a 1&7/8" at each end (Sentalloys®). The maximum distance that the grips could be apart at the beginning of the tensile test was 1 & 3/8", and still allow for 1/4" of wire for gripping in each grip. Since only a 1" extensometer was available for use, at least 1&1/4" of wire was necessary to provide attachment of the extensometer on the wire extending

between the upper and lower grip. The rectangular (1" x 2") Instron flat type grip faces were used, but the corners had to be ground off at 45° angle to allow room for the extensometer specimen clips to fit on the wire and not touch any part of the grips or clamps (see Figures 7 and 8). The maximal about of specimen was strived for between the grips as this improved the gripping process.

A cross-head speed of 1mm/min (in a range similar to that previously used by Howe *et al.*, 1968; and Asgharnia, 1983) was selected and a data sampling at 1 second intervals provided for a sufficient amount of data points for analysis. Assuming specimen elongation rate at the gage length of 1mm/min (0.039 in/min) as per the set cross-head speed, the elongation rate of the specimen would be, 0.039 in/60 sec., and a strain rate of, 6.5×10^{-3} mm/mm/sec, for a 1" gage length. This is considered to be a medium strain rate for a tensile tests (Dieter, 1976).

The tensile modulus of elasticity (E_t) was determine by means of verifying the initial linear portion of the stress-strain plots by linear regression. Once the raw data from the data acquisition system had been converted to stress-strain units, a plot was made using a Macintosh® SE FD/HD computer with added memory capabilities computer with the *Data Desk Professional® Program. The stress-strain diagram was plotted and the initial linear portion of the curve was determined. The portion of the curve selected to represent the initial linear portion was tested for linearity by means of selecting upper and lower limits of this linear portion so a linear regression of the points in this line could be done to satisfy that the

*Odesta Corp., Northbrook, Ill.

adjusted coefficient of determination, the adjusted R^2, was equal to or greater than 99.8% (values tending toward 100% indicate that variation is explain by the linear regression model). The computer assisted in location of the initial linear portion as any part of the original data curve could be magnified by the Data Desk Professional® graphical software. The tensile modulus of elasticity (E_t) is define as the slope of this line. Once this line was determined to be sufficiently linear, it was extrapolated (drawn) to its intercept with the horizontal (strain) axis. This intercept was considered to be the new (actual) origin. A new axis scale was superimposed over the old scale so that the new origin would be at this point (a duplicate of the scale was overlaid on the old scale but now starting at the linear portion intercept on the strain (horizontal) axis). This procedure was necessary because some artifacts generally produced a small curvilinear line at the beginning of the test do to specimen slack or slack in the gripping apparatus, and theoretically the initial linear portion of the curve should originate at the origin. The tensile yield strength (YS) at the 0.2% offset was found by extending a line parallel to the initial linear section starting on the horizontal (strain) axis at the a strain of 0.002 ln(in/in) and extending to where it intersect with the original data curve. The reading from the vertical (stress) axis at this point of intersection gives the yield strength at the 0.2% offset. The reading from the horizontal (strain) axis given the corresponding strain at the yield strength at the 0.2% offset. For each group of wires the value for the modulus of elasticity (E) and the yield strength at the 0.2% offset and the corresponding strain at the 0.2% offset will be recorded. The average and standard deviation will be determined for each of these values for each test condition.

The actual location of the elastic limit was not attempted in this study by these graphical means because in order to determine the exact elastic limit requires that tedious incremental loading-unloading tests procedures be done (Dieter, 1976).

Protocol for the Three-Point-Bend Test:

In addition to presenting bend test data in load-deflection diagram form, the results from the bend test were manipulated into approximated flexural stress-strain diagram form. This allowed a more direct comparison with tensile test data and as discussed earlier it is more convenient for the wire designer to use stress-strain diagrams since there is only one curve per material and he is free to plug in parameters such as wire size and shape during new wire design. On the other hand, when selecting wires for clinical use, since the clinician has wires in a set limited number of size and shaped wires to choose from, it is more convenient for him to look at a load-deflection diagram of a particular wire to determine if it will respond appropriately for his intended use.

The load-deflection diagrams can be directly plotted from data taken from the three-point-bend test. The load is recorded from the load cell and the deflection is converted directly from the movement of the crosshead. Load-deflection diagrams were plotted were the abscissa (horizontal axis) was the deflection, in (mm) and the ordinate (vertical axis) was load, lbf (Newtons). The stress-strain diagrams were plotted were the abscissa was the stress, lbf/sq in (N/m^2) and the ordinate was given as the strain (engineering), in/in (m/m).

In order to plot a load-deflection diagram, the changes in voltage provided by the load cell

were converted to give load and the rate of movement of the crosshead was converted to give the deflection by using the following equations. The load, P, is given by,

$$P=c^{*}V_{p}$$

where P=load, the converted ordinate data, lbf (N)

c=data acquisition conversion factor, lbf/volts (N/volts)

V_p= voltage from the meter detecting load, volts

and deflection, δ, is given by

$$\delta=t^{*}C_{h}/(60 \text{ seconds/min})$$

where δ=deflection, the converted abscissa data, in (m)

t=elapsed time, seconds

C_h=rate of the crosshead movement, 1mm/min (0.0394 in/min)

In order to manipulate raw data from the three-point-bend test in to a form that could be used to plot an approximated flexural stress-strain diagram, the following standard definition that applies to the initial linear portion of the stress-strain curve will be used,

$$E=\sigma/\varepsilon$$

Where E=modulus of elasticity, psi (N/m^2)

s=stress, psi (N/m^2)

ε=strain, in/in (mm/mm)

With this relationship, the following is true for a three-point-bend test if the conditions of linear elastic deformation and idea three-point-bending geometry are maintained. The flexural modulus of elasticity is given by the equation (Van Krevelen, 1976), for the condition of a

three-point-bend test,

$$E_f=4*P*L^3/3*\pi*D^4*y$$

where E_f=the flexural modulus of elasticity, psi (N/m^2),

P=load applied to the wire, lbf (N)

L=span length, the distance between the supports, in (mm)

D=diameter of wire, in (mm)

y=maximum wire deflection (center of the span length), in (mm)

or for convenience,

$$E_f=(4*L^3/3*\pi*D^4)*S$$

where S=slope of initial linear portion of the load-deflection curve, $\Delta P/\Delta y$, lbf/in (N/m),

and since $E_f=\sigma/\varepsilon$,

$$\sigma=8*P*L/\pi*D^3$$

and,

$$\varepsilon=6*D*y/L^2$$

(the above equations are specifically for the case of *round wires). The equations for stress, σ, and strain, ε, here apply were the deflection, y, is maximal (at the center of the test span were load, P, is placed by the crosshead). Data from the three-point-bend test can be plugged into the above *equations for stress, σ, and strain, ε, to construct an approximated flextural stress-strain diagram. Although the above equations are valid for the initial linear

*Rectangular wires have different equations, see Van Krevelen, 1976.

portion of the curve, some error will be accepted as the equation is applied through curvilinear portions of the curve to define a curve up to at least were the 0.2% offset yield point occurs. While some errors will occur in the curvilinear portions of the constructed three-point-bend test stress-strain curve, it will still render useful comparison to the everywhere accurate tensile stress-strain curve. Since the above equations relate specifically to the initial linear part of the curve, and because the equation will be applied to some curvilinear portions of load-deflection data during the construction of flexural stress-stress diagrams, these plots are call approximated flexural stress-strain diagrams.

Since stress-strain diagrams are presented for tensile and bending data, this allows for further comparison of characteristics the two test techniques, however, when comparing stress-strain data between the tensile and bend test inherent differences in the manner of load should be kept in mind (see Literature Review section). The units of strain used on the tensile stress-strain diagram were given in ln(in/in) or true stain and the units used of the bending (flexural) stress-strain diagram were given in in/in or the engineering (conventional) strain. These two definitions of strain are approximately equal up to values of strain of 0.1 in/in, but after that the progressively become more unequal. Therefore, comparisons of information made between plots which use different definitions of strain should be accurate, if the data of interest does not exceed strain of 0.1 in/in.

The bend test data originated from the origin, generally in a linear manner, and in the bend test there were no factors of specimen and machine slack which influenced the very initial portions of the curve as was the case with the tensile test. Such as the case, the origin

point and strain (horizontal) scale did not have to be adjusted for bend test data as it was with the tensile data. In the case of the bend test, since the data generally started at the true origin, as opposed to the tensile test that had to have the origin adjusted, the interval of the data plot that represented the initial linear portion was defined by selecting a data point to only represent the upper limit of the initial linear portion that was define a linear segment that meet the criterion of the minimal acceptable value for the adjusted coefficient of determination (the adjusted R^2 greater than or equal to 99.8%). The slope of this line was later included into bend test equations that provided values for the flexural modulus of elasticity (E_f). Occasionally, the first few points of the bend test data were not included in the determination initial linear portion of the data plot if it was obvious they were not linear. The yield strength at the 0.2% offset and the associate strain at the 0.2% offset were established by simply drawing a parallel to the initial linear portion of the original curve at a strain of 0.002 in/in (mm/mm) which equals 0.2% strain to a point were it intersected the curvilinear portion of the original data plot. Using the equation, $E=\sigma/\varepsilon$, for the flexural modulus of elasticity (E_f) and understanding the potential errors in using this equations outside of the initial linear portion of the curve, back-calculations were done to approximate load and deflection on the load-deflection diagrams that would correspond to the yield strength at 0.2% offset and the associated strain on the approximated flexural stress-strain diagram. These values, the load and corresponding deflection (that is the load and deflection that corresponds to the 0.2% strain offset from the approximated fextural stress-strain diagram) represented a standardized technique for defining a clinical reference point between elastic and plastic deformation on the

load-deflection diagrams.

Three wire specimens trails were run for each test condition. An *Instron Model 1125 Universal Testing Machine was used for all trials. The data acquisition system was the same as for the tensile test. A 2000 gram **Instron Compression Load Cell (see Figures 9, 10, and 11) with full scale calibration (sensitivity) ranges of 2000, 1000, 500, 200, 100 grams was used to detect changes in load. A full scale calibration range was selected for each specimen type so that the resulting curve would have its maximal flexural strength in the middle or upper third of the Instron chart recorder in order to maximized the sensitivity of the load cell for each specimen type. The load cell was calibrated with standard weights at zero, mid-range, and full-scale. The average error over the load range of each of the full scale calibration range used, 1000, 500, 200, and 100 g, were ± 2 g (± 0.0044 lbs), ±1 g (± 0.0022 lbs), ± 0.2 g (± 0.0004 lbs), ± 0.4 g (± 0.0009 lbs), respectively. As actual graphicall interpretation of data was used from data plotted from the data acquisition system, the Instron chart recorder graph was only used so the operator could view the progression of each test and select the proper load cell sensitivity on trial runs prior to the actual recorded specimen runs. The data acquisition system sampled one data point every 1 second. A custom made three-point-bend fixture was designed to accommodation the small specimen size and small test span lengths. Since considerations had to be given to the selection of a appropriate span length do to the geometric conditions of pure bend test, the test fixture had adjustable

*Instron Corp.,Canton,Mass.

**Catalog #2511-201, Instron Corp., Ibid.

specimen supports that allowed for appropriate span lengths for all test conditions. Test span lengths can influence the accuracy of data if it is too short in relation to the amount of deflection that will occur in the elastic range of the wire being tested. As the test span becomes shorter in relation to the amount of deflection in the elastic range, the likelihood of torsional, shear, and other none pure bending influences tends to increase. The critical question that immediately arises is at what point do these influences cause a significant deviation to pure bending mechanics for a given situation. The answer to this question is that the investigator must choose test parameters that provide data that is within a desired level of accuracy.

When choosing a span length for test purposes, it is necessary to take in to consideration the initial assumptions made in the development of elastic bending theory so that the span is not to short as to violated assumptions made and introduce intolerable errors. It is assumed that during the bend test the change in length of the specimen, dy, will be much less the amount of deflection, dx or

$$dy/dx << 1$$

and this implies for the bending angle, θ , that,

$$\tan\theta = dy/dx \approx \theta$$

So with the assumption that $dy/dx = \theta$ (Byars and Synder, 1969), the derivation of the modulus of elasticity in bending equation continues. With the above assumptions it is seen that with a small bending angle, θ, of 10° only an error of 1% will occur, with a bending angle, θ, of 20° an error of 4% will occur, and with a bending angle, θ, of 30° an error of 9% will occur. This

discussion demonstrates why the pure bending theory stipulates that the specimen be of a long length with respect to the deflection and that only small deflections on less than 10° occur prior to reaching the proportional limit in the bend test. Kusy and Dilley (1984) found by maintaining a test span that was 20 times the length of deflection, and for deflections of their wire specimens were between 0.04 and 0.13 cm (purposely kept with in the linear elastic range for each particular wire tested), the maximum wire increase in length in this range was less than 0.2%.

Data from preliminary trial runs demonstrated that deflections up to the 0.2% yield strength offset rarely exceeded 0.05" (1.27 mm) when tested at a support span length of 0.5" (12.7 mm). In the light of this information and the clinical relevance of a small test span, a test span of 0.5" (12.7 mm) was selected to test all specimens, except the Glastic® wire which was only available in the smallest size of 0.030". Because The Glastic® wire was 0.030" in diameter, in addition to its relative stiffness, it was tested at a 1" (25.4 mm) span length because it was necessary to increase the span length so the specimen would under go the full range of elastic bending without exceeding the load limit of the 2000 g load cell (as test span is increase the load required to cause a given deflection decreases). Exceeding the load limit of a load cell can damage it. A small test support span was also necessary because highly flexible wires (Respond® multistranded stainless steel and the unfilled polymer wires) may bow between the supports if the supports were too far apart.

Wires were cut into to 3/4" sections for the three-point-bend test at a support span length of 0.5", this length was chosen since it allowed a little extra wire for ease of placement on the

test fixture, but was not excessively long as this may introduce unexplained deformations of the portion of the between the test supports. The Glastic® wire tested at a 1" test span length was cut into 2 & 1/2" sections for testing.

The unfilled polymer wires which were delivered on spools and preformed Sentalloy® arch wires did not appear to have perfectly straight lengths when cut into the 3/4" test length. However, as consistent with bend test theory, wires that are not perfectly straight can be tolerated to a certain extent. If the wire is slightly curved, the depth of curvature must be less than 1/10th of the test span length to maintain the desired level of accuracy. Arch wires that were delivered in preformed arch wire shape had 3/4" specimen length taken from the straightest portion of the wire, usually at the ends.

The crosshead was aligned so that it was dead center (within ± 0.010" of dead center) between the two test supports. Specimens were laid across the two supports so it would also be centered (± 0.025" of dead center) on each support. The crosshead was moved downward with the manual control knob until it was about 0.005" to 0.010" away from the specimen (see Figures 9, 10, 11, and 12). The data acquisition system was started just prior to starting the crosshead motion. A crosshead speed of 1 mm/min (0.0394 in/min) was selected since this was the same crosshead speed that was used for the tensile test and when combined with a data point selection of 1 point/second from the data acquisition system, gave an ample number of points to draw a significantly linear line through linear regions on the final data plots. The crosshead was stopped and the test completed for each specimen when the maximal flexure strength had been obtained or obvious wire slippage

occurred.

The contribution of the dead weight of the wire specimen across the test span can potentially result in wire deflection that could contribute to errors in calculation of the flexural modulus of Elasticity (E_f). Kusy and Dilley (1984) studied the influence of the dead weight deflections of wire during a three-point-bend test and found that at as load of 1 N (0.225 lbf) was placed, the dead weight deflection was only 0.05% of the total wire deflection. Since the dead weight deflection does not vary with load, the dead weight deflection becomes more significant at low loads. At a load of 0.01 N (0.00225 lbs), the dead weight deflection was 5% of the total wire deflection. The load ranges encountered by the specimens tested here at the 0.2% yield strength ranged from 12.0 N (2.7 lbf) to 0.05 N (0.012 lbf) so the dead weight effect of the wire was considered negligible.

The machine error occurring during the three-point-bend test, that is the deflection caused by the load cell itself and other parts of the machine during testing was determine by placing a stainless steel specimen of a very large diameter 0.8764" (22.26 mm) on the test supports that would undergo no deflection when laoded throughout the full range of loads used during actual specimen testing. Great care was taken to stop the crosshead movement as soon as the full scale calibration load had been meet since damage to the load cell could occur if the 2000 grams maximum limit was exceeded. Three trials for the machine deflection were done, and average slope of the resulting load-deflection curves (the load-deflection data for the machine deflection were linear throughtout the entire range of loads used during all of the specimen tests) were compared to the average slope of the initial linear portions of the

actual specimen load-deflection curves to see if the machine deflection was a comparatively vertical line. The three-point-bend test data of the test condition (the particular type of wire specimen) with the smallest average initial linear load-deflection slope was 0.94 ± 0.01 lbf/in (164.6 ± 1.8 N/m) and that of the largest average initial linear laod-deflection slope was 52.49 ± 0.58 lbf/in (9,191 ± 101 N/m). The load-deflection slope of the large diameter stainless steel specimen (or the machine deflection) was 1658.24 ± 7.10 lbf/in (290,387 ± 1,244 N/m). In terms of percentages, the test conditions with the smallest and largest initial linear load-deflection slopes were 0.06% and 3% of the linear load-deflection of the machine deflection, respectively. Since the load-deflection slope of the machine deflection was so much greater than that of the range of test conditions, it was considered to be relatively vertical and thus considered to contribute negligibly to the slopes of the test conditions and was not factored-out in subsequent calculations.

Summary of Statistical Methods

For each test condition, the three replications where averaged and a mean was presented with the accompanying standard deviation for the group for each of the reported values of the tensile modulus of elasticity (E_t), the tensile yield strength at a 0.2% offset, the corresponding tensile strain at the 0.2% offset, the flexural modulus of elasticity (E_f), the flexural yield strength at the 0.2% offset, the corresponding strain at the 0.2% offset, the flexural load corresponding to the 0.2% strain offset, and the flexural deflection corresponding to the 0.2% strain offset.

The portion of the curve selected to represent the initial linear portion of the curve in the tensile test was tested for linearity by means of selecting upper and lower limits of this linear portion so a linear regression of the points in this line could be done to satisfy that the adjusted coefficient of determination, the adjusted R^2, was equal to or greater than 99.8% (values tending toward 100% indicate that variation is explain by the linear regression model). The slope of this line then was taken as the tensile modulus of elasticity (E_t). Similarly with the bend test data a linear portion of the stress-strain data was select and the interval adjusted until the condition of an adjusted coefficient of determination, the adjusted R^2, was equal to or greater than 99.8%. In the case of the bend test, since the data general started at the true origin, as opposed to the tensile test that had to have the origin adjusted, usually only the upper limit of the initial linear portion had to be varied to meet the criterion of the minimal acceptable value for the adjusted coefficient of determination. Occasionally, the first few points of the bend test data were not included in the determination initial linear portion of the data plot if it was obvious they were not linear.

The average error in the loads detected in each full scale calibration range of the load cells were established by averaging the difference between actual weight of the calibration weights used and the experimental weight of each of the three calibration weights read off of the data acquisition load meter after calibration was complete and after this voltage data was converted to lbf. Three different calibration weights were weighed and recorded that represented zero, mid-range, and full scale. Three replication of each weight were repeated and reported. The average of all these replications was the average error for determining the

load at a given full scale calibration (sensitivity). The average error for each full scale (sensitivity) strain was done similar to the average error for the load cell calibration except the measure of strain gage movement (inches) replaced the measurement of weight. The difference between the actual length as given by the extensometer calibrator scale and the unit converted value for experimental length as read from the data acquisition strain meter was determined for each of three replications at each of three different lengths representing the zero, mid-range , and full scale lengths. These differences were averaged and this gave the average error in the reported value of elongation that was used in further calculation to determine the true stain.

An indication of the repeatability of experimentation was compared between the tensile and bend tests by taking the standard deviation and dividing by the mean of the various reported values and multiplied by 100%, {(std. dev./mean)x100%}, for each test condition, and then the summation of this ratio for all test conditions was divided by the number of test conditions, [Σ{(std. dev./mean)100%}/(number of test conditions)]. This value is the overall average percent of the standard deviation divided by the mean.

TABLE II
The Metal Wires That Were Tested

Wire Produce Name, Size (inch)	Wire Composition
*Tru-Chrome, .014	Soft Austenitic Stainless Steel
*Tru-Chrome, .016	Soft Austenitic Stainless Steel
*Tru-Chrome, .018	Soft Austenitic Stainless Steel
*Tru-Chrome, .020	Soft Austenitic Stainless Steel
**A. J. Wilcox Aust. Reg., .018	Resilient Stainless Steel
**A. J. Wilcox Aust. Spec.+, .018	Very Resilient Stainless Steel
*Blue Elgiloy, .018	Soft Cobalt-Chromium-Nickel
*Red Elgiloy, .018	Very Resilient Cobalt-Chromium-Nickel
***TMA, .018	Beta-Phase Titanium-Molybdenum
***NiTi, .018	Nickel-Titanium
***Respond, .0175	6-Strand Multistrand Stainless Steel
***Triple-Flex, .0195	3-Strand Multistrand Stainless Steel
^Titanal, .018	Nickel-Titanium
^Titanal XR, .018	Nickel-Titanium
^^Sentalloy Light, .018	Nickel-Titanium
^^Sentalloy Medium, .018	Nickel-Titanium
^^Sentalloy Heavy, .018	Nickel-Titanium
^^Neo-Sentalloy, .018 x .025	Nickel-Titanium

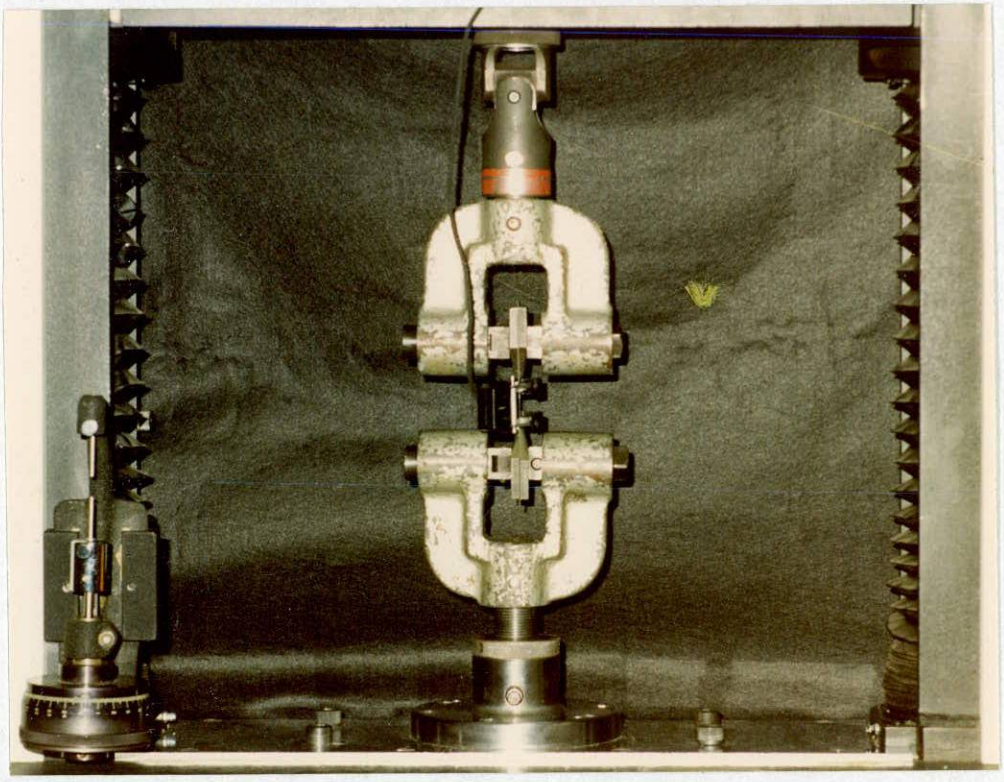
*RMO, Inc., Denver, Co.
**TP Orthodontics, La Porte, Ind.
***Ormco Corporation, Glendora, Calif.
^Lancer Orthodontics, Carlsbad, Calif.
^^GAC International, Central Islip, N.Y.

TABLE III
The Esthetic Wires That Were Tested

Wire Product Name, Size (inch)	Wire Composition
*Glastic, .030	63-64 volume %, longitudinal, continuous, uniaxial fiberglass in an acrylated epoxy matrix (semi-transparent)
**MX-501, .023	polyether ether ketone (PEEK), extruded, air quenched for smoother surface (brownish color)
**WOX-3, .0157	polyether ether ketone (PEEK), extruded, water queched (brownish color)
**WP-89, .0138	polyethylene terephthalate (PET) polyester, extruded, high molecular weight (available in clear and colors)
**WP-320, .0157	polyethylele terephthalate (PET) polyester, extruded, high molecular weight (available in clear and colors)
**WN-101, .014	polyamide Nylon 6/6, extruded, (available in clear and colors)
***Optiflex, .020	190 micron fiber-optic fiberglass core in a nylon matrix, commercially available orthodontic wire (clear)

*Glastic Corporation, Cleveland, Oh.
**Shakespeare Monoflilament, Col., S.C.
***Ormco Corporation, Glendora, Calif.

FIGURE 5
The Tensile Clamps, Grips, and Extensometer in Place on the Instron Universal Testing Machine with a Wire Specimen in Position and Ready for Testing and the Extensometer Calibrator is Shown at the Lower Left.



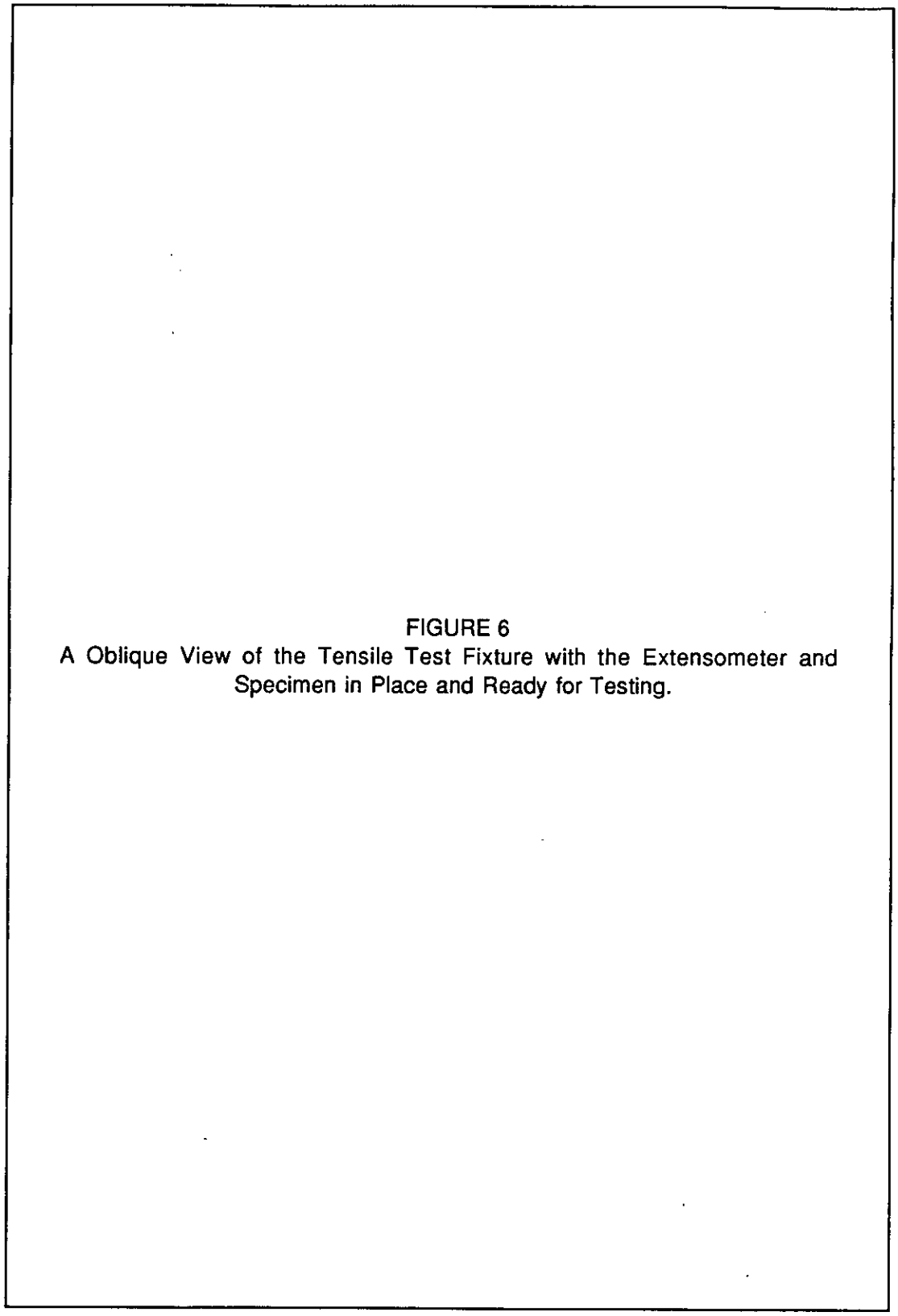
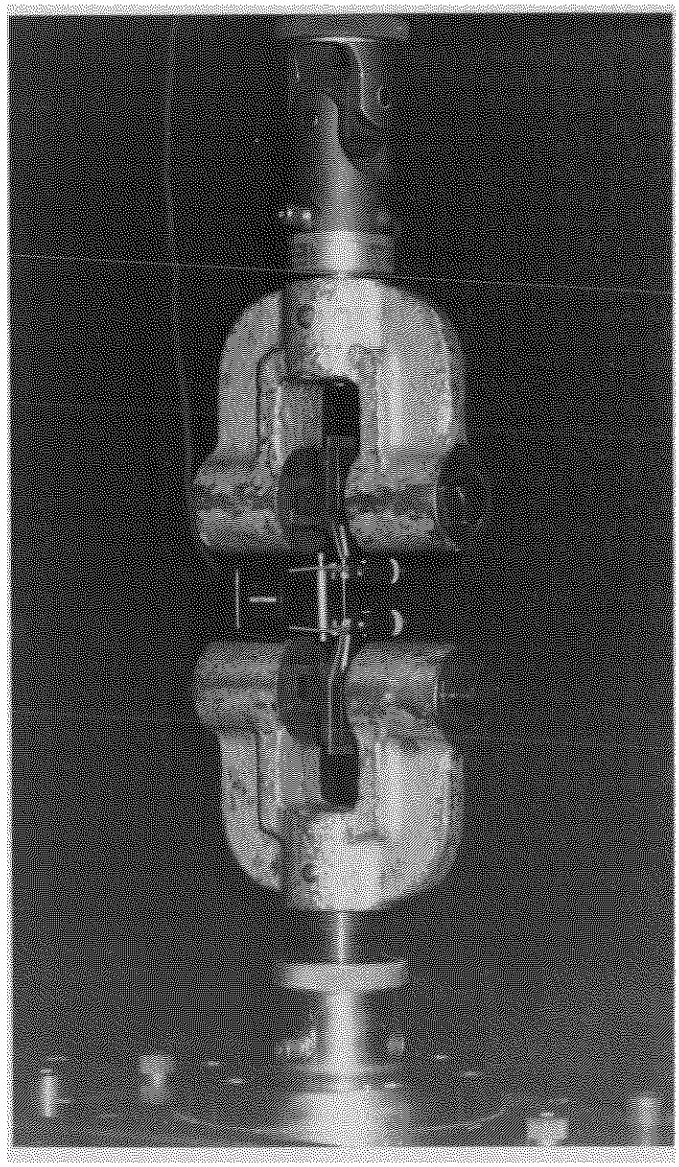


FIGURE 6
A Oblique View of the Tensile Test Fixture with the Extensometer and Specimen in Place and Ready for Testing.



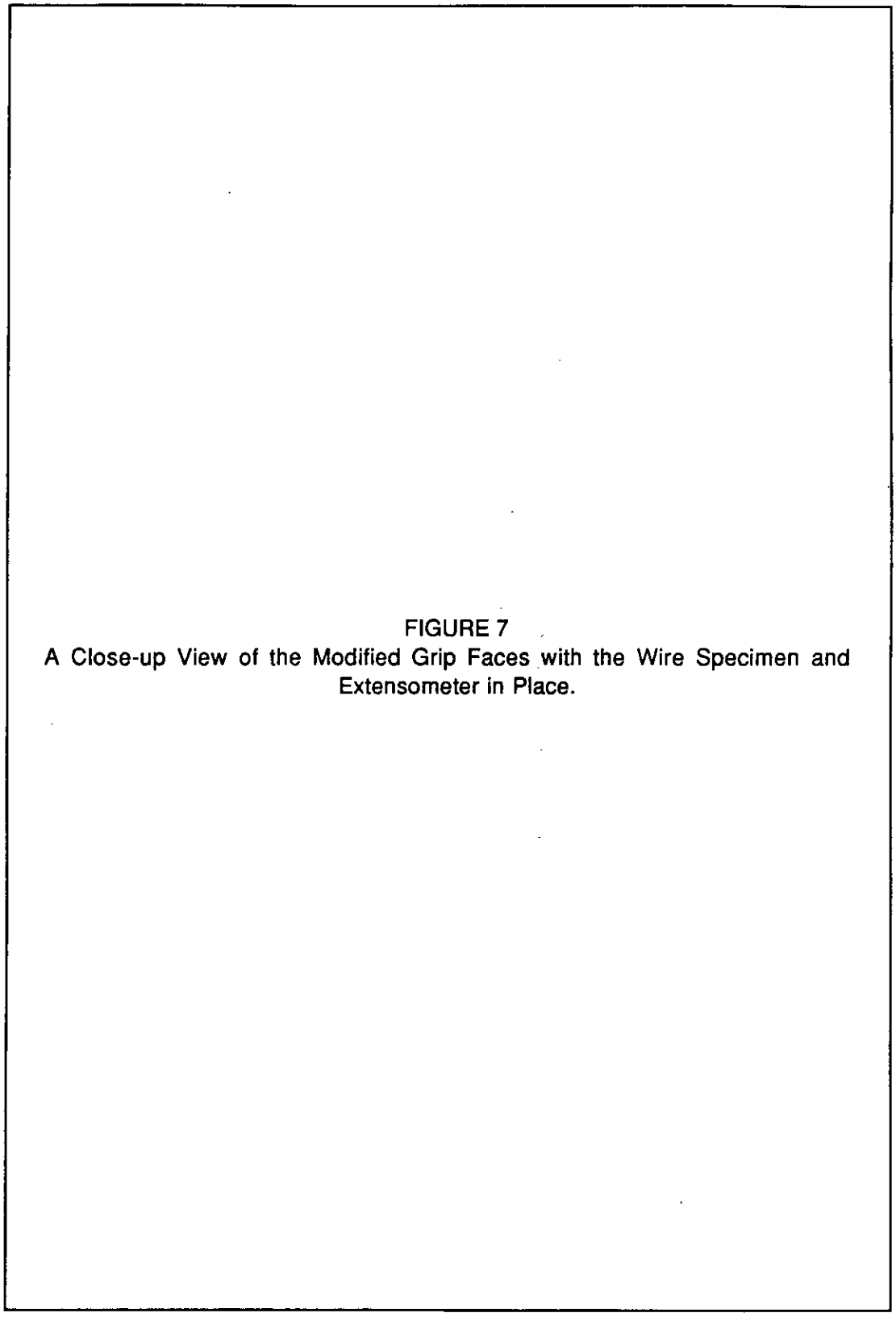


FIGURE 7
A Close-up View of the Modified Grip Faces with the Wire Specimen and Extensometer in Place.


INSTRON

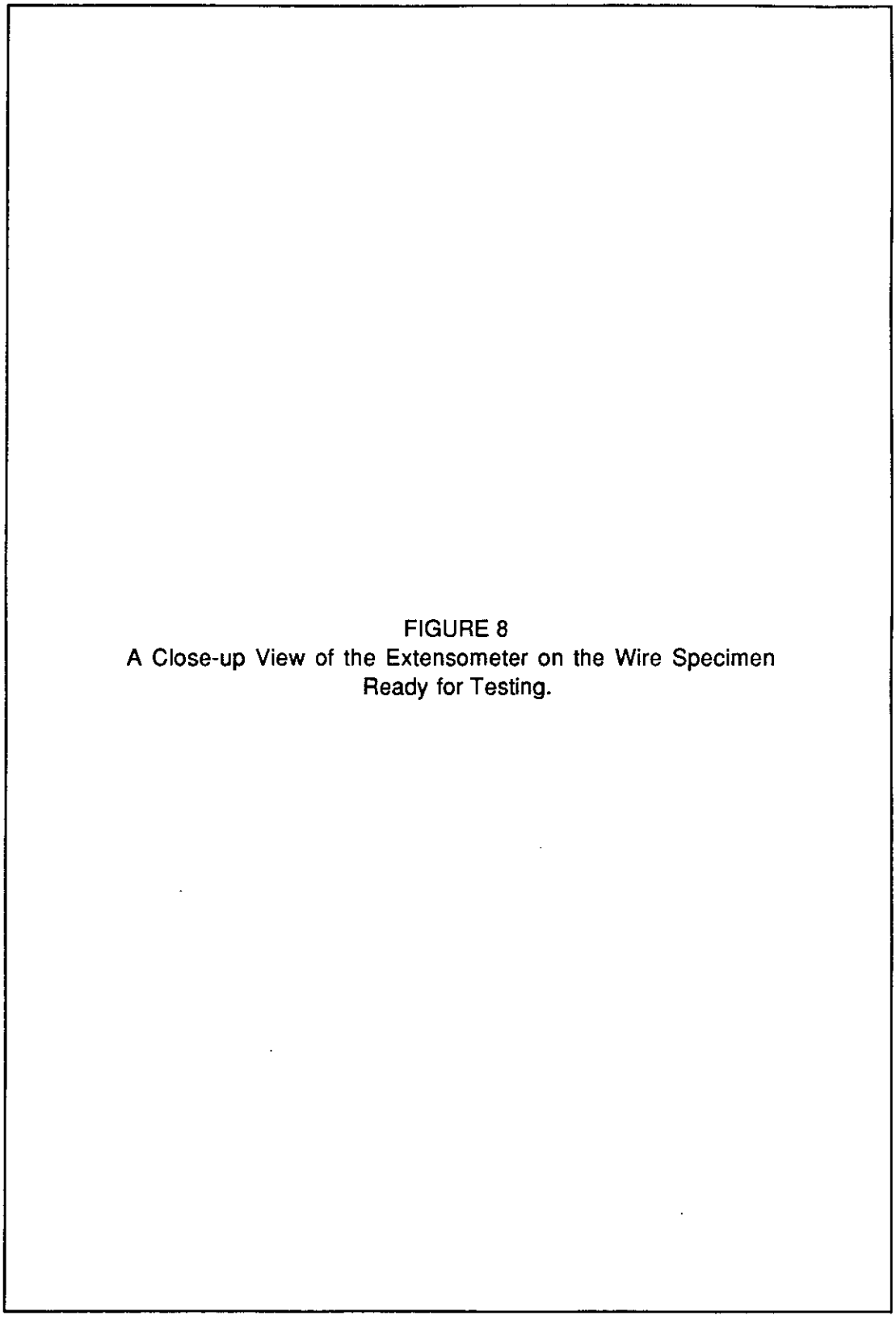
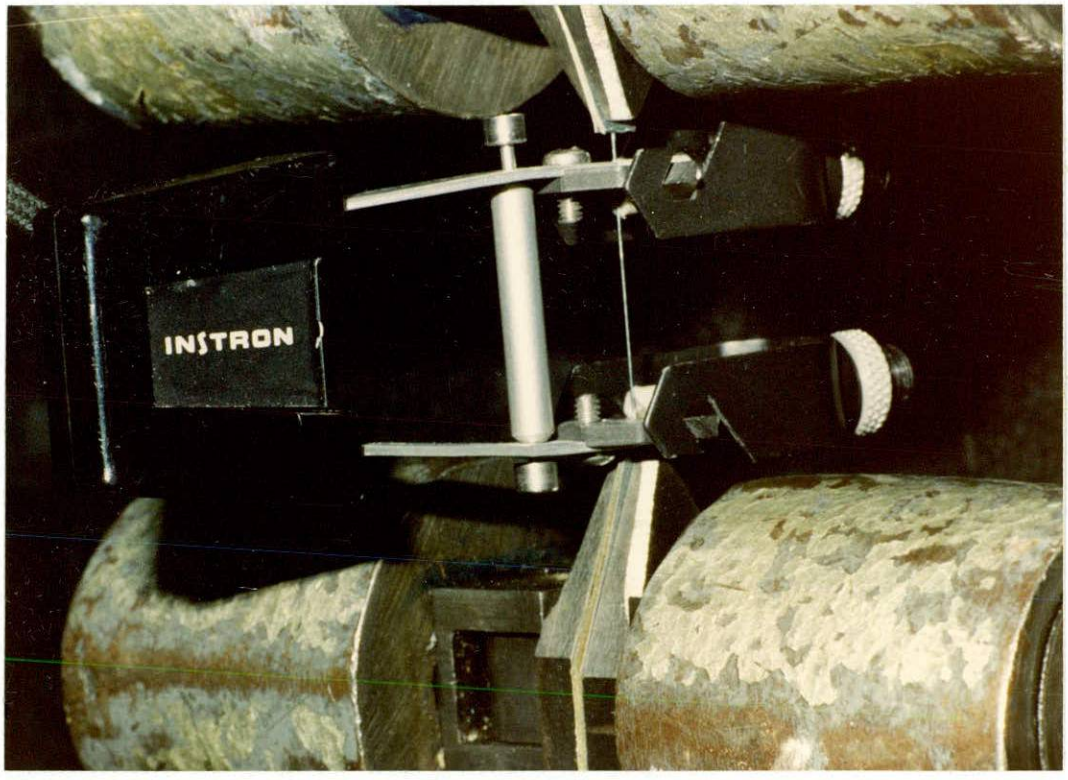


FIGURE 8
A Close-up View of the Extensometer on the Wire Specimen
Ready for Testing.


INSTRON

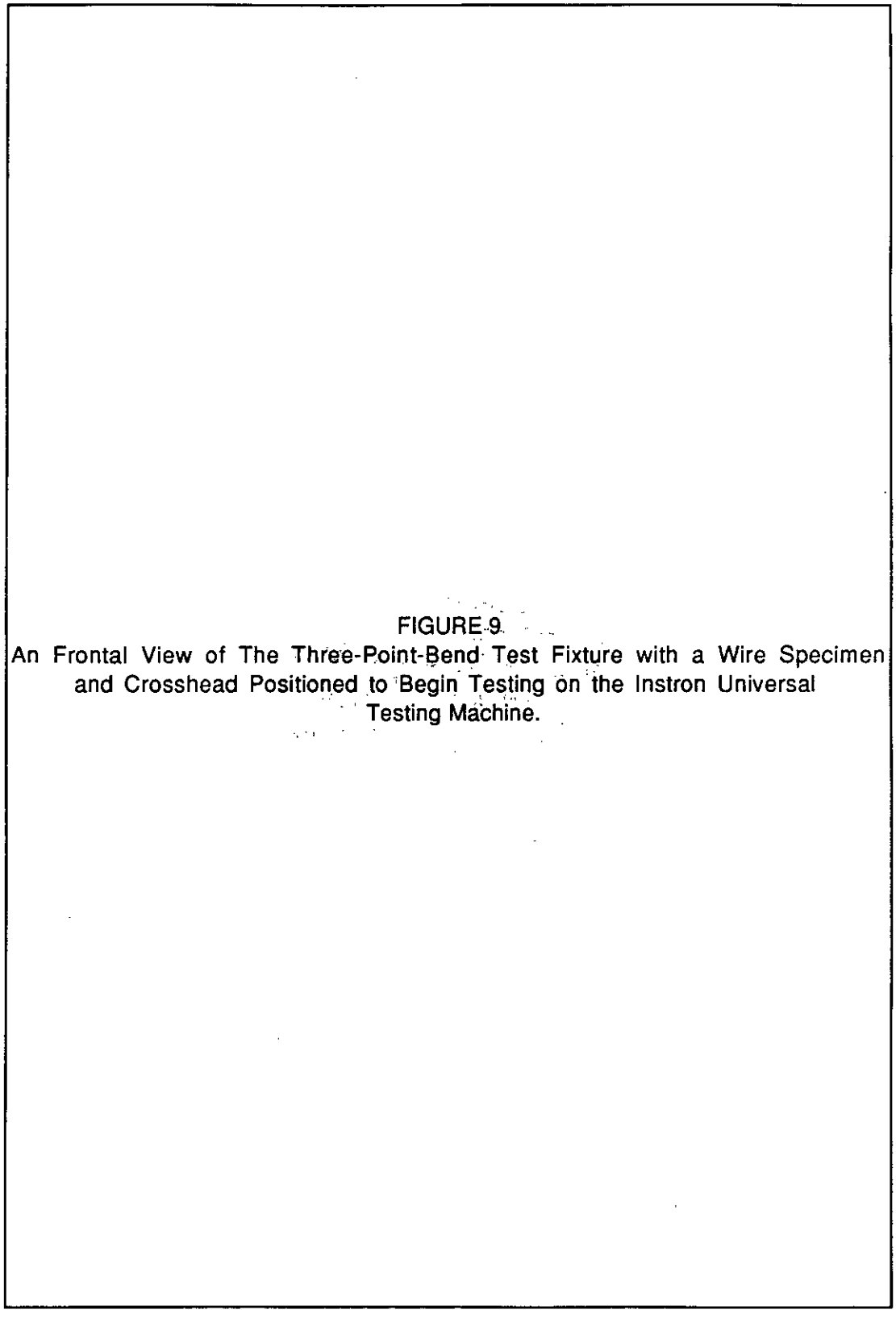
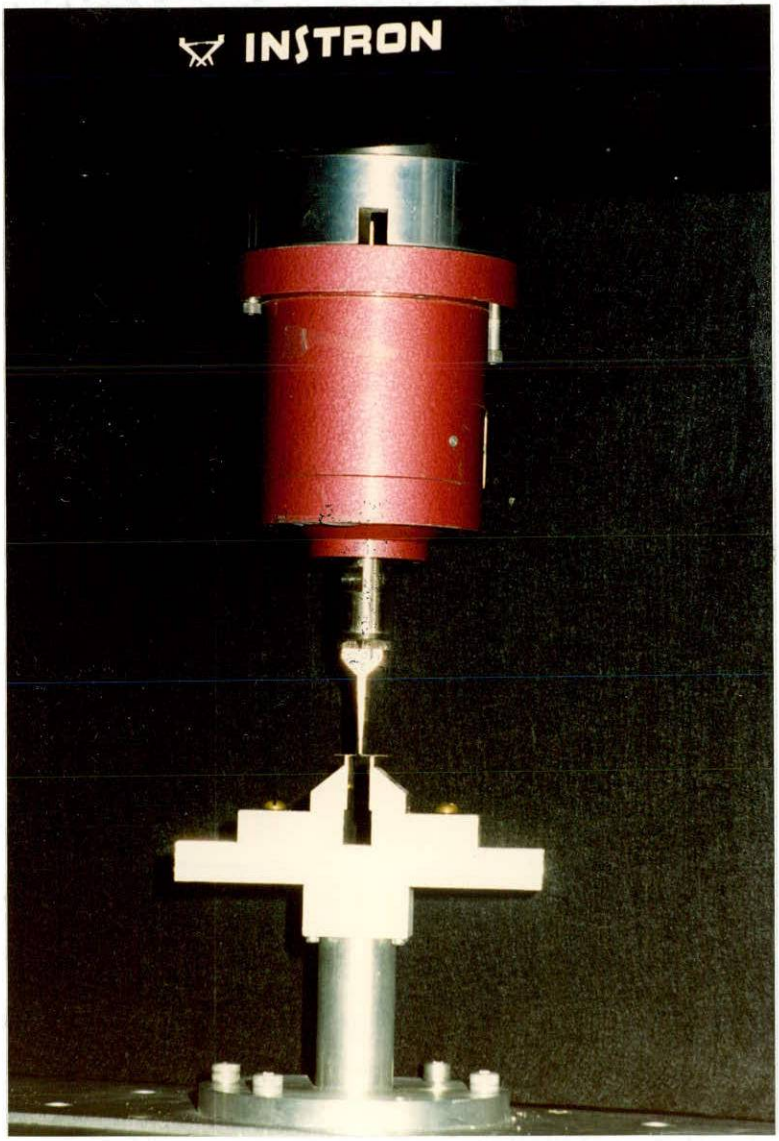


FIGURE 9.
An Frontal View of The Three-Point-Bend Test Fixture with a Wire Specimen and Crosshead Positioned to Begin Testing on the Instron Universal Testing Machine.


INSTRON

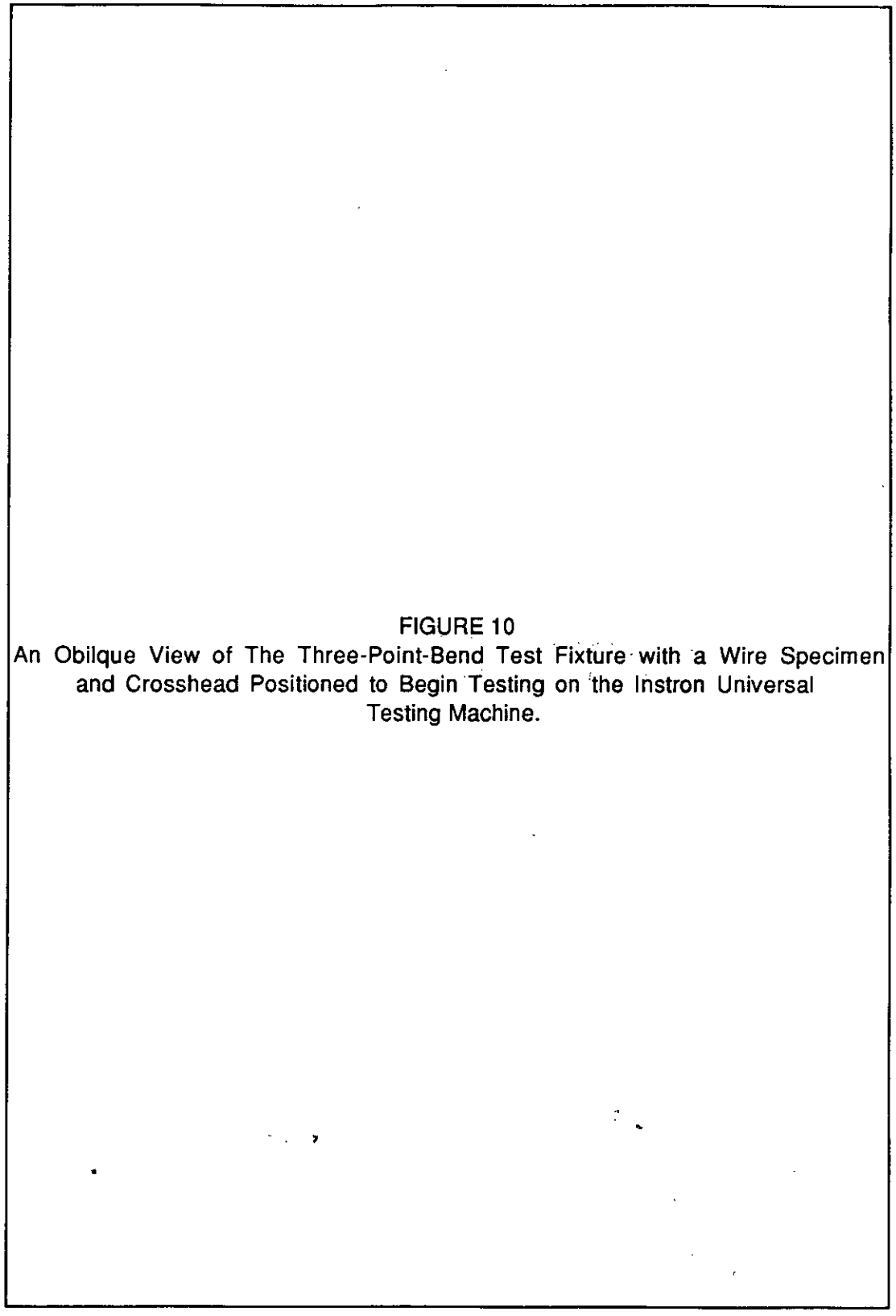


FIGURE 10
An Obilque View of The Three-Point-Bend Test Fixture with a Wire Specimen and Crosshead Positioned to Begin Testing on the Instron Universal Testing Machine.

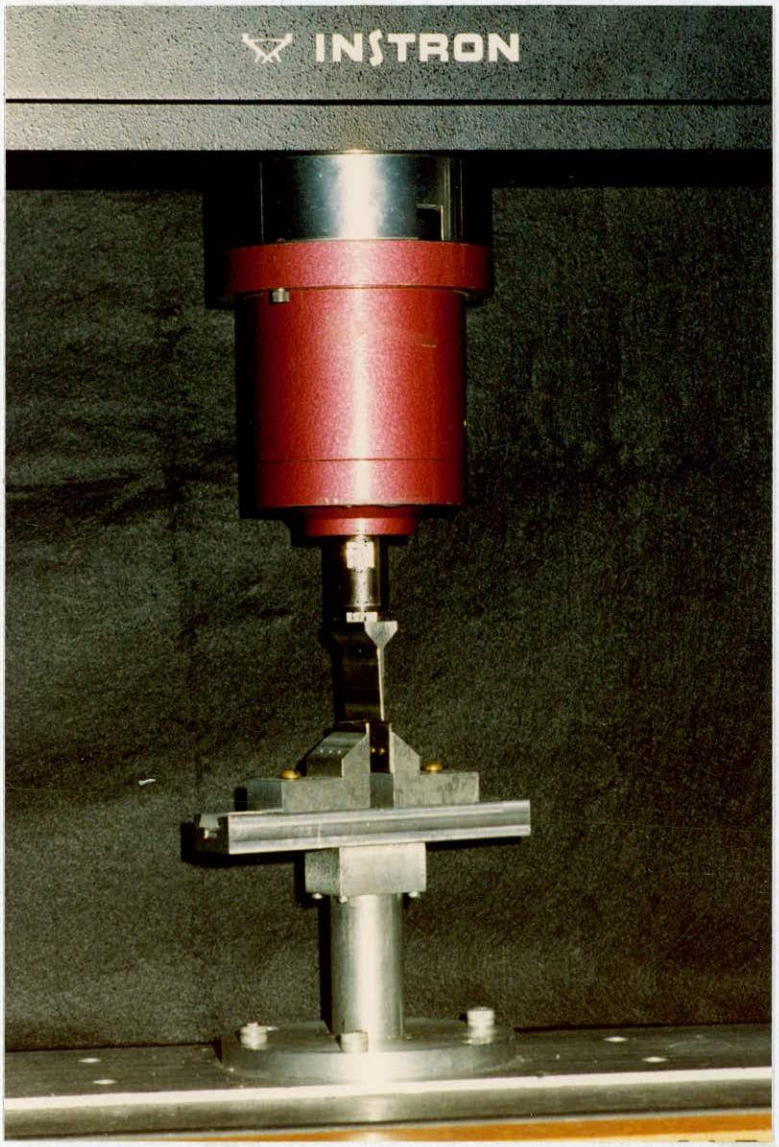
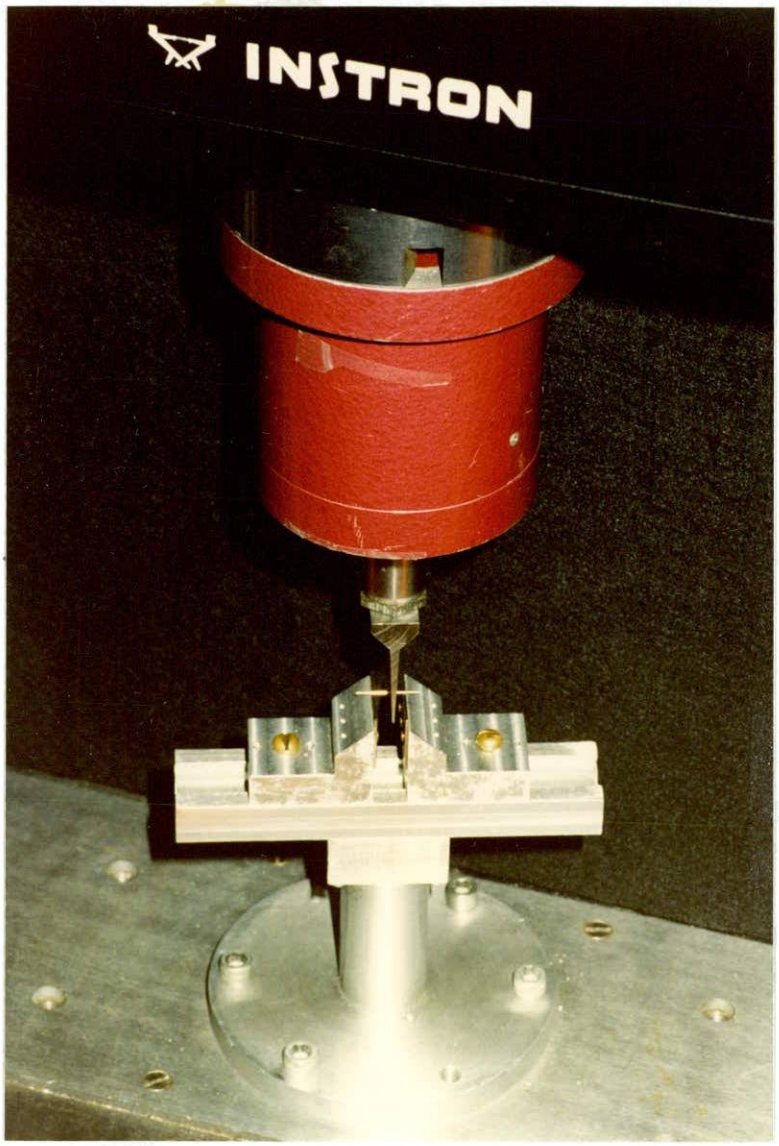

INSTRON

FIGURE 11
A Top View of The Three-Point-Bend Test Fixture with a Wire Specimen and Crosshead Positioned to Begin Testing on the Instron Universal Testing Machine.


INSTRON

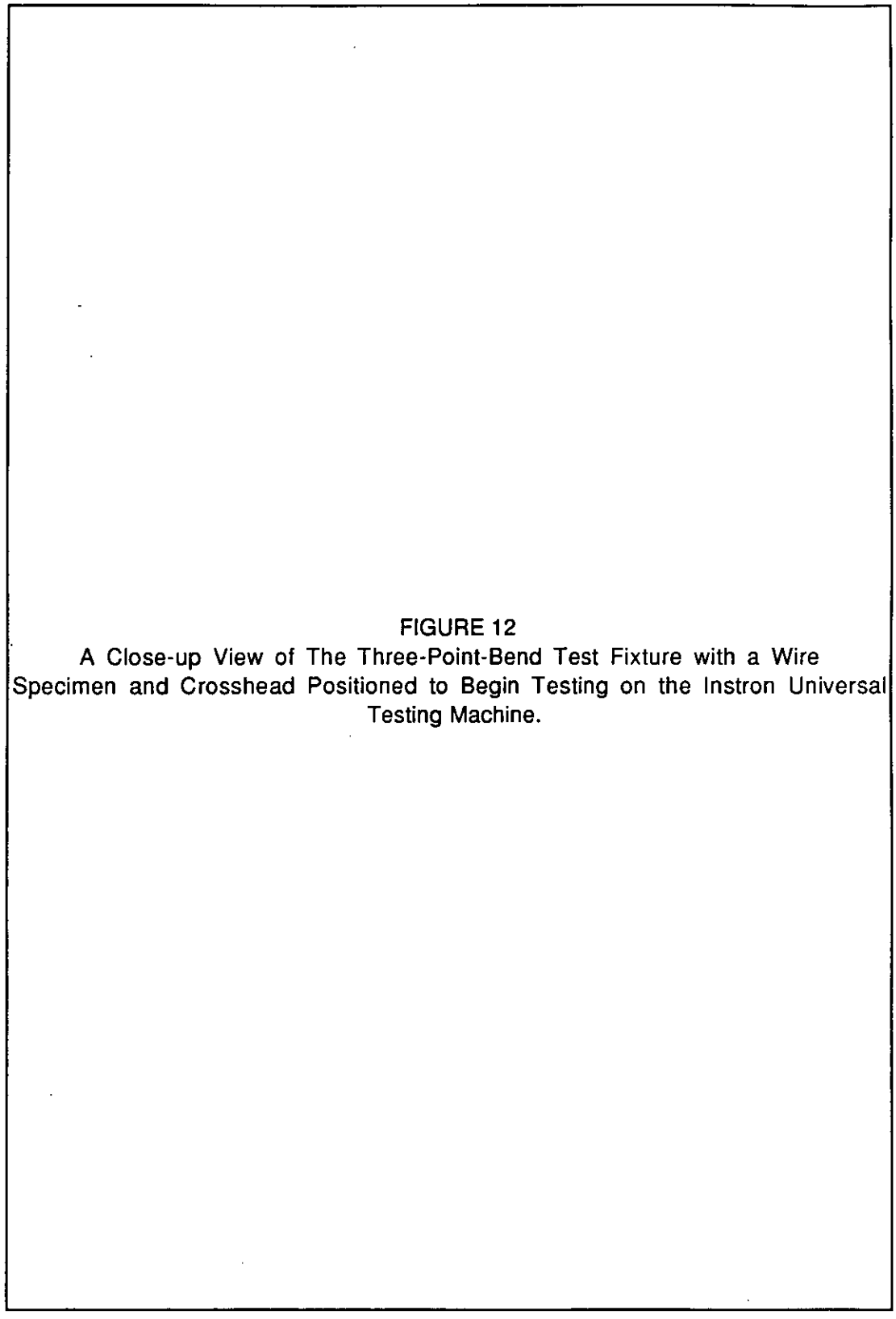
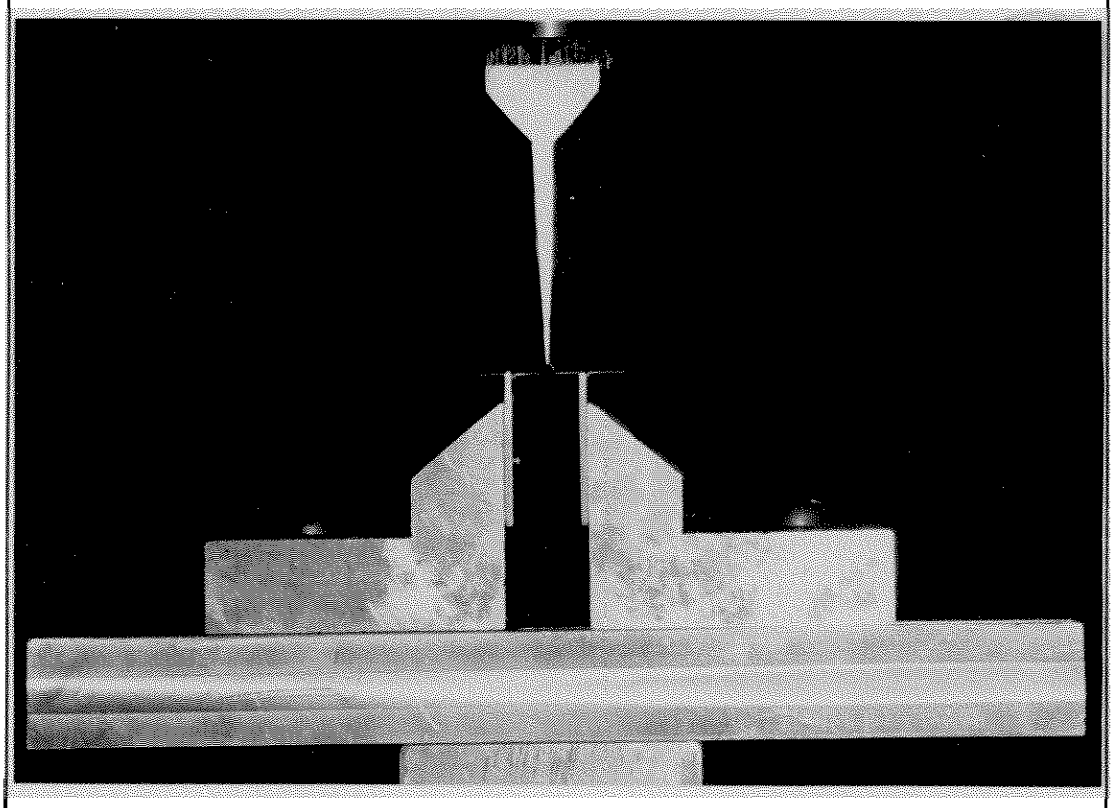


FIGURE 12
A Close-up View of The Three-Point-Bend Test Fixture with a Wire Specimen and Crosshead Positioned to Begin Testing on the Instron Universal Testing Machine.



RESULTS

The tensile test

The experimental results of this investigation involving the tensile modulus of elasticity (E_t), the yield strength, YS, at the 0.2% offset and the corresponding strain at a 0.2% offset are presented in Tables IV, V, and VI, repectively, as averages and standard deviations for each particular test conditions. A variety of representative comparative stress-strain diagrams are included in the results section to compare various metals to other metals and esthetic materials (Figures 13 to 20). A representative stress-strain diagram for each tensile test condition (material) in this investigation is presented in this section as a means of cataloging results for future reference (Figures 21 to 27). The material(s) presented in each Figure are listed in the Table of Contents. The significance of these diagrams will be addressed in the discussion. The testing of specimens was uneventful although very flexible samples such as the unfilled polymer were more difficult to obtain a zero load reading after the extensometer was placed because the weight of the extensometer had a slight torquing effect on these light wires. The fiber glass (fiberoptic) core in the Optiflex™ wire would separate after mild stress was placed so stress-strain data could only be collected for a brief time before the fiber glass (fiberoptic) core was pulled through the nylon matrix that remained in the test grips. This was due to the fact that as the nylon matrix was deformed during the grip tightening process the fiberoptic core was loosen from the surrounding nylon matrix. No other gripping problems were encountered with any other specimen type.

The tensile test produced curve shapes that varied drastically with different materials (Figures 13 to 20). The nature of the shapes of the curves will considered in the discussion in detail.

A linear regression plot was done of the average tensile modulus of elasticity (E_t) of each of the 0.014", 0.016", 0.018" and 0.020" Tru-chrome® wires to see if there was a relationship with varied diameter size. The adjusted coefficient of determination, the adjusted R^2, was -41.5%, (values tending toward 100% indicate a relationship explained by the linear regression model) and this demonstrated that the tensile modulus of elasticity (E_t) was independent of specimen diameter during the tensile test. The tensile tests for the multistranded wires, Tripleflex™ and Respond® wires really have no significance, since strand shape and configuration considerations were not accounted for in the equations used, other than to demonstrate that wire configurational effects in comparison of the tensile and bend test data and diagrams (the modulus is much lower in bending than in tension). The multistranded wires, Tripleflex™ and Respond® wires, do have important apparent properties in bending, however, as this is their manner of deformation when used intraorally.

The bend test

The experimental result of this investigation relating to the flexural modulus of elasticity (E_f), the flexural yield strength (FYS) at 0.2% offset, the corresponding strain at a 0.2% offset are present as averages with standard deviations for each of the test conditions on Tables VII, VIII, and IX, repectively. For the load-deflection data, the load corresponding to the

flexural yield strength (FYS) at a 0.2% offset on the approxiamted flexural stress-strain diagrams and the deflection corresponding strain at a 0.2% offset on the approximated flexural stress-strain diagrams are reported on Tables X and XI, respectively. A variety of comparative approximated flexural stress-strain diagrams and load-deflection diagrams are included in the results section to compare various metal with other metals and esthetic materials (Figures 28 to 36). A representative load-deflection diagram for each test condition done (material), and the corresponding approximated flexural stress-strain diagram (the flexural stress-strain diagrams were approximated by using the corresponding load-deflection data and the defining equation for the modulus of elasticity, $E=\sigma/\varepsilon$, see Methods section) in this investigation is presented in this section as a means of cataloging results for future reference (Figures 37 to 49). The material(s) presented in each Figure are listed in the Table of Contents. The significance of these diagrams will be considered in the discussion section.

A linear regression plot was done of the average flexural modulus of elasticity (E_f) of the 0.014", 0.0160" 0.018", and 0.020" Tru-Chrome® wires to determine if it was dependent on specimen diameter. The adjusted coefficient of determination , adjusted R^2, was 90.2%, and this demonstrates a very mild relationship between to flexural modulus of elasticity (E_f) and the specimen diameter under the given test equations and conditions. The flexural modulus of elasticity (E_f) tends to increase with decreased specimen diameters at least in the case of Tru-Chrome® wires. Also the overall average of values for the four wire sizes gives a much higher standard deviation that any of the separated wire size groups so this also tends to demonstrate a slight diameter dependence of the flexural.modulus of elasticity (E_f).

During the bend test all materials produced single, very smooth arc shaped curves at least to the point of obvious permanent deformation, except the Sentalloy® wires, which appeared have a dual curvature (Figures 44a, 44b, 44c, 44d, 45a, 45b, 45c, and 45d, in particular). This phenomenon will be discussed at length in the discussion.

TABLE IV
The Tensile Modulus of Elasticity, E_t
Uniaxial Tensile Test

Wire Product Name, Size " " , inch	The Tensile Modulus of Elasticity, E_t	
	$x10^6$ psi {std. dev.}	($x10^9$ N/m^2) {std. dev.}
Metal Wires		
Tru-Chrome, Overall Average	24.2 {0.6}	(166.7 {10.0})
Tru-Chrome, .020	23.8 {1.4}	(164.2 {4})
Tru-Chrome, .018	25.9 {1.2}	(178.6 {8.6})
Tru-Chrome, .016	22.9 {0.4}	(158.1 {2.9})
Tru-Chrome, .014	24.1 {1.6}	(166.0 {10.8})
A. J. Wilcox Aust. Reg., .018	26.2 {1.9}	(180.8 {12.9})
A. J. Wilcox Aust. Spec+ .018	26.2 {0.9}	(180.6 {6.3})
Blue Elgiloy, .018	26.6 {1.1}	(183.2 {7.3})
Red Elgiloy, .018	24.2 {2.5}	(166.7 {17.2})
TMA, .018	11.9 {0.4}	(82.1 {2.6})
*Respond, .0175	3.67 {1.8}	(25.3 {1.3})
*Triple-Flex, .0195	10.6 {0.6}	(72.9 {4.2})
NiTi, .018	8.9 {0.65}	(61.3 {4.5})
Titanal, .018	5.0 {0.47}	(34.4 {3.2})
Titanal XR, .018	4.24 {0.26}	(29.2 {1.8})
Sentalloy Light, .018	4.13 {0.58}	(28.5 {4.0})
Sentalloy Medium, .018	6.43 {0.8}	(42.3 {4.2})
Sentalloy Heavy, .018	6.13 {0.61}	(44.3 {5.5})
Neo-Sentalloy, .018 x .025	5.35 {0.09}	(36.8 {0.6})
Esthetic Wires		
MX-501 PEEK, .0236	0.72 {0.02}	(4.9 {0.13})
WP-320 PET, .0157	1.15 {0.03}	(7.9 {0.2})
WOX-3 PEEK, .0157	0.72 {0.06}	(5.0 {0.39})
WP-89 PET, .0138	1.14 {0.03}	(7.8 {0.21})
WN-101 Nylon 6/6, .014	0.24 {0.01}	(1.7 {0.08})
Glastic, .030	7.81 {0.2}	(166.7 {10.0})
**Optiflex, .020	0.98 {0.15}	(6.7 {1.0})

*Apparent property only, material property not found because strand configuration was not accounted for.

**Optiflex tensile data is unreliable because the fiber glass core was pulled out of the matrix do to tensile stresses prior to failure.

TABLE V
The Tensile Yield Strength at the 0.2% Offset, YS
Uniaxial Tensile Test

Wire Product Name, Size " " , inch	The Tensile Yield Strength at the 0.2% Offset, YS	
	$x10^6$ psi {std. dev.}	($x10^9$ N/m^2) {std. dev.}
Metal Wires		
Tru-Chrome, Overall Average	272 {27}	(187 {18.9})
Tru-Chrome, .020	300 {6}	(207 {4})
Tru-Chrome, .018	243 {7}	(168 {4.6})
Tru-Chrome, .016	249 {4}	(171 {2.9})
Tru-Chrome, .014	295 {6}	(203 {4.4})
A. J. Wilcox Aust. Reg., .018	256 {4}	(176 {2.4})
A. J. Wilcox Aust. Spec+ .018	331 {18}	(228 {12.1})
Blue Elgiloy, .018	157 {5}	(108 {3.2})
Red Elgiloy, .018	225 {29}	(155 {20})
TMA, .018	15 {3}	(103 {2.2})
*Respond, .0175	46 {5}	(32 {3.4})
*Triple-Flex, .0195	155 {9}	(106 {6.2})
NiTi, .018	57 {2}	(40 {1.1})
Titanal, .018	70 {4}	(49 {2.7})
Titanal XR, .018	55 {2}	(38 {1.1})
Sentalloy Light, .018	39 {0.4}	(27 {3})
Sentalloy Medium, .018	43 {8}	(30 {5.7})
Sentalloy Heavy, .018	59 {14}	(40 {9.3})
Neo-Sentalloy, .018 x .025	35 {0.3}	(24 {0.2})
Esthetic Wires		
MX-501 PEEK, .0236	13 {0.3}	(9 {0.2})
**WP-320 PET, .0157	81 {1}	(56 {0.8})
WOX-3 PEEK, .0157	17 {0.8}	(12 {0.5})
WP-89 PET, .0138	86 {7}	(59 {4.5})
**WN-101 Nylon 6/6, .014	18 {1}	(13 {1})
***Glastic, .030	* * *	* * *
^Optiflex, .020	^	^

*Apparent property only, material property not found because strand configuration was not accounted for.

**These stress-train curves were actually concave so the offset was taken at the -0.2% offset in order to get an intersection.

***Glastic fiber glass composite failed before the 0.2% occured by progressive splintering of the glass fibers.

^Optiflex fiber glass composite had its fiber glass core pulled through the matrix before the 0.2% offset occured.

TABLE VI
The Tensile Strain at the 0.2% Offset
Uniaxial Tensile Test

Wire Product Name, Size " " , inch	The Tensile Strain at the 0.2% Offset ln(in/in) or ln(mm/mm) {std. dev.}
Metal Wires	
Tru-Chrome, Overall Average	0.0135 {0.0012}
Tru-Chrome, .020	0.0146 {0.00006}
Tru-Chrome, .018	0.012 {0.0004}
Tru-Chrome, .016	0.0132 {0.00003}
Tru-Chrome, .014	0.0142 {0.0009}
A. J. Wilcox Aust. Reg., .018	0.0119 {0.0006}
A. J. Wilcox Aust. Spec+ .018	0.0147 {0.0013}
Blue Elgiloy, .018	0.008 {0.00009}
Red Elgiloy, .018	0.0112 {0.0024}
TMA, .018	0.0147 {0.0007}
*Respond, .0175	0.0143 {0.0022}
*Triple-Flex, .0195	0.0168 {0.0015}
NiTi, .018	0.008 {0.0007}
Titanal, .018	0.0164 {0.0022}
Titanal XR, .018	0.0149 {0.0012}
Sentalloy Light, .018	0.0116 {0.0013}
Sentalloy Medium, .018	0.0095 {0.0021}
Sentalloy Heavy, .018	0.0123 {0.0015}
Neo-Sentalloy, .018 x .025	0.0083 {0.00021}
Esthetic Wires	
MX-501 PEEK, .0236	0.0193 {0.0006}
**WP-320 PET, .0157	0.0836 {0.0122}
WOX-3 PEEK, .0157	0.0267 {0.0033}
WP-89 PET, .0138	0.0759 {0.0101}
**WN-101 Nylon 6/6, .014	0.0691 {0.0043}
***Glastic, .030	*** ***
^Optiflex, .020	^ ^

*Apparent property only, material property not found because strand configuration was not accounted for.

**These stress-train curves were actually concave so the offset was taken at the -0.2% offset in order to get an intersection.

***Glastic fiber glass composite failed before the 0.2% occured by progressive splintering of the glass fibers.

^Optiflex fiber glass composite had its fiber glass core pulled through the matrix before the 0.2% offset occured.

TABLE VII
The Flexural Modulus of Elasticity, E_f
Three-Point-Bend Test, 0.5" Span Length

Wire Product Name, Size " " , inch	The Flexural Modulus of Elasticity, E_f	
	$x10^6$ psi {std. dev.}	($x10^9$ N/m^2) {std. dev.}
Metal Wires		
Tru-Chrome, Overall Average	28.1 {0.7}	(193.6 {4.6})
Tru-Chrome, .020	27.5 {0.5}	(189.6 {3.6})
Tru-Chrome, .018	27.6 {0.3}	(190.3 {2.3})
Tru-Chrome, .016	28.4 {0.4}	(195.6 {2.8})
Tru-Chrome, .014	28.9 {0.07}	(199.1 {0.5})
A. J. Wilcox Aust. Reg., .018	28.4 {0.3}	(195.6 {2.4})
A. J. Wilcox Aust. Spec+ .018	29.2 {0.1}	(201.0 {0.8})
Blue Elgiloy, .018	29.6 {0.7}	(203.8 {4.6})
Red Elgiloy, .018	28.6 {0.4}	(196.7 {2.7})
TMA, .018	12.9 {0.4}	(89.1 {2.6})
*Respond, .0175	1.64 {0.02}	(11.3 {0.11})
*Triple-Flex, .0195	3.59 {0.07}	(24.8 {0.48})
NiTi, .018	10.1 {0.11}	(69.8 {0.78})
Titanal, .018	6.78 {0.56}	(46.7 {3.8})
Titanal XR, .018	5.65 {0.32}	(38.9 {2.2})
**Sentalloy Light, .018	8.37 {0.23}	(57.7 {1.6})
**Sentalloy Medium, .018	9.28 {0.31}	(64.0 {2.2})
**Sentalloy Heavy, .018	8.87 {0.1}	(61.1 {0.65})
**Neo-Sentalloy, .018 x .025	8.23 {0.09}	(56.7 {0.61})
Esthetic Wires		
MX-501 PEEK, .0236	0.97 {0.03}	(6.68 {0.22})
WP-320 PET, .0157	2.24 {0.02}	(15.4 {0.16})
WOX-3 PEEK, .0157	1.05 {0.11}	(7.26 {0.74})
WP-89 PET, .0138	2.43 {0.04}	(16.7 {0.26})
WN-101 Nylon 6/6, .014	0.56 {0.009}	(3.84 {0.06})
***Glastic, .030	7.32 {0.37}	(50.4 {2.5})
Optiflex, .020	0.36 {0.004}	(2.46 {0.3})

*Apparent property only, material property not found because strand configuration was not accounted for.
**See corresponding Figures, and the Results, and Discussion sections as to why values may appear to be elevated.
***Glastic fiber glass composite tested at 1" span length instead of 0.5".

TABLE VIII
The Flexural Yield Strength at the 0.2% Offset, FYS*
Three-Point-Bend Test, 0.5" Span Length

Wire Product Name, Size " " , inch	The Flexural Yield Strength at the 0.2% Offset, FYS*	
	$x10^6$ psi {std. dev.}	($x10^9$ N/m^2) {std. dev.}
Metal Wires		
Tru-Chrome, Overall Average	395 {49.3}	(272 {33.9})
Tru-Chrome, .020	454 {14.2}	(313 {9.8}
Tru-Chrome, .018	363 {6.3}	(250 {4.3})
Tru-Chrome, .016	338 {8}	(233 {5.5})
Tru-Chrome, .014	426 {8.7}	(293 {6})
A. J. Wilcox Aust. Reg., .018	416 {2.5}	(287 {1.7})
A. J. Wilcox Aust. Spec+ .018	452 {20.8}	(312 {14.3})
Blue Elgiloy, .018	262 {1.2}	(180 {0.8})
Red Elgiloy, .018	362 {6.2}	(249 {4.3})
TMA, .018	243 {16.6}	(168 {11.4})
**Respond, .0175	37 {2.5}	(25 {1.7})
**Triple-Flex, .0195	84 {7}	(58 {4.8})
NiTi, .018	97 {2.1}	(67 {1.4})
Titanal, .018	137 {15.6}	(94 {10.8})
Titanal XR, .018	108 {2.2}	(74 {1.5})
***Sentalloy Light, .018	24 {1.7}	(17 {1.2 })
***Sentalloy Medium, .018	68 {7}	(47 {4.8})
***Sentalloy Heavy, .018	105 {2.8}	(73 {1.9})
***Neo-Sentalloy, .018 x .025	33 {0.9}	(23 {0.6})
Esthetic Wires		
MX-501 PEEK, .0236	17 {0.8}	(12 {0.6})
WP-320 PET, .0157	22 {0.3}	(15 {0.2})
WOX-3 PEEK, .0157	15 {0.9}	(10 {0.6})
WP-89 PET, .0138	23 {1}	(16 {0.7})
WN-101 Nylon 6/6, .014	6 {0.2}	(4.1 {0.1})
^Glastic, .030	15 {13}	(107 {8.9})
Optiflex, .020	9 {0.5}	(6 {0.3})

*Approximated from the equations defining the flexural modulus of elasticity, see Methods section.
**Apparent property only, material property not found because strand configuration was not accounted for.
***Values may appear to be underestimated due to unusual curve shape, see corresponding Figures, and the Results and Discussion sections.
^Glastic fiber glass composite was tested at 1" span length instead of .5".

TABLE IX
The Flexural Strain at the 0.2% Offset*
Three-Point-Bend Test, 0.5" Span Length

Wire Product Name, Size " " , inch	The Flexural Strain at the 0.2% Offset* (in/in) or (mm/mm) {std. dev.}
Metal Wires	
Tru-Chrome, Overall Average	0.0164 {0.0018}
Tru-Chrome, .020	0.0188 {0.0003}
Tru-Chrome, .018	0.0156 {0.00008}
Tru-Chrome, .016	0.0142 {0.0003}
Tru-Chrome, .014	0.0171 {0.0002}
A. J. Wilcox Aust. Reg., .018	0.0172 {0.00006}
A. J. Wilcox Aust. Spec+ .018	0.0175 {0.0008}
Blue Elgiloy, .018	0.0109 {0.0002}
Red Elgiloy, .018	0.0151 {0.0004}
TMA, .018	0.0211 {0.0016}
**Respond, .0175	0.0249 {0.0017}
**Triple-Flex, .0195	0.0245 {0.0008}
NiTi, .018	0.0119 {0.0003}
Titanal, .018	0.0226 {0.0009}
Titanal XR, .018	0.0218 {0.0012}
**Sentalloy Light, .018	0.0049 {0.0004}
**Sentalloy Medium, .018	0.0093 {0.0004}
**Sentalloy Heavy, .018	0.0143 {0.0004}
**Neo-Sentalloy, .018 x .025	0.0061 {0.0001}
Esthetic Wires	
MX-501 PEEK, .0236	0.0199 {0.0007}
WP-320 PET, .0157	0.0116 {0.0001}
WOX-3 PEEK, .0157	0.0160 {0.0014}
WP-89 PET, .0138	0.0116 {0.0006}
WN-101 Nylon 6/6, .014	0.0125 {0.0006}
^Glastic, .030	0.0235 {0.0023}
Optiflex, .020	0.0268 {0.0013}

*Approximated from the equations defining the flexural modulus of elasticity, see Methods section.
**Apparent property only, material property not found because strand configuration was not accounted for.
***Values may appear to be underestimated due to unusual curve shape, see corresponding Figures, and the Results and Discussion sections.
^Glastic fiber glass composite was tested at 1" span length instead of .5".

TABLE X

The Load Corresponding to the Flexural Yield Strength at the 0.2% Offset, FYS* Three-Point-Bend Test, 0.5" Span Length

Wire Product Name, Size " " , inch	The Load Corresponding to the Flexural Yield Strength at the 0.2% Offset, FYS*	
	Lbf {std. dev.}	N {std. dev.}
Metal Wires		
Tru-Chrome, Overall Average	* *	* *
Tru-Chrome, .020	2.62 {0.7}	(11.63 {0.31})
Tru-Chrome, .018	1.52 {0.2}	(6.75 {0.11})
Tru-Chrome, .016	0.97 {0.02}	(4.32 {0.1})
Tru-Chrome, .014	0.82 {0.02}	(3.66 {0.07})
A. J. Wilcox Aust. Reg., .018	1.74 {0.02}	(7.75 {0.08})
A. J. Wilcox Aust. Spec+ .018	1.94 {0.09}	(8.61 {0.4})
Blue Elgiloy, .018	1.09 {0.01}	(4.85 {0.07})
Red Elgiloy, .018	1.55 {0.03}	(6.9 {0.12})
TMA, .018	1.01 {0.07}	(4.48 {0.33})
***Respond, .0175	0.15 {0.009}	(0.68 {0.04})
***Triple-Flex, .0195	0.49 {0.04}	(2.18 {0.2})
NiTi, .018	0.43 {0.009}	(1.93 {0.04})
Titanal, .018	0.57 {0.06}	(2.54 {0.26})
Titanal XR, .018	0.44 {0.02}	(1.95 {0.1})
^Sentalloy Light, .018	0.11 {0.007}	(0.48 {0.03})
^Sentalloy Medium, .018	0.31 {0.03}	(1.37 {0.13})
^Sentalloy Heavy, .018	0.48 {0.01}	(2.11 {0.06})
^Neo-Sentalloy, .018 x .025	0.35 {0.01}	(1.55 {0.04})
Esthetic Wires		
MX-501 PEEK, .0236	0.16 {0.001}	(0.7 {0.006})
WP-320 PET, .0157	0.067{0.0009}	(0.3 {0.004})
WOX-3 PEEK, .0157	0.046 {0.005}	(0.21 {0.02})
WP-89 PET, .0138	0.046 {0.002}	(0.2 {0.009})
WN-101 Nylon 6/6, .014	0.013{0.0004}	(0.06 {0.002})
^^Glastic, .030	1.65 {0.18}	(7.34 {0.81})
Optiflex, .020	0.048 {0.002}	(0.21 {0.01})

*Approximated from the equations defining the flexural modulus of elasticity, see Methods section.

**Not reported because load varies with diameter of wire.

***Apparent property only, material property not found because strand configuration was not accounted for.

^Values may appear to be underestimated due to unusual curve shape, see corresponding Figures, and the Results and Discussion sections.

^^Glastic fiber glass composite was tested at 1" span length instead of .5".

TABLE XI
The Deflection Corresponding to the Flexural Yield Strength
at the 0.2% Offset, FYS*
Three-Point-Bend Test, 0.5" Span Length

Wire Product Name, Size " " , inch	The Deflection Corresponding to the Flexural Yield Strength at the 0.2% Offset, FYS*			
Metal Wires	inch	{std. dev.}	mm	{std. dev.}
Tru-Chrome, Overall Average	* *		* *	
Tru-Chrome, .020	0.0404	{0.0007}	(1.03	{0.02})
Tru-Chrome, .018	0.0372	{0.0003}	(0.94	{0.007})
Tru-Chrome, .016	0.0384	{0.0009}	(0.98	{0.02})
Tru-Chrome, .014	0.0526	{0.0007}	(1.34	{0.02})
A. J. Wilcox Aust. Reg., .018	0.041	{0.001}	(1.04	{0.003})
A. J. Wilcox Aust. Spec+ .018	0.0413	{0.0019}	(1.05	{0.05})
Blue Elgiloy, .018	0.0261	{0.0005}	(0.66	{0.01})
Red Elgiloy, .018	0.0359	{0.001}	(0.91	{0.03})
TMA, .018	0.0506	{0.0036}	(1.28	{0.09})
***Respond, .0175	0.0595	{0.0042}	(1.51	{0.11})
***Triple-Flex, .0195	0.0526	{0.0019}	(1.34	{0.05})
NiTi, .018	0.0277	{0.0006}	(0.7	{0.02})
Titanal, .018	0.054	{0.0023}	(1.37	{0.06})
Titanal XR, .018	0.0524	{0.0024}	(1.33	{0.06})
^Sentalloy Light, .018	0.0115	{0.0008}	(0.29	{0.02})
^Sentalloy Medium, .018	0.0215	{0.0009}	(0.55	{0.02})
^Sentalloy Heavy, .018	0.0332	{0.001}	(0.84	{0.03})
^Neo-Sentalloy, .018 x .025	0.0103	{0.0002}	(0.26	{0.004})
Esthetic Wires				
MX-501 PEEK, .0236	0.0366	{0.0017}	(0.93	{0.04})
WP-320 PET, .0157	0.0306	{0.0003}	(0.78	{0.009})
WOX-3 PEEK, .0157	0.0419	{0.0023}	(1.06	{0.06})
WP-89 PET, .0138	0.0355	{0.0017}	(0.9	{0.04})
WN-101 Nylon 6/6, .014	0.0372	{0.0018}	(0.94	{0.05})
^^Glastic, .030	0.1305	{0.0115}	(3.31	{0.29})
Optiflex, .020	0.0581	{0.003}	(1.48	{0.08})

*Approximated from the equations defining the flexural modulus of elasticity, see Methods section.
**Not reported because deflection varies with diameter of wire.
***Apparent property only, material property not found because strand configuration was not accounted for.
^Values may appear to be underestimated due to unusual curve shape, see corresponding Figures, and the Results and Discussion sections.
^^Glastic fiber glass composite was tested at 1" span length instead of .5".

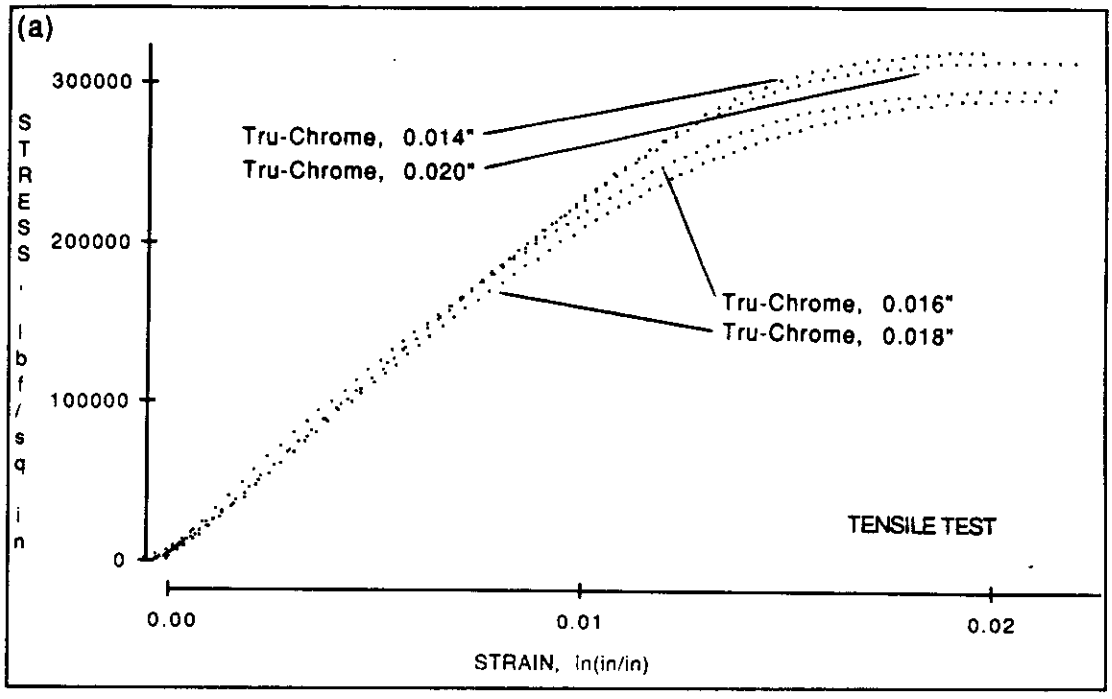
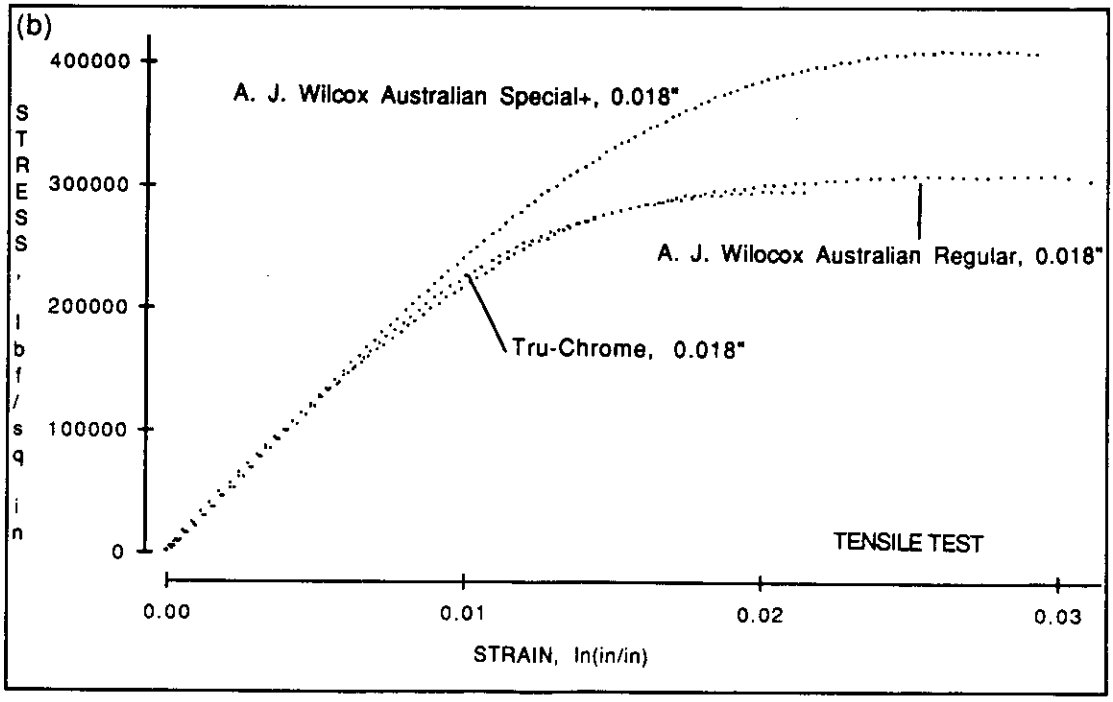


FIGURE 13
Comparison of Tensile Test Stress/Strain Diagrams -- (a) Tru-Chrome 0.020", Tru-Chrome 0.018", Tru-Chrome 0.016", and Tru-Chrome 0.014"; (b) Tru-Chrome 0.018", A. J. Wilcox Australian Regular 0.018", and A. J. Wilcox Australian Special+ 0.018"



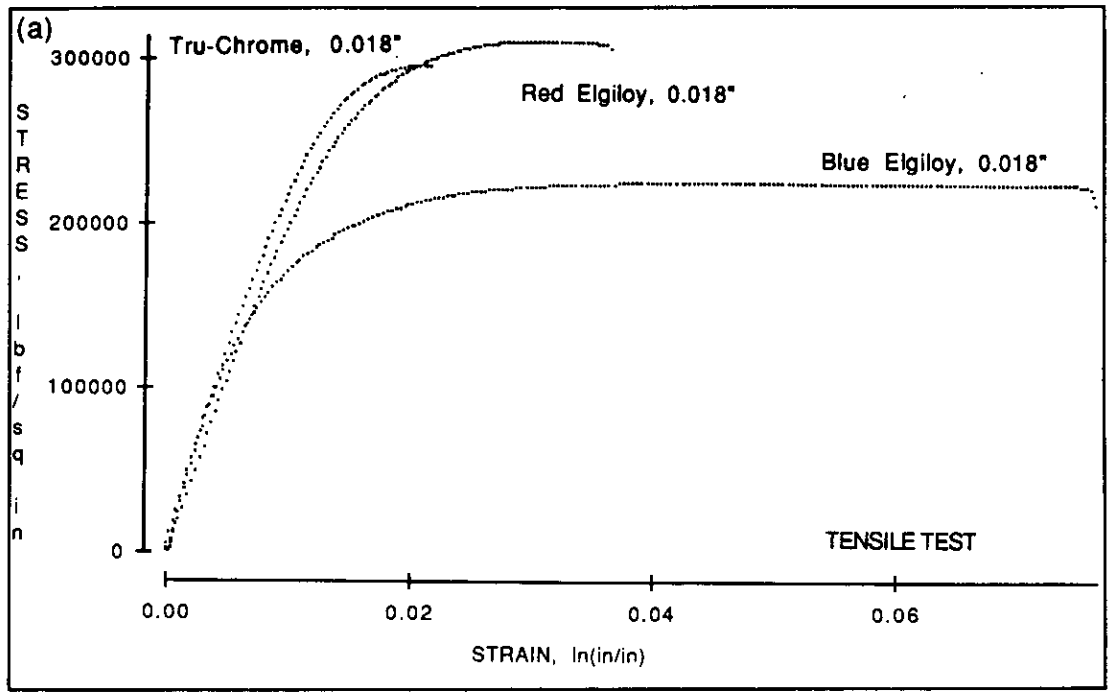
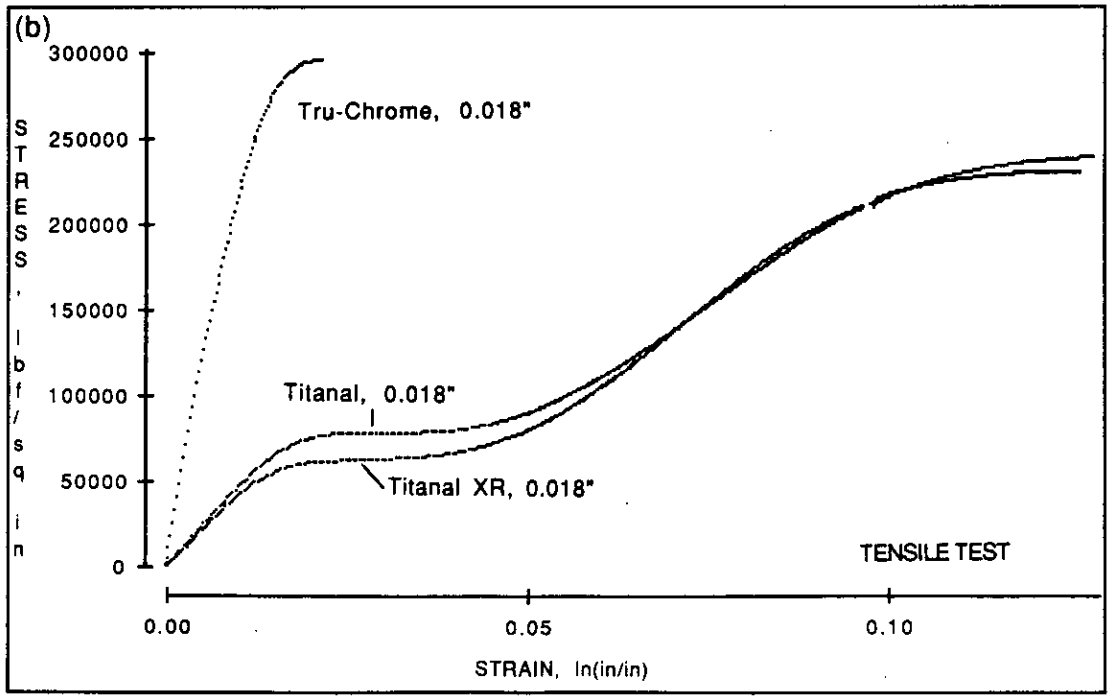


FIGURE 14
Comparison of Tensile Test Stress/Strain Diagrams -- (a) Tru-Chrome 0.018", Blue Elgiloy 0.018", and Red Elgiloy 0.018"; (b) Tru-Chrome 0.018", Titanal 0.018" and Titanal XR 0.018"



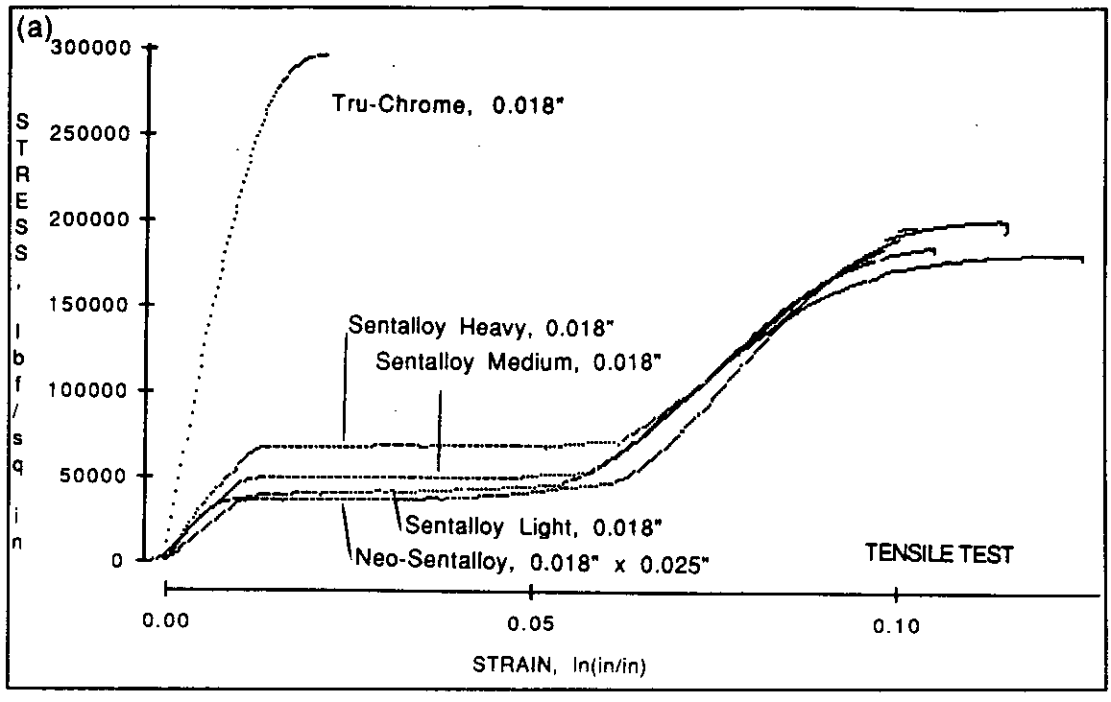
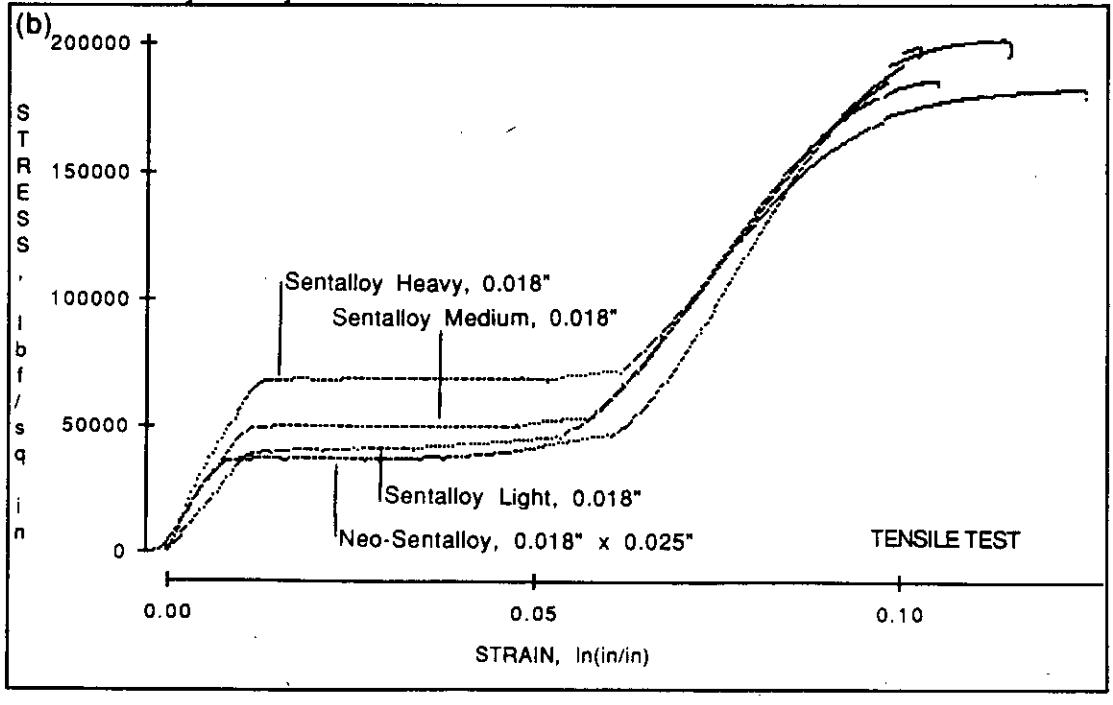


FIGURE 15

Comparison of Tensile Test Stress/Strain Diagrams -- (a) Tru-Chrome 0.018", Neo-Sentalloy 0.018" x 0.025", Sentalloy Light 0.018", Sentalloy Medium 0.018", and Sentalloy Heavy 0.018"; (b) Neo-Sentalloy 0.018" x 0.025", Sentalloy Light 0.018", Sentalloy Medium 0.018", and Sentalloy Heavy 0.018"



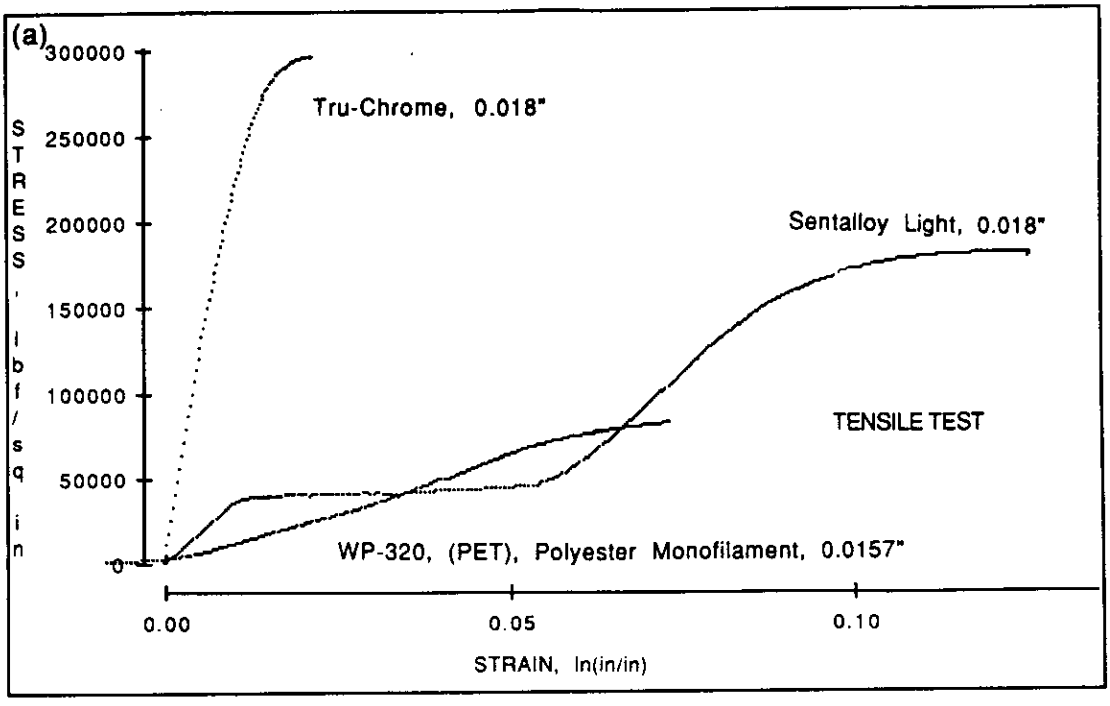
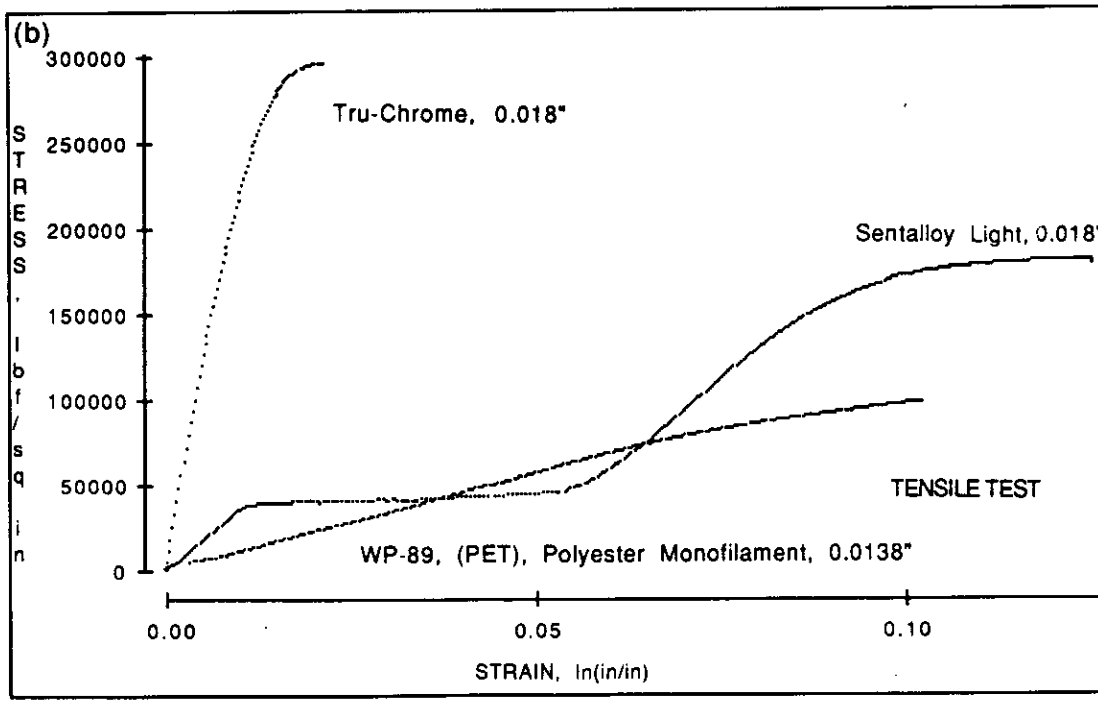


FIGURE 16
Comparison of Tensile Test Stress/Strain Diagrams -- (a) Tru-Chrome 0.018", WP-320 (PET) Polyester Monofilament 0.0157", and Sentalloy Light 0.018"; (b) Tru-Chrome 0.018", WP-89 (PET) Polyester Monofilament 0.0138", and Sentalloy Light 0.018"



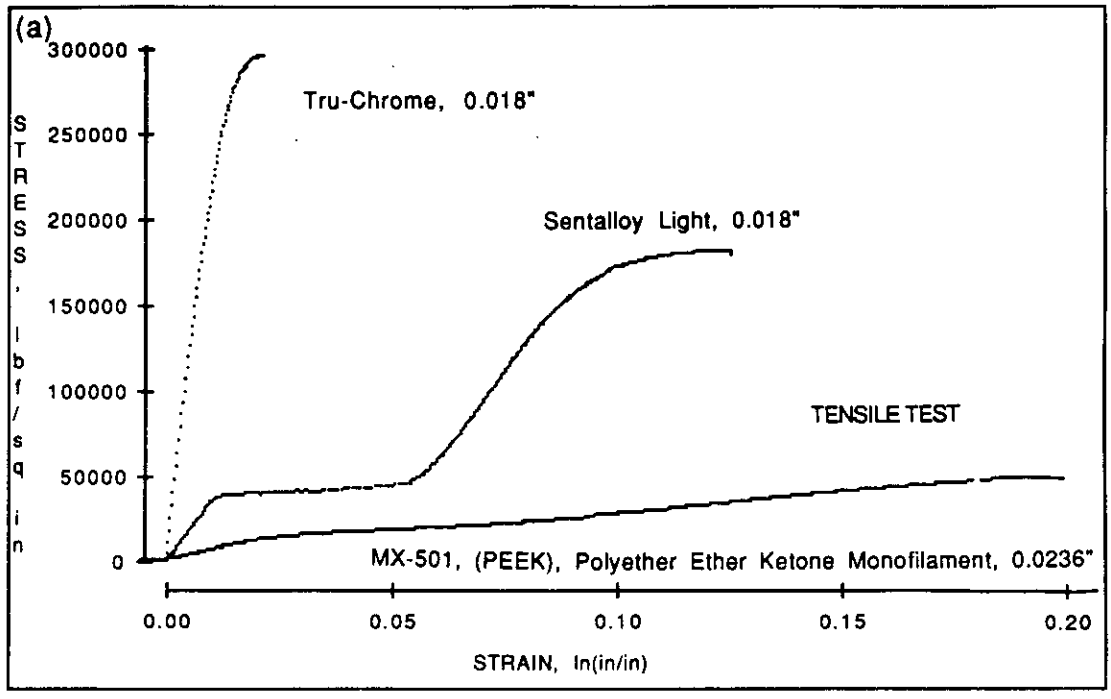
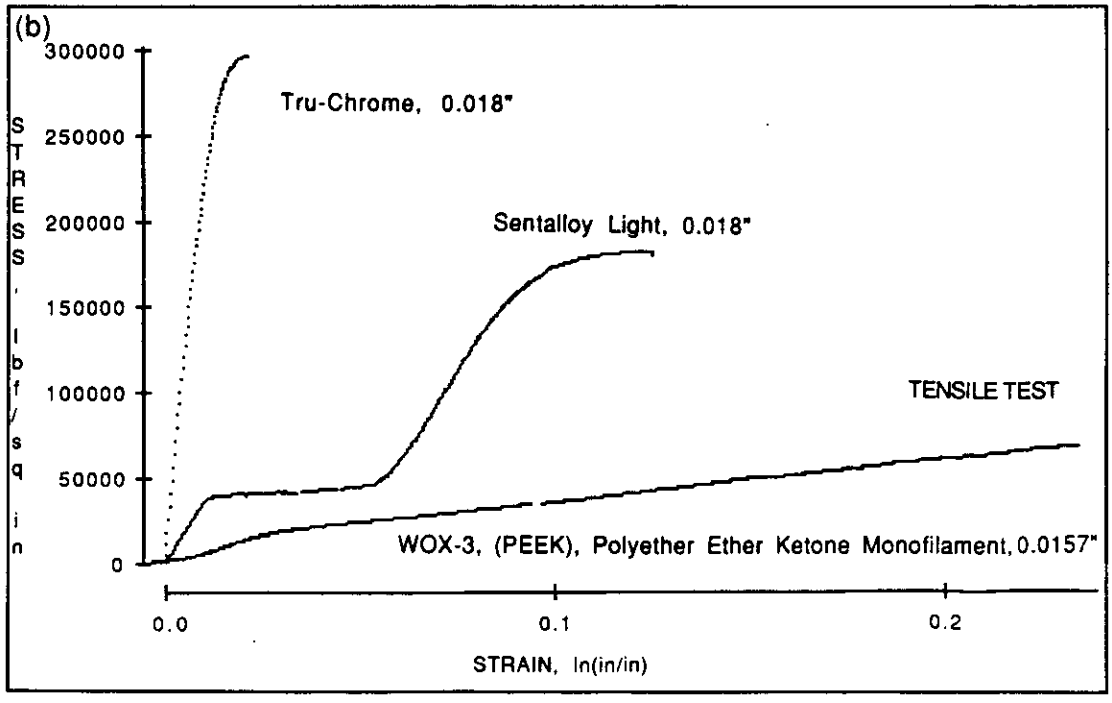


FIGURE 17
Comparison of Tensile Test Stress/Strain Diagrams -- (a) Tru-Chrome 0.018", MX-501 (PEEK) Monofilament 0.0236", and Sentalloy Light 0.018"; (b) Tru-Chrome 0.018", WOX-3 (PEEK) Monofilament 0.0157", and Sentalloy Light 0.018"



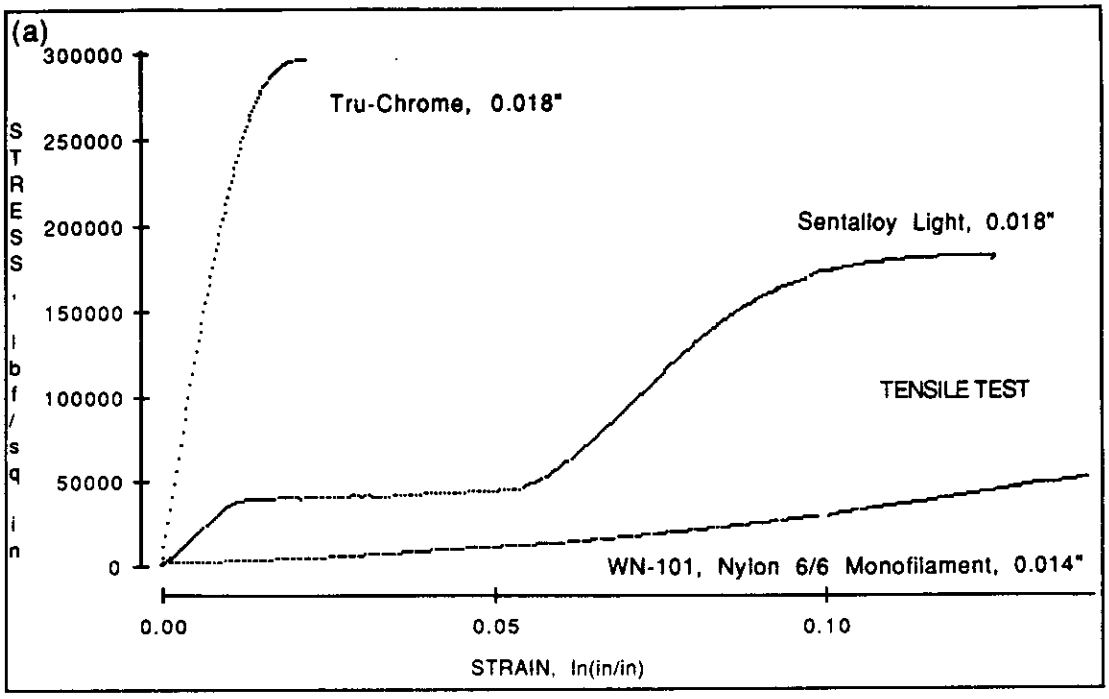
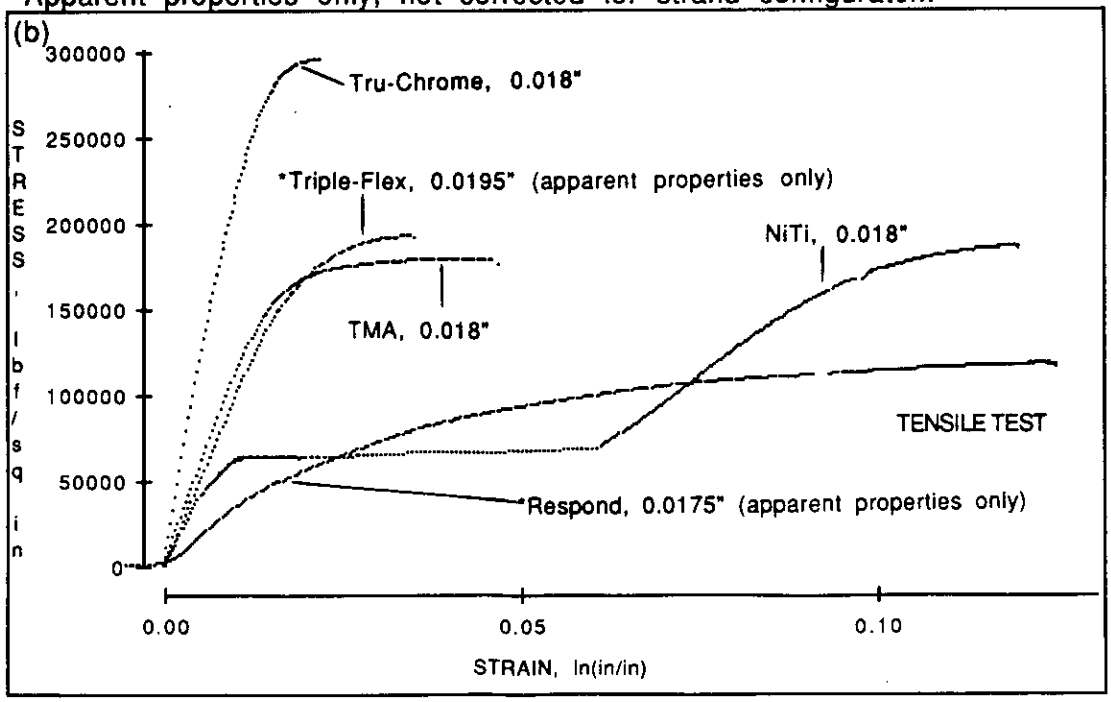


FIGURE 18

Comparison of Tensile Test Stress/Strain Diagrams -- (a) Tru-Chrome 0.018", WN-101 Nylon 6/6 Monofilament 0.014", and Sentalloy Light 0.018"; (b) Tru-Chrome 0.018", *Triple-Flex 0.0195", TMA 0.018", NiTi 0.018", and *Respond 0.0175"

*Apparent properties only, not corrected for strand configuraton.



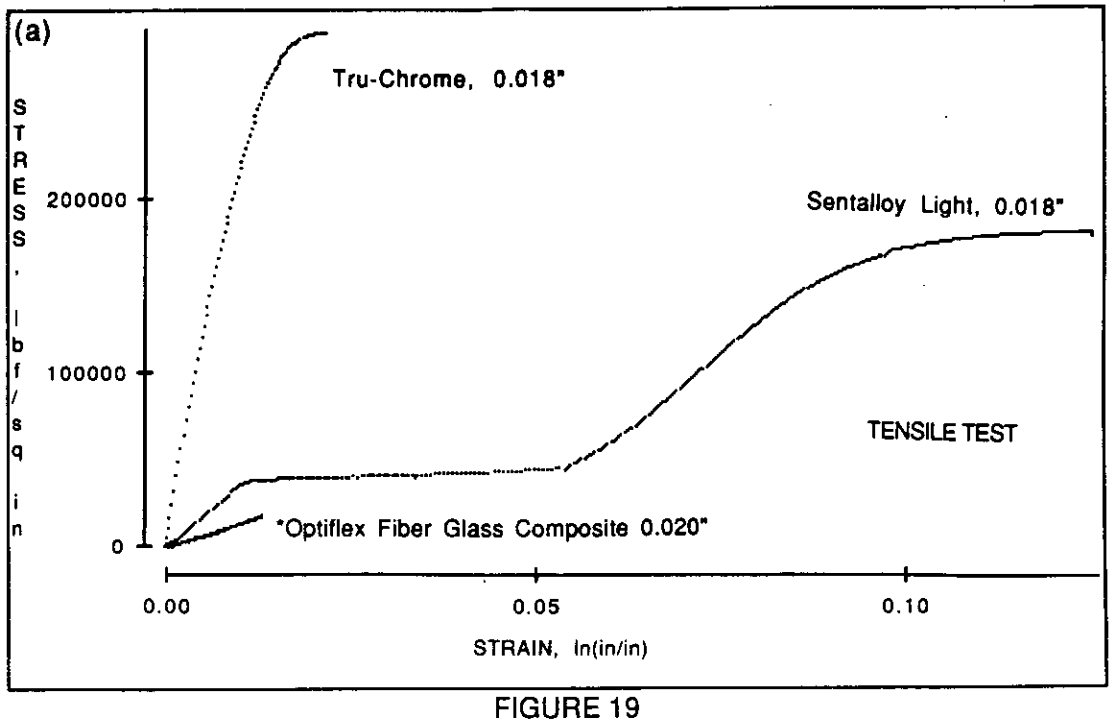


FIGURE 19

Comparison of Tensile Test Stress/Strain Diagrams -- (a) Tru-Chrome 0.018", *Optiflex Fiber Glass Composite 0.020", and Sentalloy Light 0.018"; and (b) Tru-Chrome 0.018", **Glastic Fiber Glass Composite 0.030", and Sentalloy Light 0.018"

*Otpiflex tensile data unreliable, Glass core pulls out of nylon matrix.

**Notice breakage of bunches of glass fibers (stepped appearence).

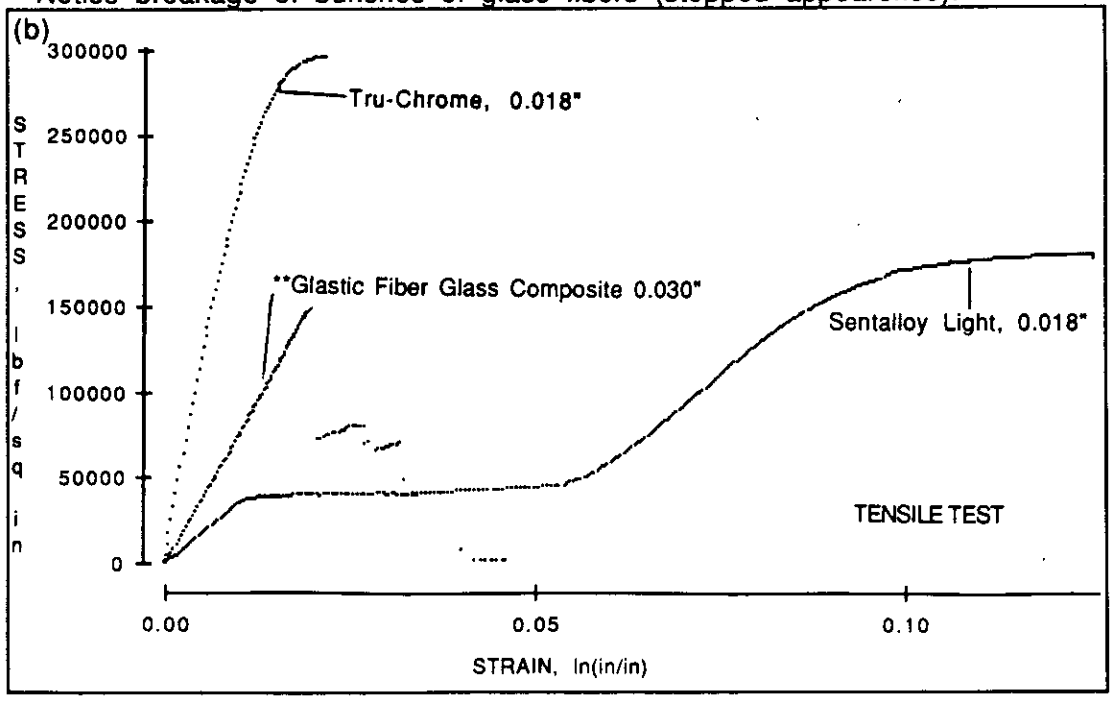
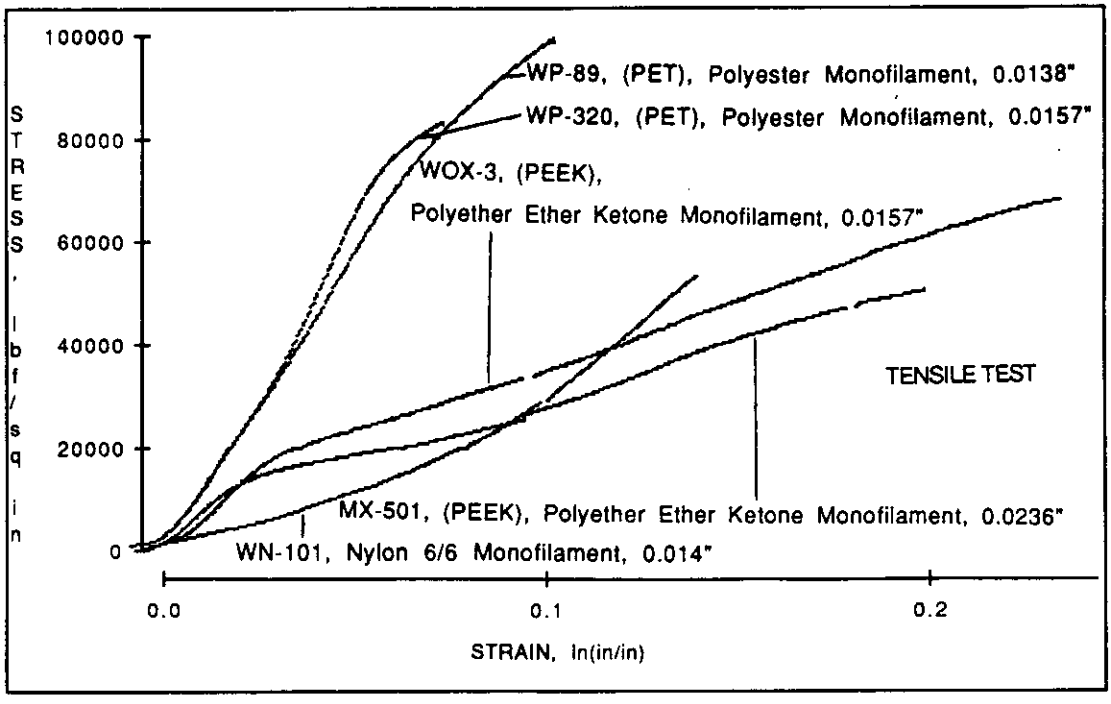


FIGURE 20

Comparison of Tensile Test Stress/Strain Diagrams -- WP-89 (PET) Polyester Monofilament 0.0138", WP-320 (PET) Polyester Monofilament 0.0157", WOX-3 (PEEK) Monofilament 0.0157", MX-501 (PEEK) Monofilament 0.0236", and WN-101 Nylon 6/6 Monofilament 0.014"



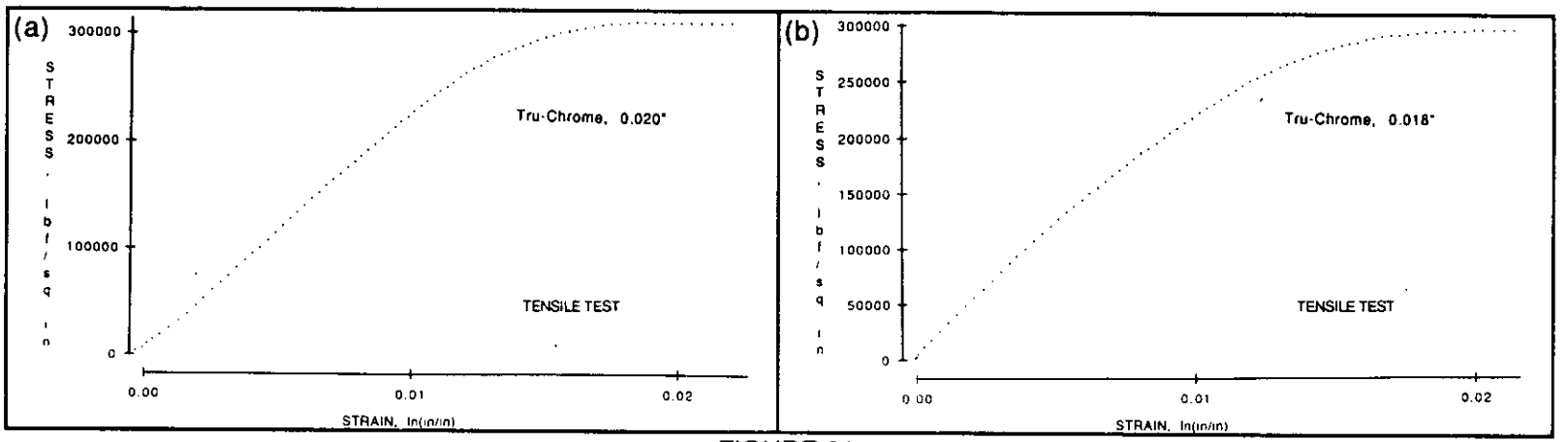
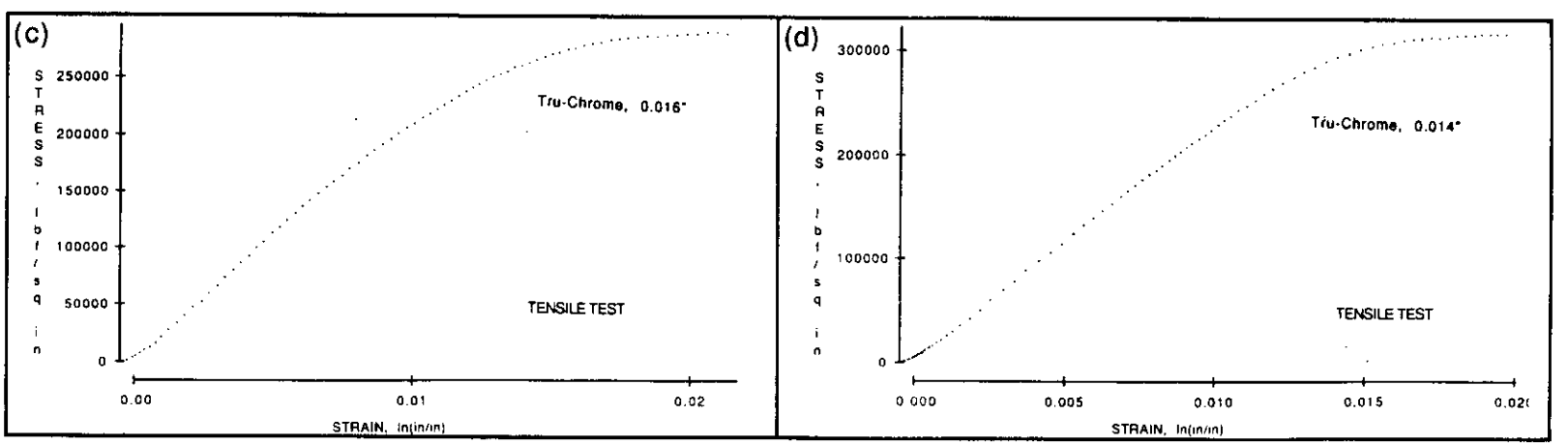


FIGURE 21

Tensile Test Stress/Strain Diagrams for Individual Materials -- (a) Tru-Chrome 0.020", (b) Tru-Chrome 0.018", (c) Tru-Chrome 0.016", and (d) Tru-Chrome 0.014"



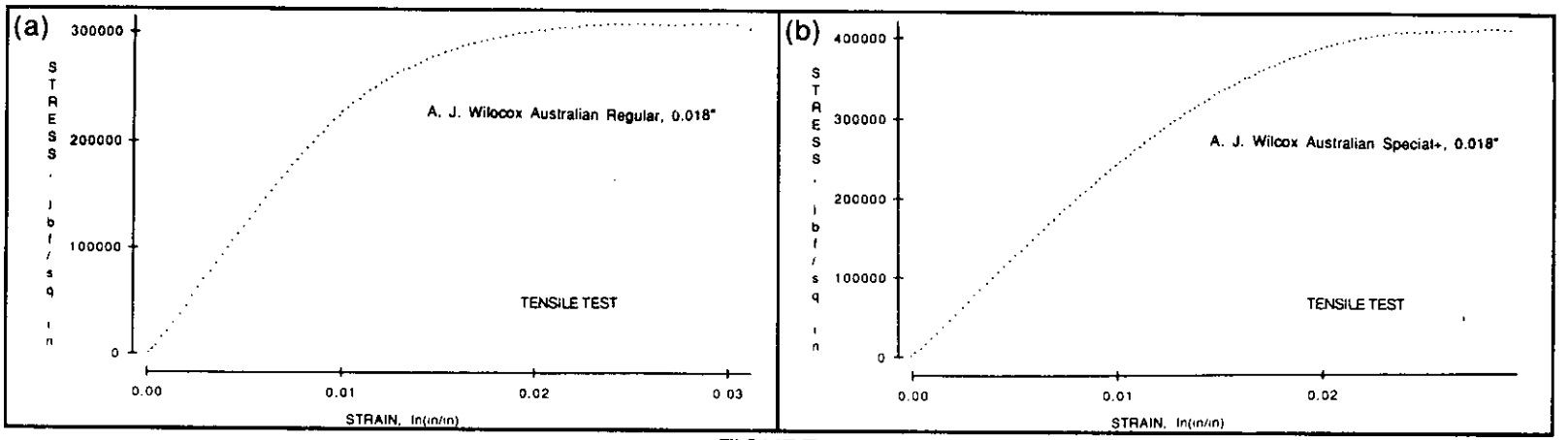
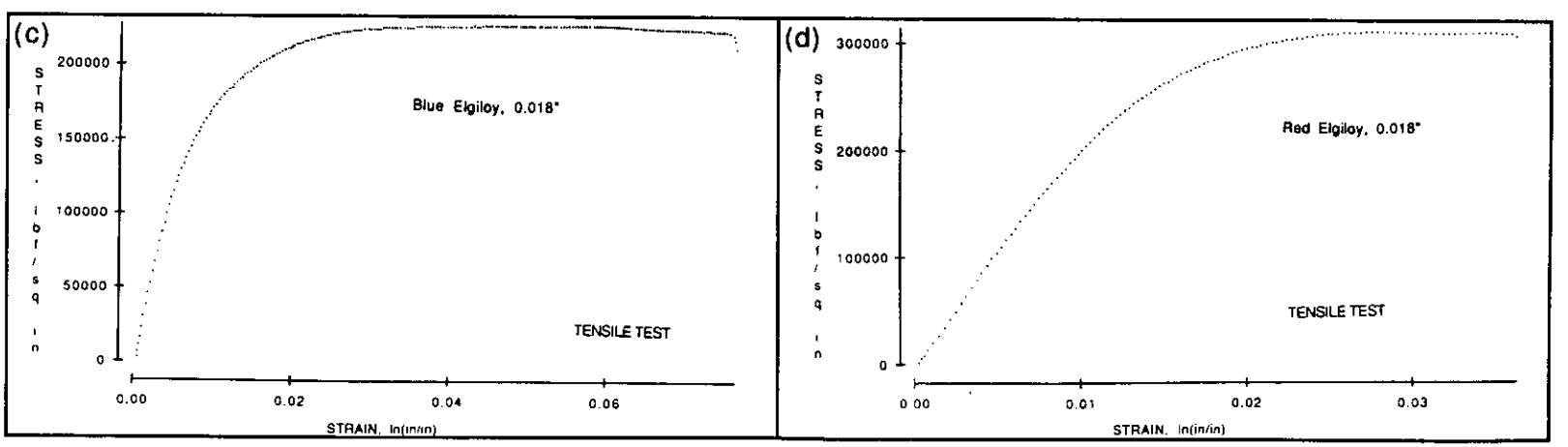


FIGURE 22

Tensile Test Stress/Strain Diagrams for Individual Materials -- (a) A. J. Wilcox Australian Regular 0.018", (b) A. J. Wilcox Australian Special+ 0.018", (c) Blue Elgiloy 0.018", and (d) Red Elgiloy 0.018"



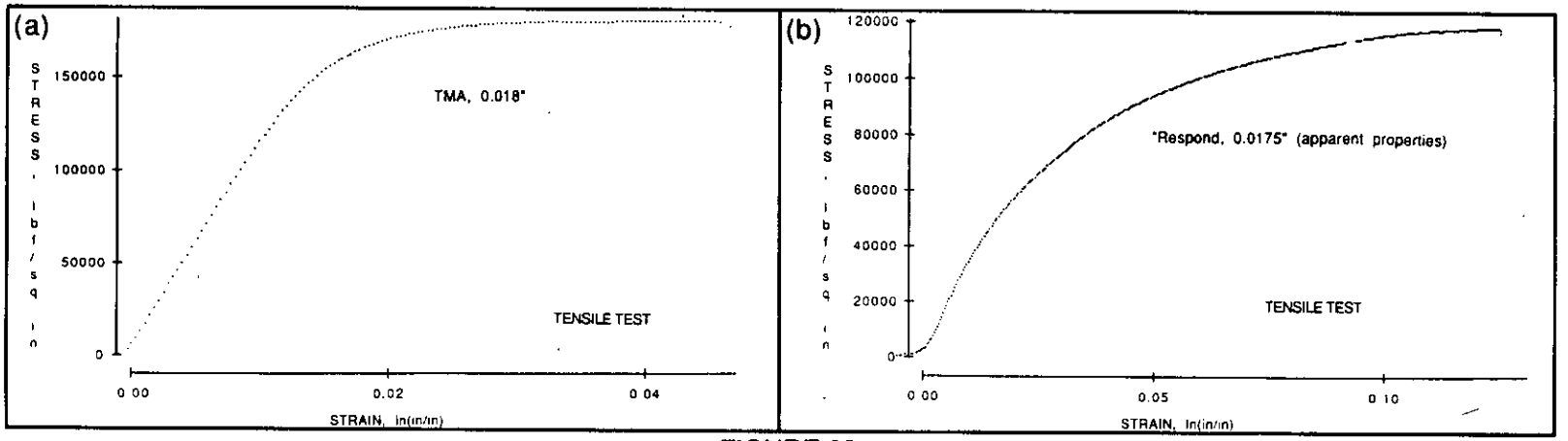
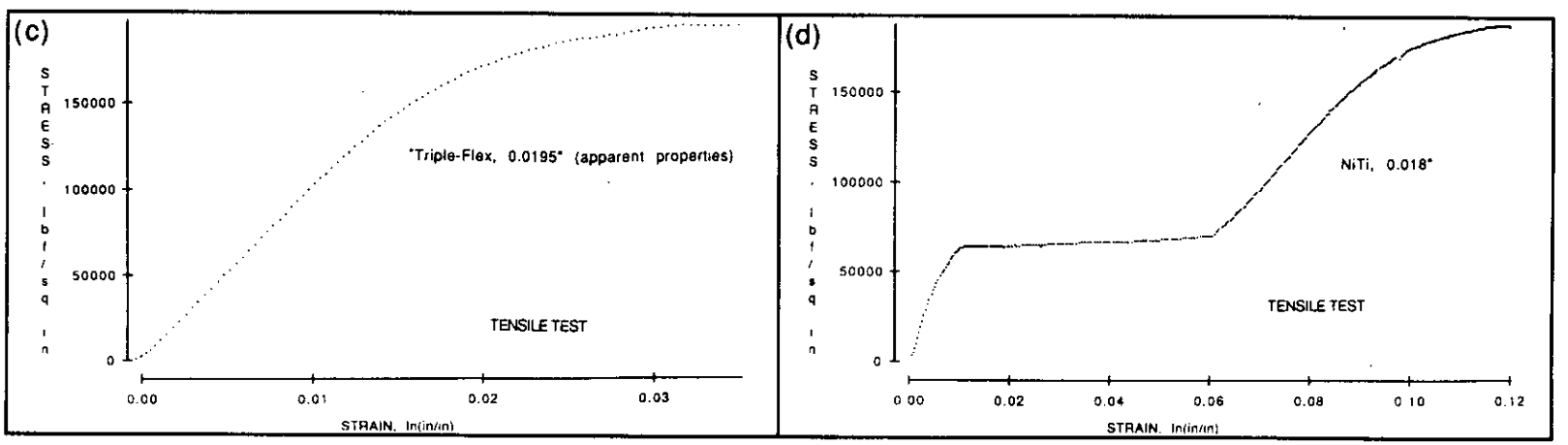


FIGURE 23

Tensile Test Stress/Strain Diagrams for Individual Materials -- (a) TMA 0.018", (b) *Respond 0.0175", (c) *Triple-flex 0.0195", and (d) NiTi 0.018"

*Apparent properties at overall diameter only, not corrected for strand configurations.



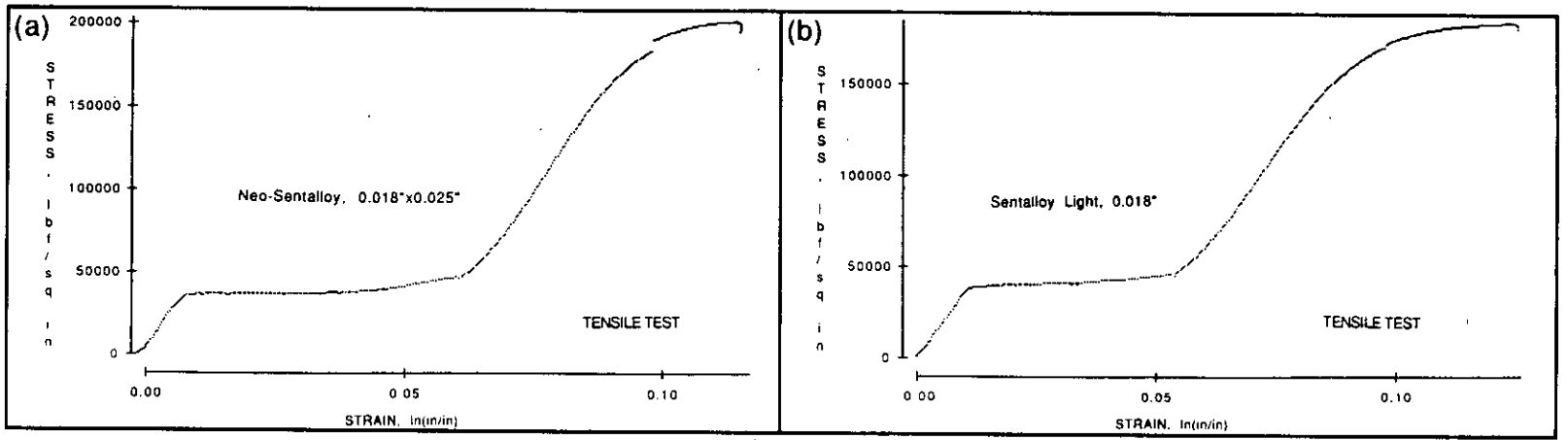
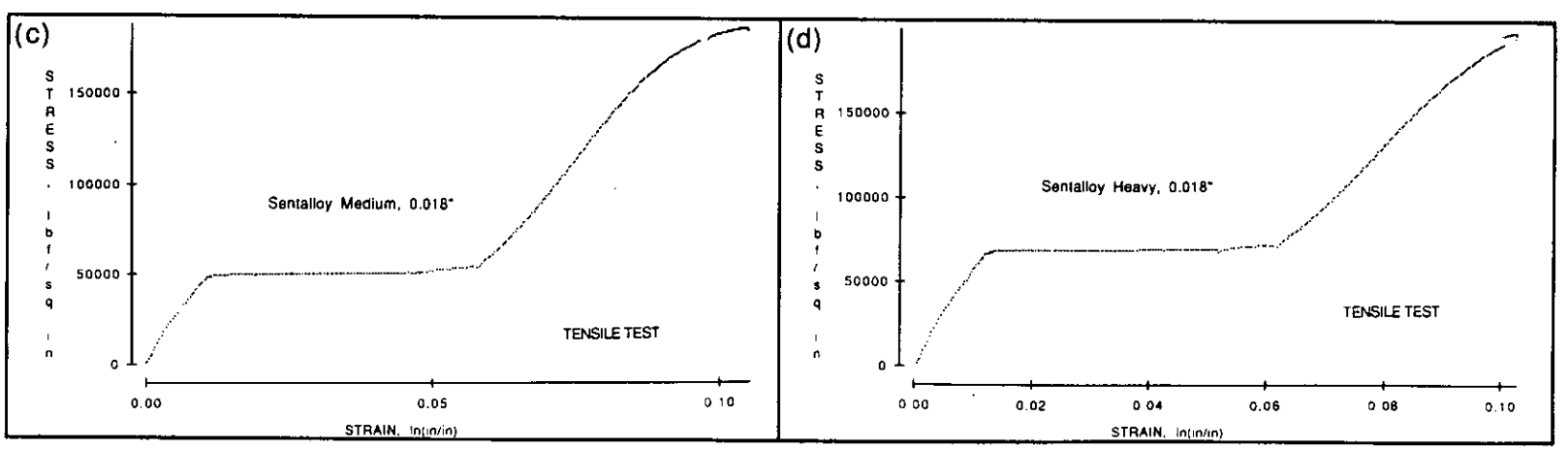


FIGURE 24

Tensile Test Stress/Strain Diagrams for Individual Materials -- (a) Neo-Sentalloy 0.018" x 0.025", (b) Sentalloy Light 0.018", (c) Sentalloy Medium 0.018", and (d) Sentalloy Heavy 0.018"



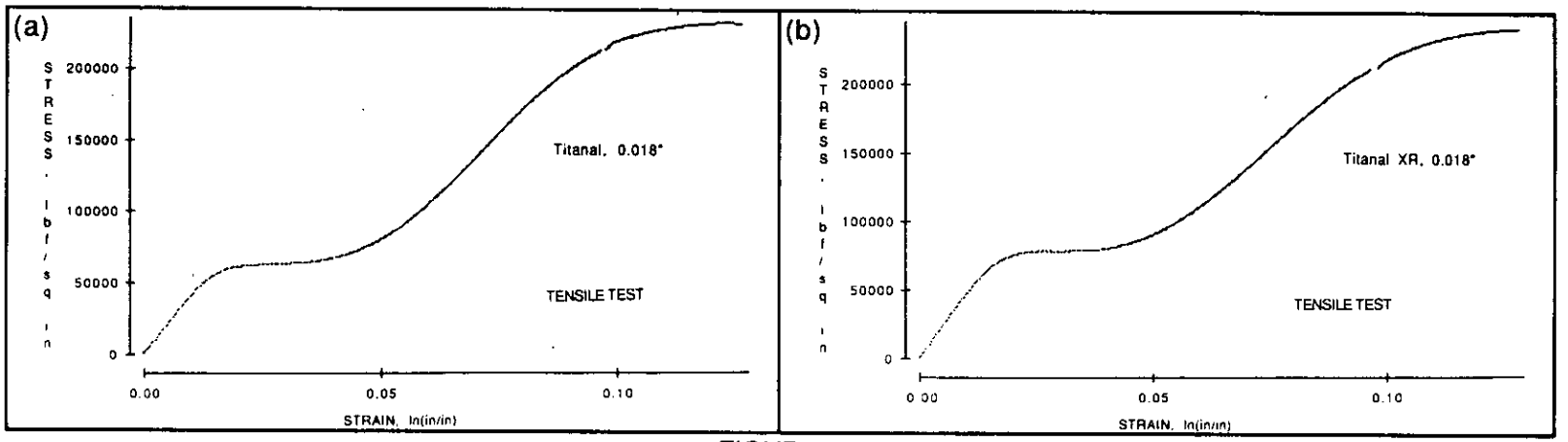
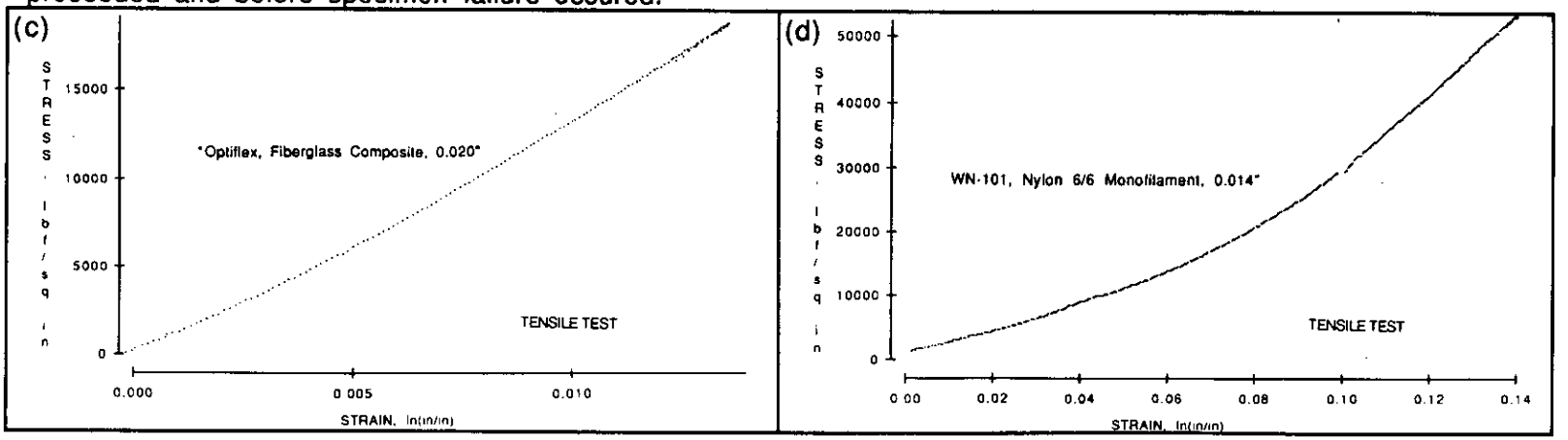


FIGURE 25

Tensile Test Stress/Strain Diagrams for Individual Materials -- (a) Titanal 0.018", (b) Titanal XR 0.018", (c) *Optiflex Fiber Glass Composite 0.020", and (d) WN-101 Nylon 6/6 Monofilament 0.014"

*Optiflex tensile data unreliable because fiber glass core was pulled through the nylon matrix (the matrix remaining between the tensile grips in a compressed state) while the specimen elongation proceeded and before specimen failure occured.



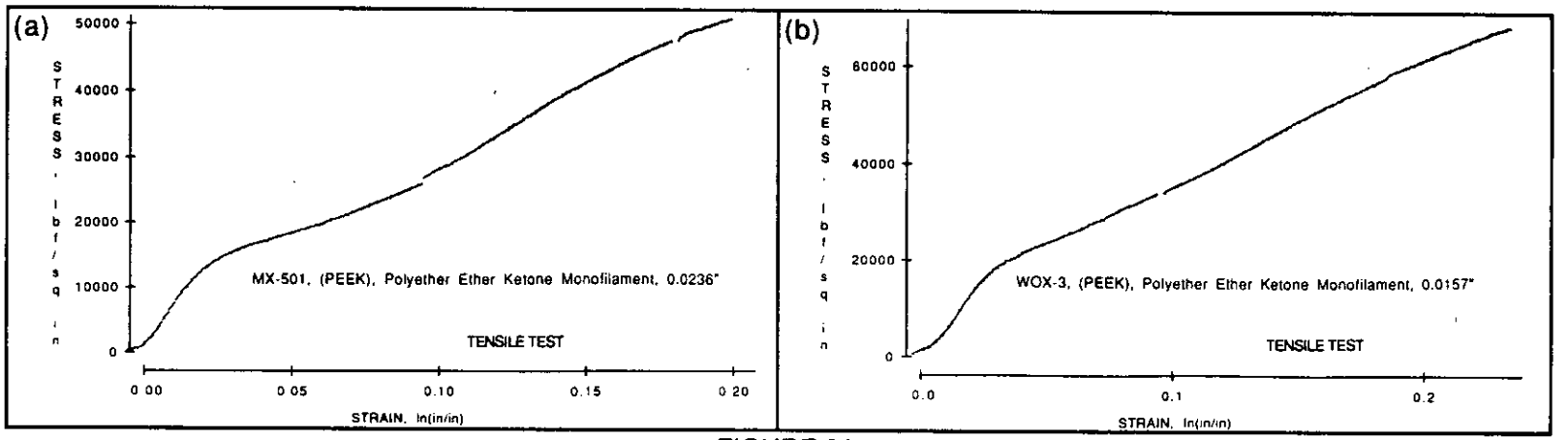
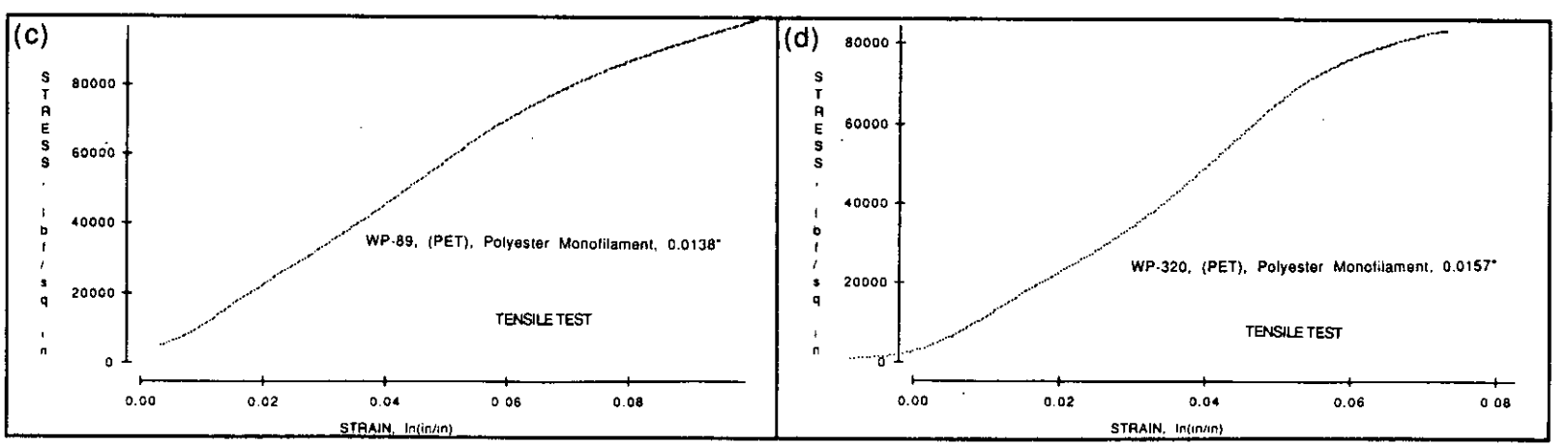


FIGURE 26

Tensile Test Stress/Strain Diagrams for Individual Materials -- (a) MX-501 (PEEK) Monofilament 0.0236", (b) WOX-3 (PEEK) Monofilament 0.0157", (c) WP-89 (PET) Polyester Monofilament 0.0138", and (d) WP-320 (PET) Polyester Monofilament 0.0157"



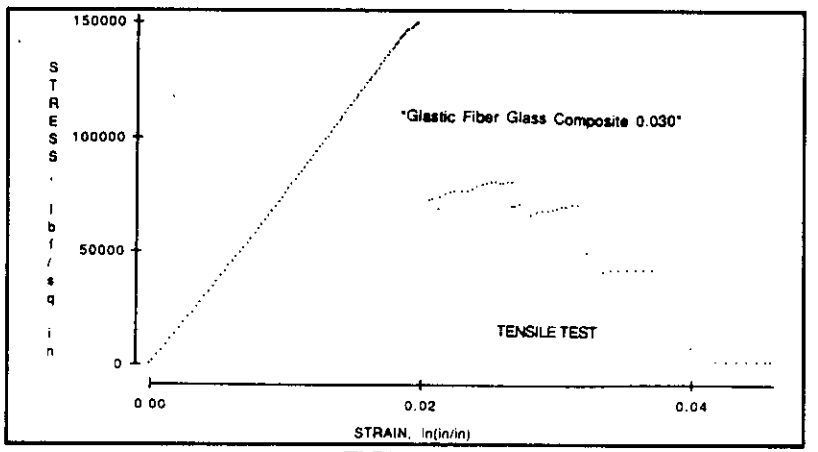


FIGURE 27

Tensile Test Stress/Strain Diagrams for Individual Materials -- *Glastic Fiber Glass Composite 0.030"

*Notice the progressive failure of bunches of fiber glass strands before total specimen failure, thus giving the plot a stepped appearence.

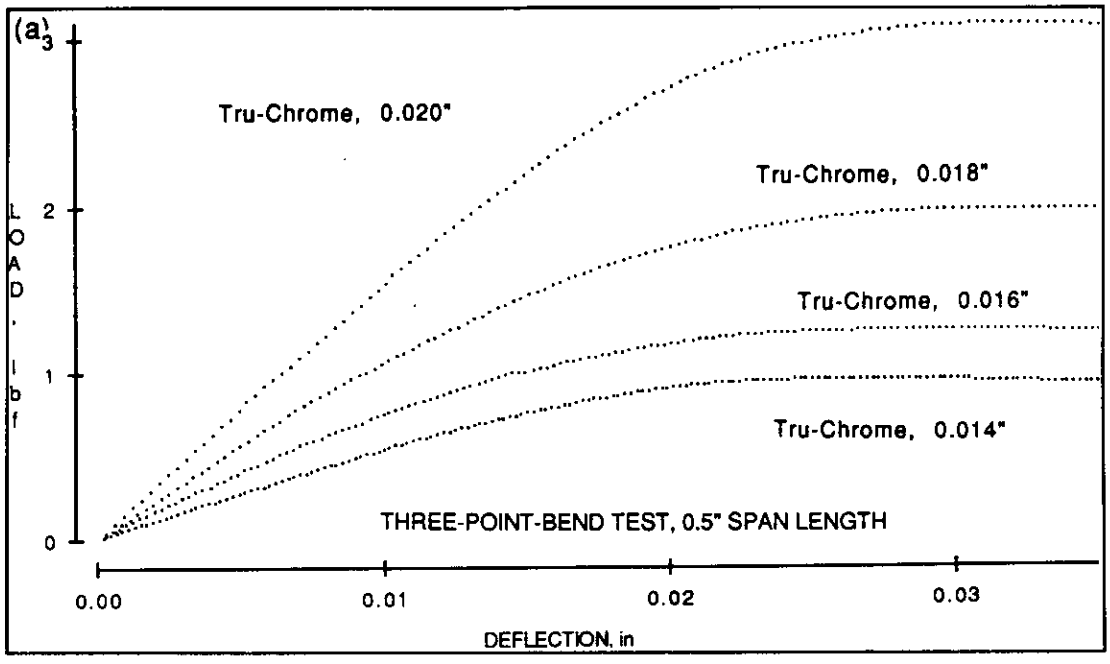
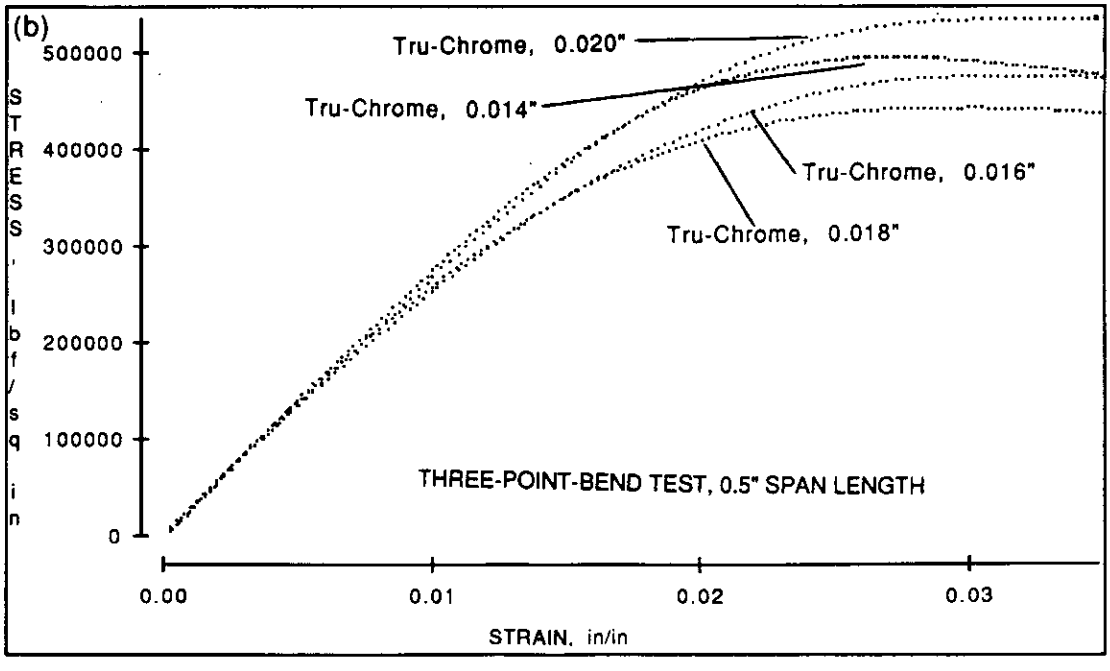


FIGURE 28

Comparison of the Three-Point-Bend Test Load/Deflection [L/D] and *Approximated Flexural Stress/Strain [S/S] Diagrams of Tru-Chrome 0.020", Tru-Chrome 0.018", Tru-Chrome 0.016", and Tru-Chrome 0.014" -- (a) [L/D] Diagrams and (b) *Approximated Flexural [S/S] Diagrams

*Approximated by the equation for the flexural modulus of elasticity.



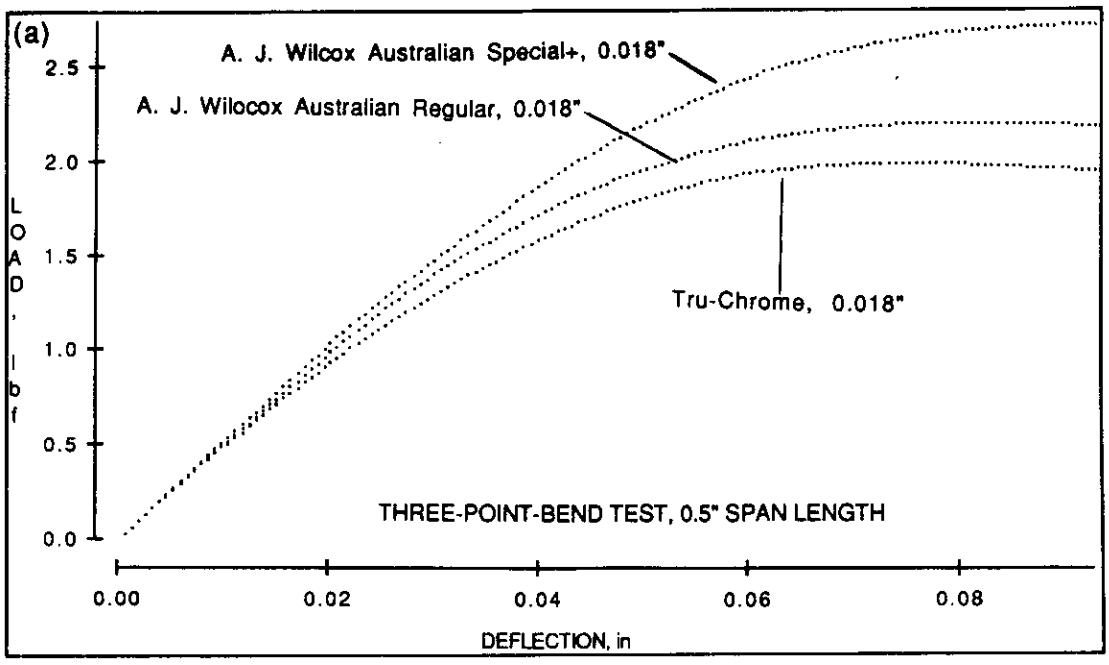
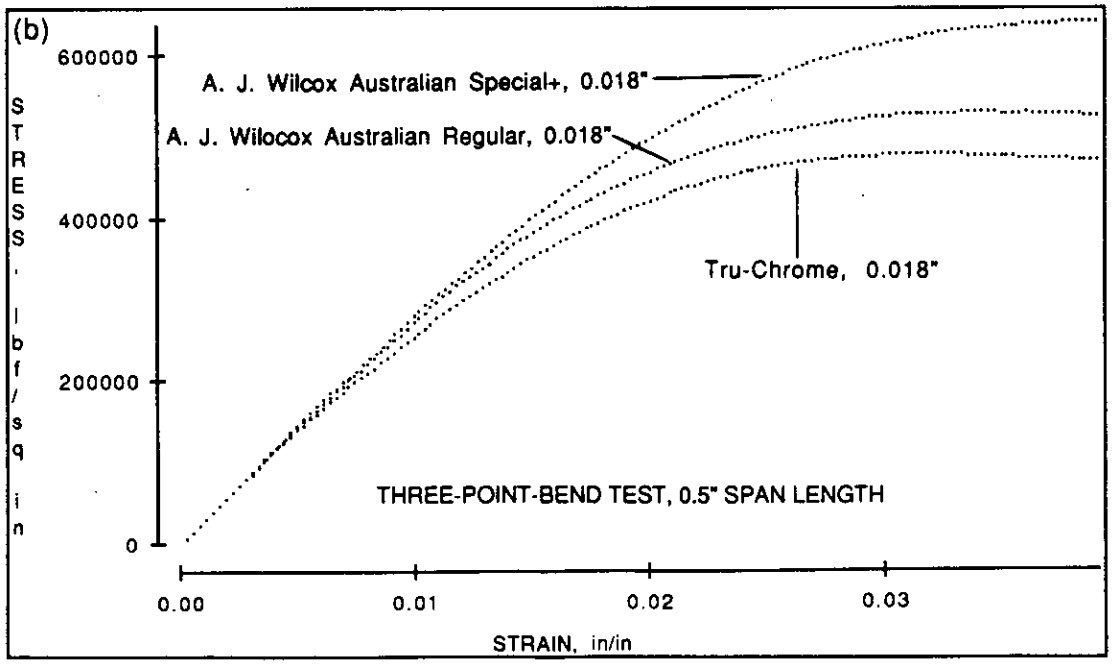


FIGURE 29
Comparison of the Three-Point-Bend Test Load/Deflection [L/D] and *Approximated Stress/Strain [S/S] Diagrams of Tru-Chrome 0.018", A. J. Wilcox Australian Regular 0.018", and A. J Wilcox Australian Special+ 0.018" -- (a) [L/D] Diagrams and (b) *Approximated [S/S] Diagrams

*Approximated by the equation for the flexural modulus of elasticity.



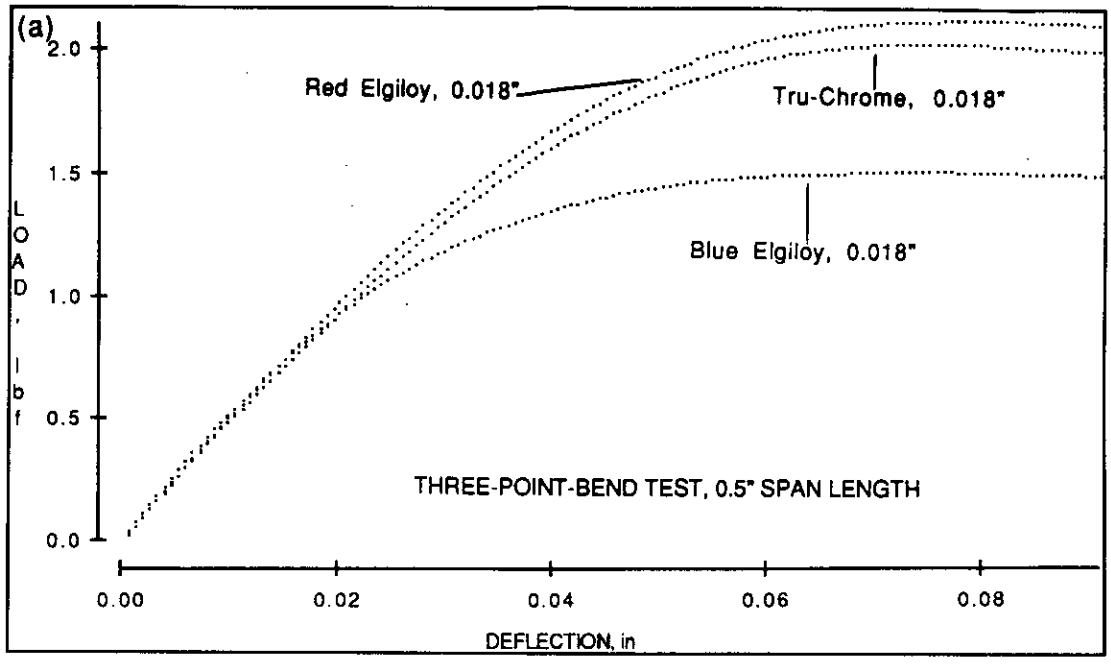
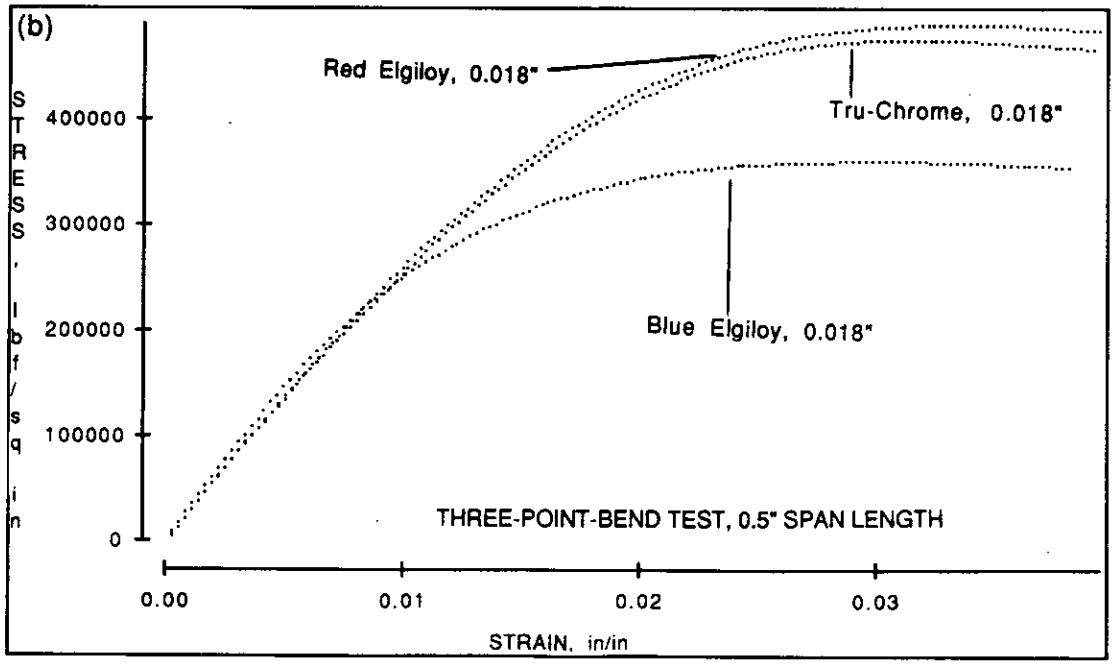


FIGURE 30

Comparison of the Three-Point-Bend Test Load/Deflection [L/D] and *Approximated Stress/Strain [S/S] Diagrams of Tru-Chrome 0.018", Blue Elgiloy 0.018", and Red Elgiloy 0.018" -- (a) [L/D] Diagrams and (b) *Approximated [S/S] Diagrams

*Approximated by the equation for the flexural modulus of elasticity.



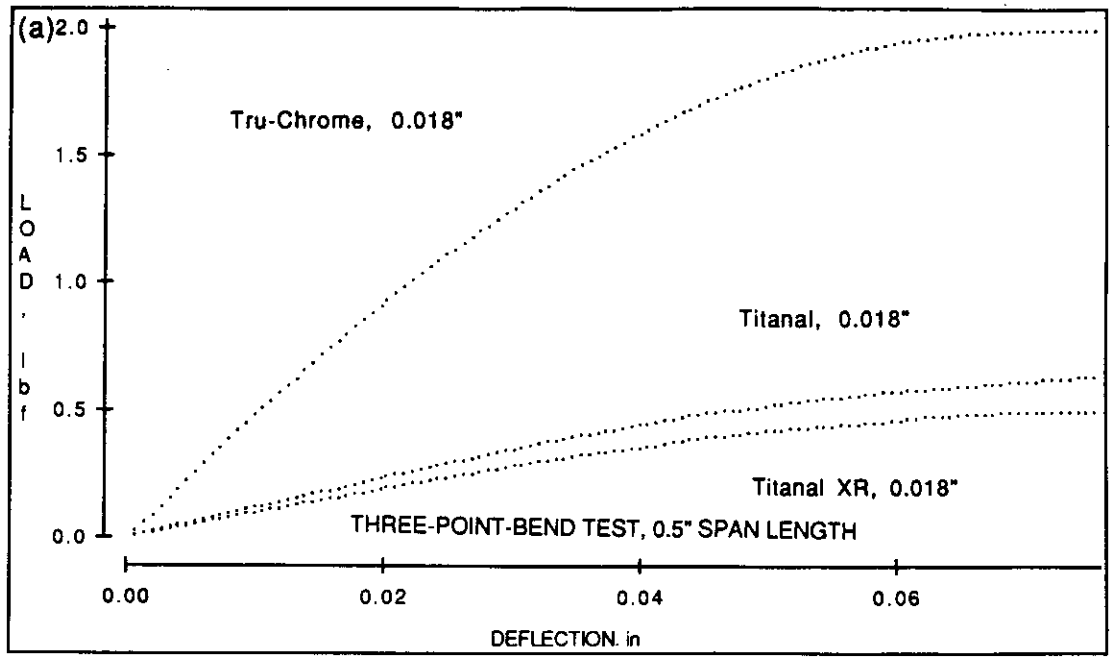
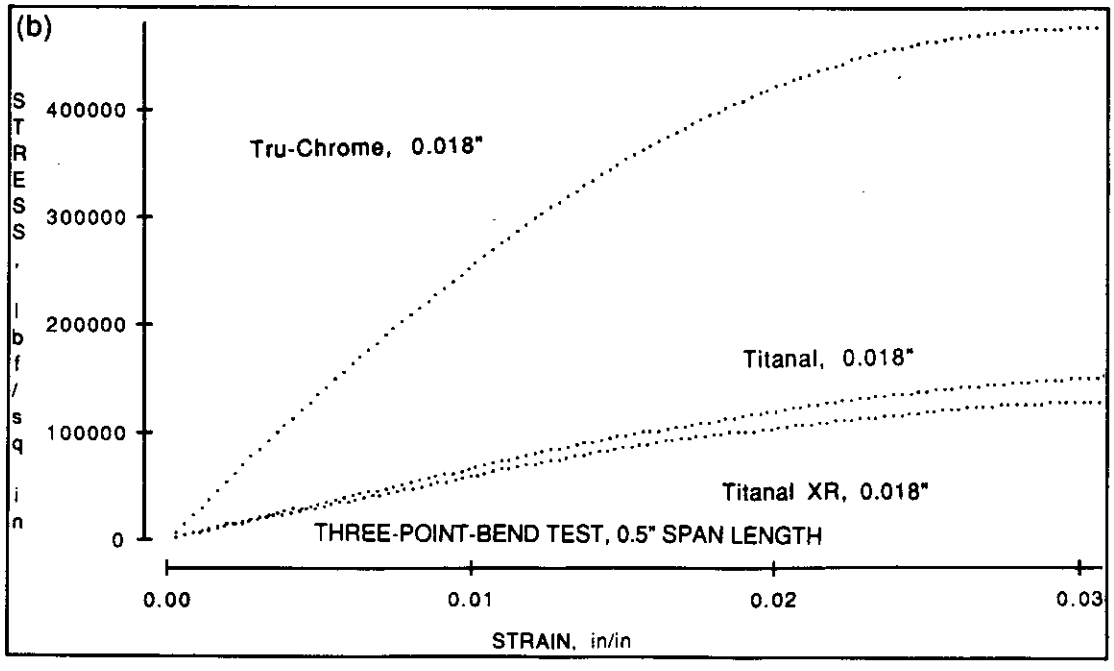


FIGURE 31
Comparison of the Three-Point-Bend Test Load/Deflection [L/D] and *Approximated Stress/Strain [S/S] Diagrams of Tru-Chrome 0.018", Titanal 0.018" and Titanal XR 0.018" -- (a) [L/D] Diagrams and (b) *Approximated [S/S] Diagrams

*Approximated by the equation for the flexural modulus of elasticity.



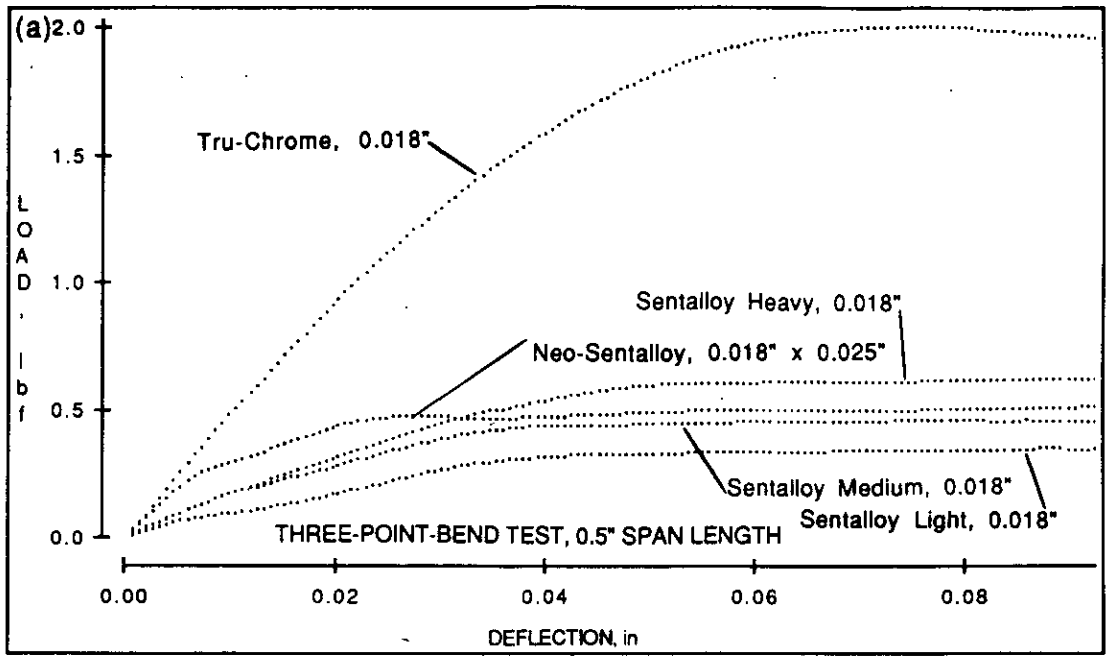
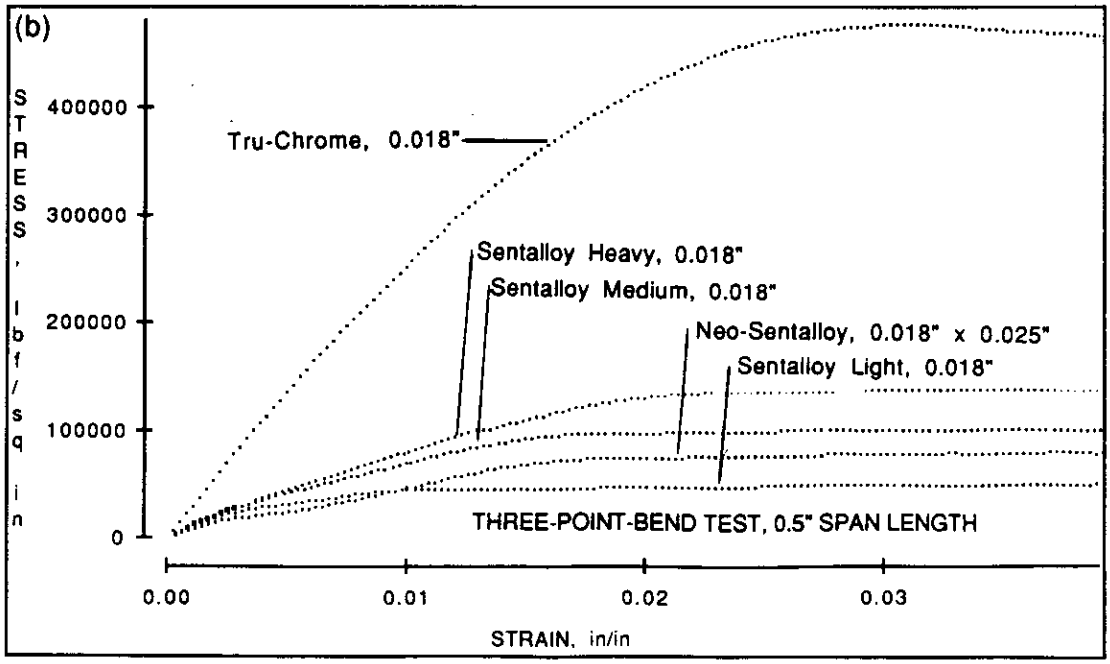


FIGURE 32

Comparison of the Three-Point-Bend Test Load/Deflection [L/D] and *Approximated Flexural Stress/Strain [S/S] Diagrams of Tru-Chrome 0.018", Neo-Sentalloy 0.018" x 0.025", Sentalloy Light 0.018", Sentalloy Medium 0.018", and Sentalloy Heavy 0.018" -- (a) [L/D] Diagrams and (b) *Approximated Flexural [S/S] Diagrams

*Approximated by the equation for the flexural modulus of elasticity.



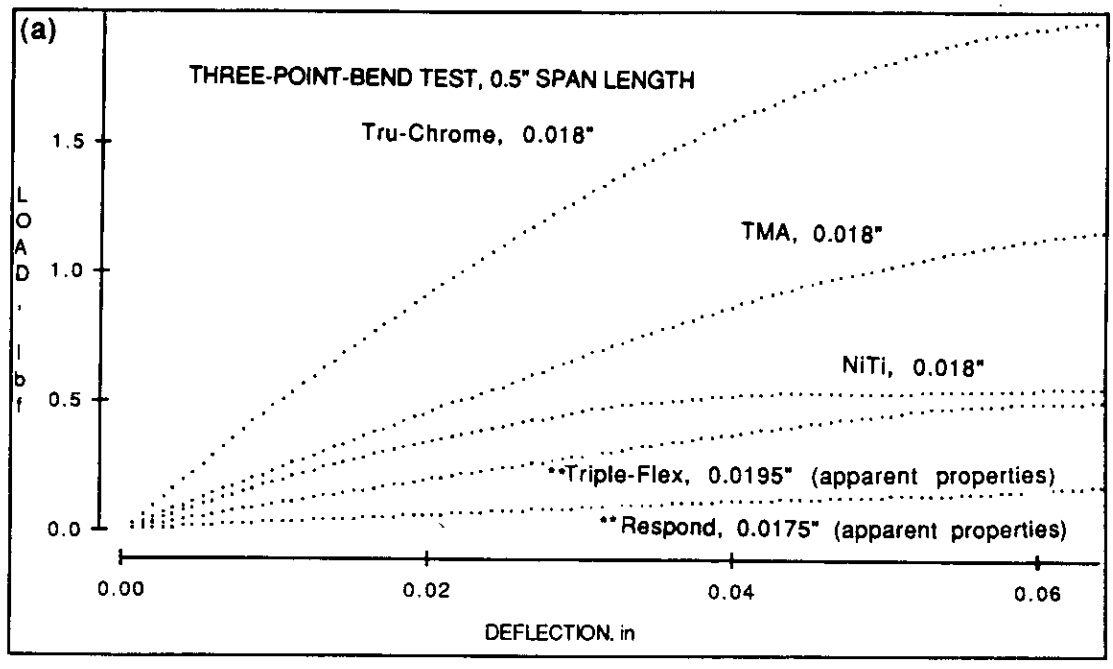
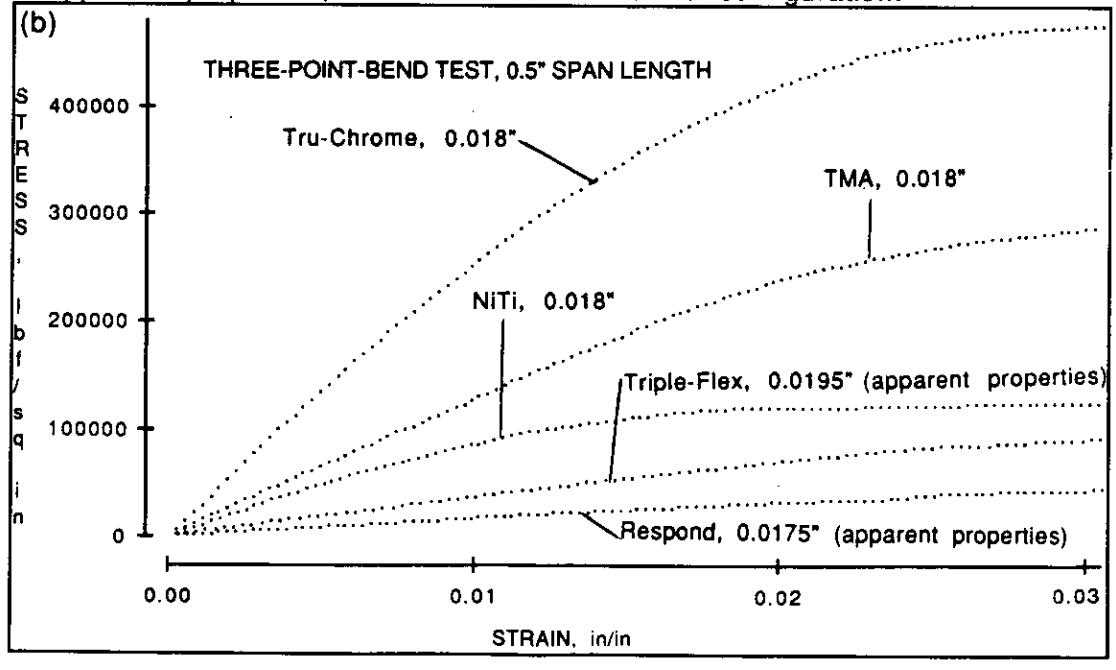


FIGURE 33
Comparison of the Three-Point-Bend Test Load/Deflection [L/D] and *Approximated Flexural Stress/Strain [S/S] Diagrams of Tru-Chrome 0.018", TMA 0.018", NiTi 0.018", **Triple-flex 0.0195", and **Respond 0.0175" -- (a) [L/D] Diagrams and *Approximated Flexural [S/S] Diagrams

*Approximated by the equation for the flexural modulus of elasticity.
**Apparent properties, not corrected for strand configuration.



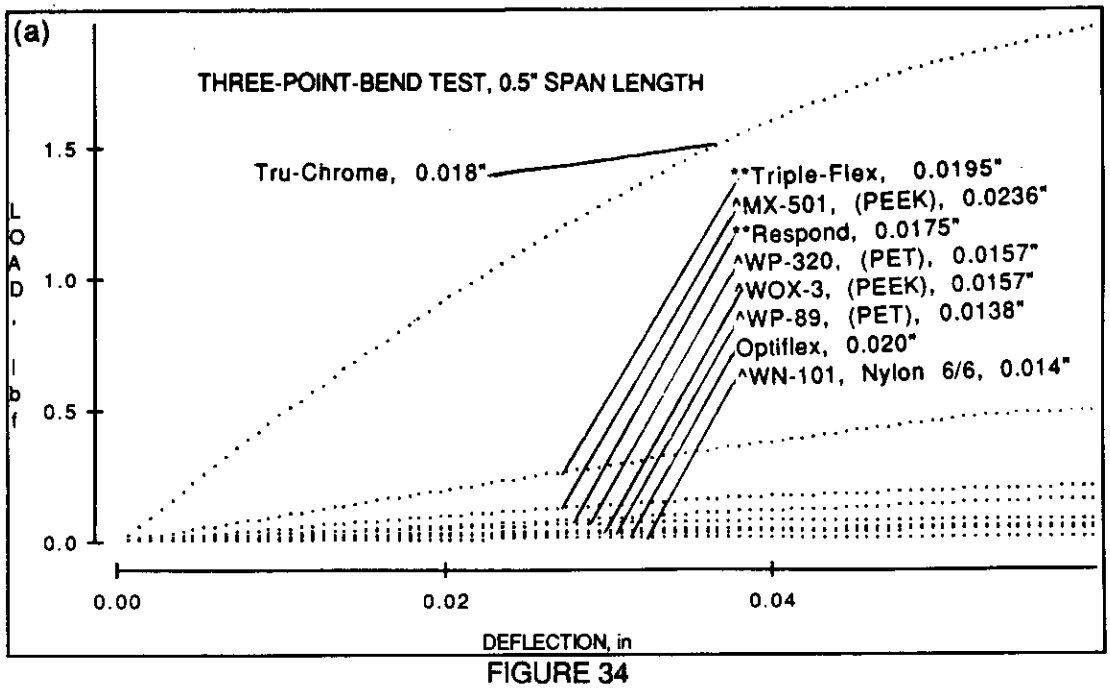
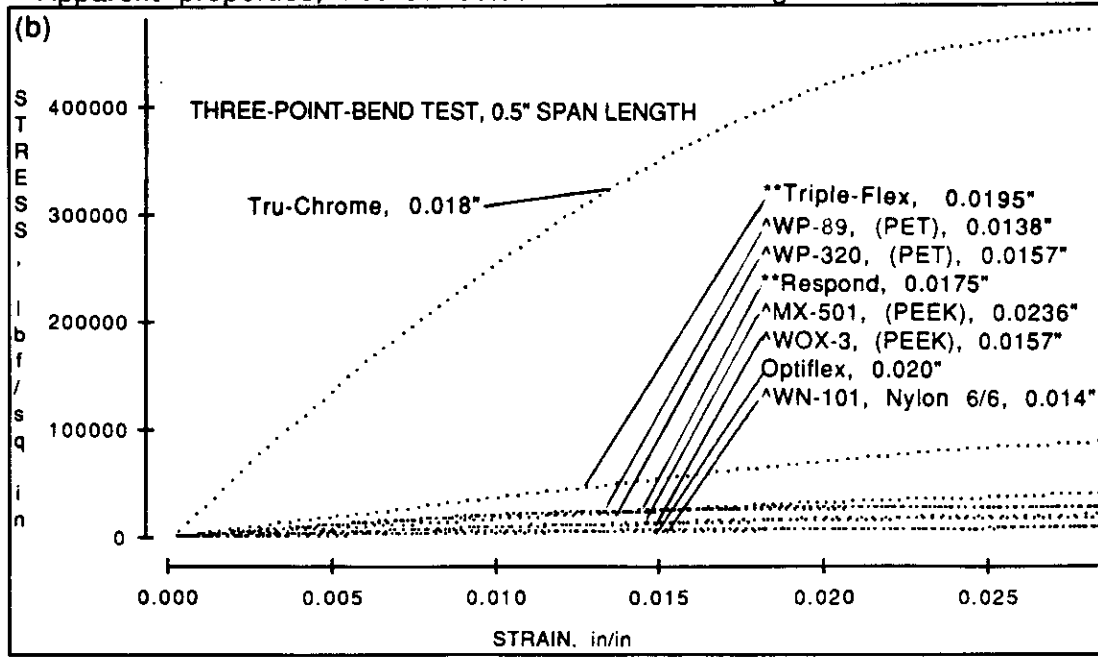


FIGURE 34

Comparison of the Three-Point-Bend Test Load/Deflection [L/D] and *Approximated Flexural Stress/Strain [S/S] Diagrams of Tru-Chrome 0.018", **Tripleflex 0.0195", *MX-501 (PEEK) 0.0236", **Respond 0.0175", ^WP-320 (PET) Polyester 0.0157", ^WOX-3 (PEEK) 0.0157", ^WP-89 (PET) Polyester 0.0138", Optiflex 0.020", ^WN-101 Nylon 6/6 0.014" -- (a) [L/D] Diagrams and (b) Approximated Flexural [S/S] Diagrams *Approximated by the equation for the flexural modulus of elasticity. **Apparent properties, not corrected for strand configuration. ^Monofilament



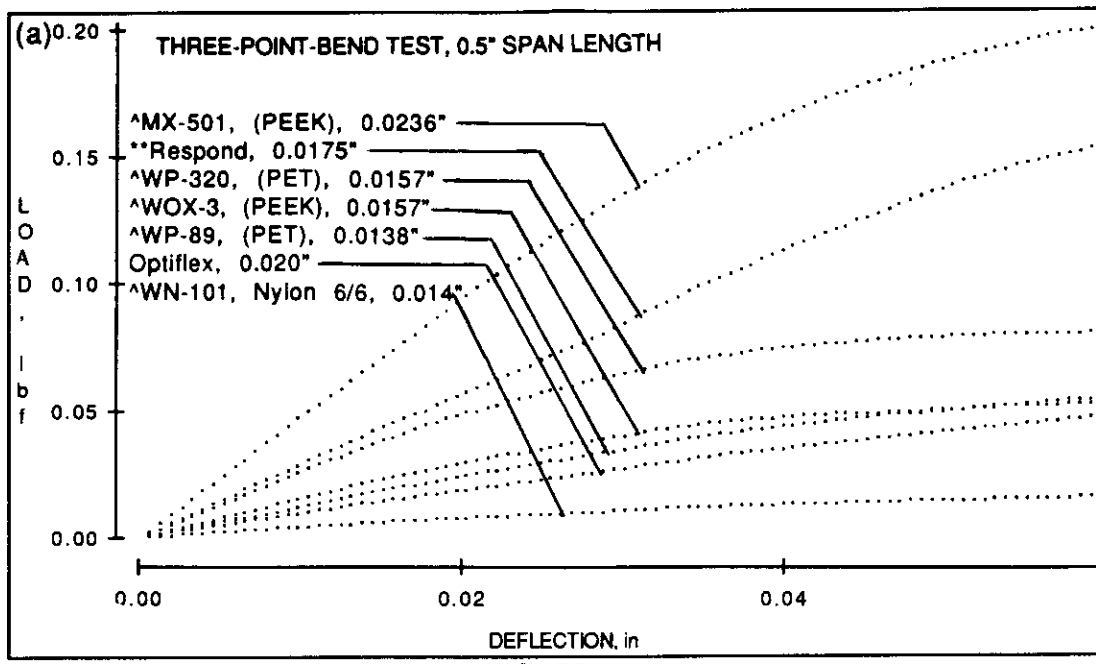
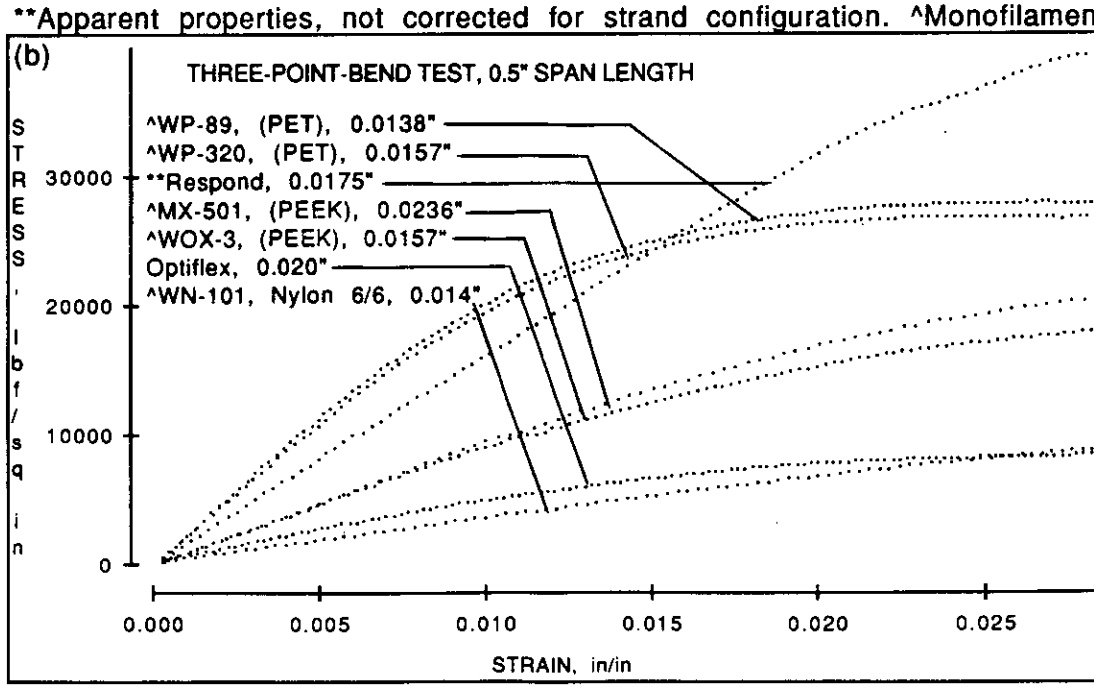


FIGURE 35

Comparison of the Three-Point-Bend Test Load/Deflection [L/D] and *Approximated Flexural Stress/Strain [S/S] Diagrams of **Tripleflex 0.0195", *MX-501 (PEEK) 0.0236", **Respond 0.0175", ^WP-320 (PET) Polyester 0.0157", ^WOX-3 (PEEK) 0.0157", ^WP-89 (PET) Polyester 0.0138", Optiflex 0.020", ^WN-101 Nylon 6/6 0.014" -- (a) [L/D] Diagrams and (b) Approximated Flexural [S/S] Diagrams *Approximated by the equation for the flexural modulus of elasticity. **Apparent properties, not corrected for strand configuration. ^Monofilament



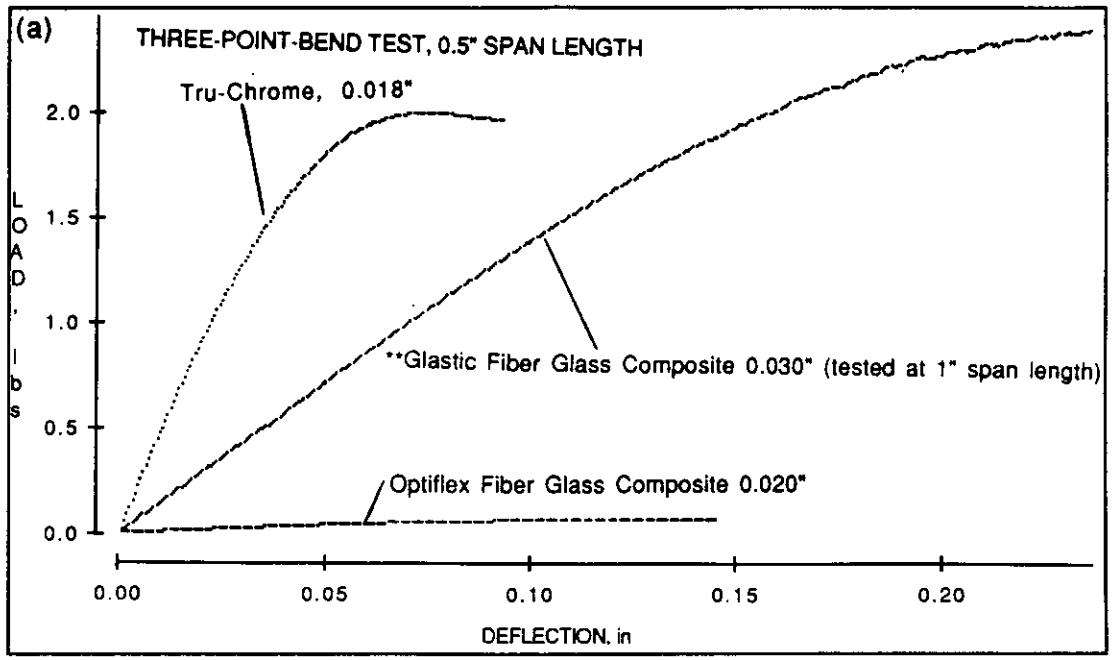
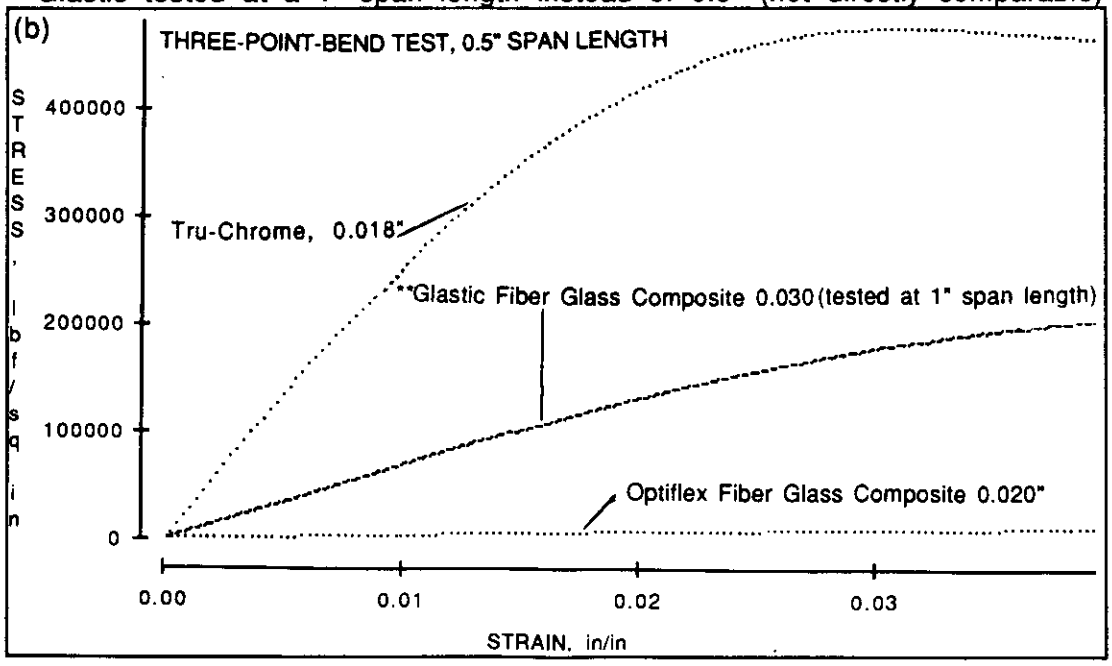


FIGURE 36

Comparison of the Three-Point-Bend Test Load/Deflection [L/D] and *Approximated Flexural Stress/Strain [S/S] Diagrams of Tru-Chrome 0.018", **Glastic Fiber Glass Composite 0.030", and Optiflex Fiber Glass Composite, 0.020" -- (a) [L/D] Diagrams and (b) *Approximated Flexural [S/S] Diagrams

*Approximated by the equation for the flexural modulus of elasticity.
**Glastic tested at a 1" span length instead of 0.5" (not directly comparable)



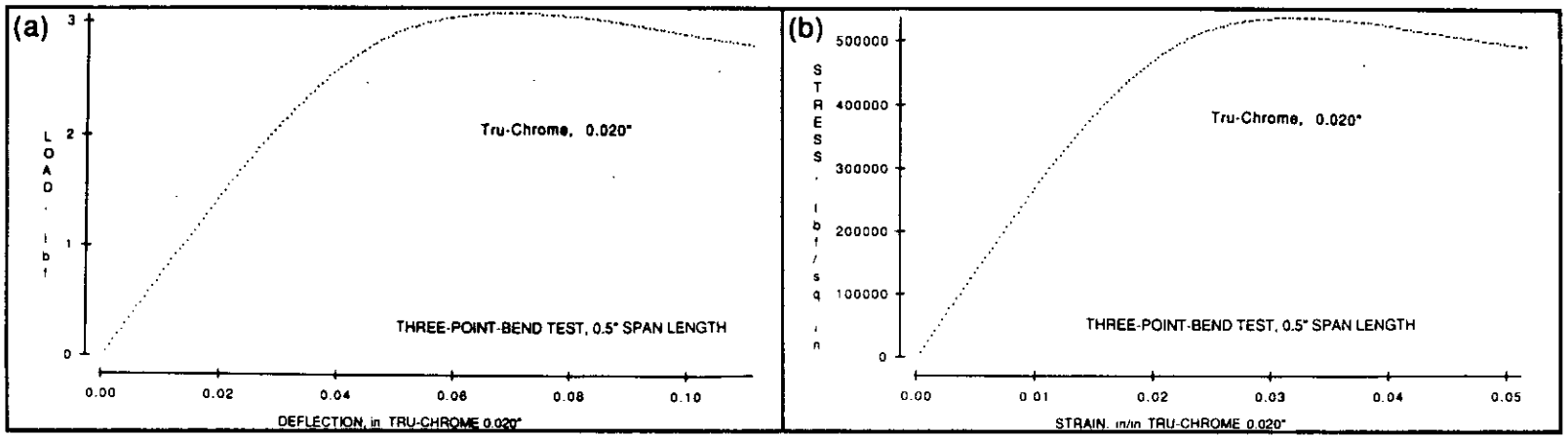
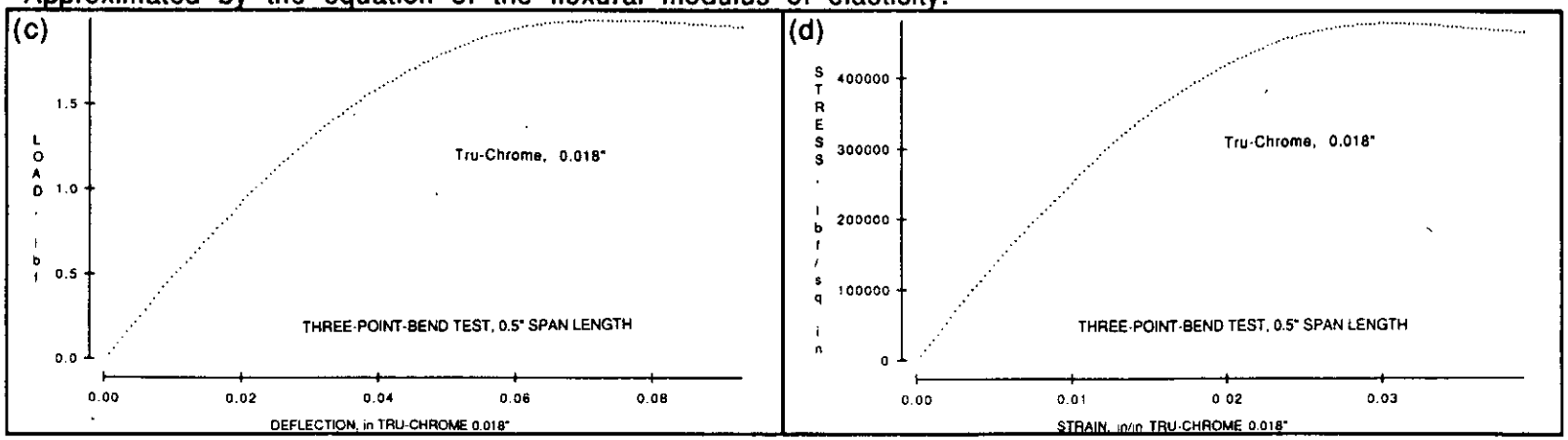


FIGURE 37

Three-point-Bend Test Load/Deflection [L/D] and *Approximated Flexural Stress/Strain [S/S] Diagrams for Individual Materials -- (a) [L/D] Diagram of Tru-Chrome 0.020", (b) *Approximated Flexural [S/S] Diagram of Tru-Chrome 0.020", (c) [L/D] Diagram of Tru-Chrome 0.018", and (d) *Approximated Flexural [S/S] Diagram of Tru-Chrome 0.018"

*Approximated by the equation of the flexural modulus of elasticity.



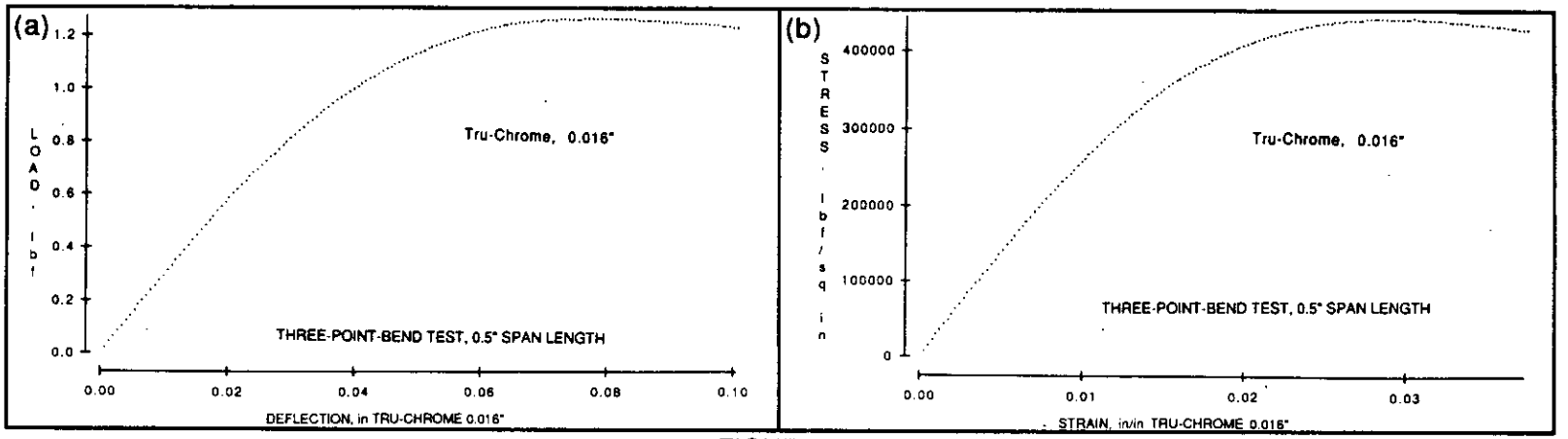
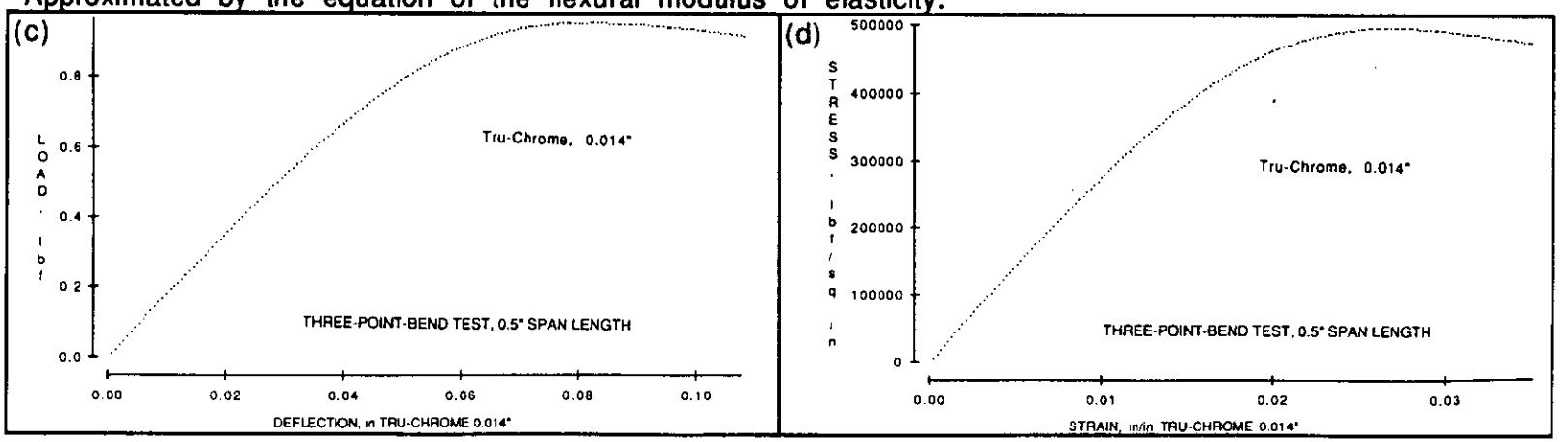


FIGURE 38

Three-point-Bend Test Load/Deflection [L/D] and *Approximated Flexural Stress/Strain [S/S] Diagrams for Individual Materials -- (a) [L/D] Diagram of Tru-Chrome 0.016", (b) *Approximated Flexural [S/S] Diagram of Tru-Chrome 0.016", (c) [L/D] Diagram of Tru-Chrome 0.014", and (d) *Approximated Flexural [S/S] Diagram of Tru-Chrome 0.014"

*Approximated by the equation of the flexural modulus of elasticity.



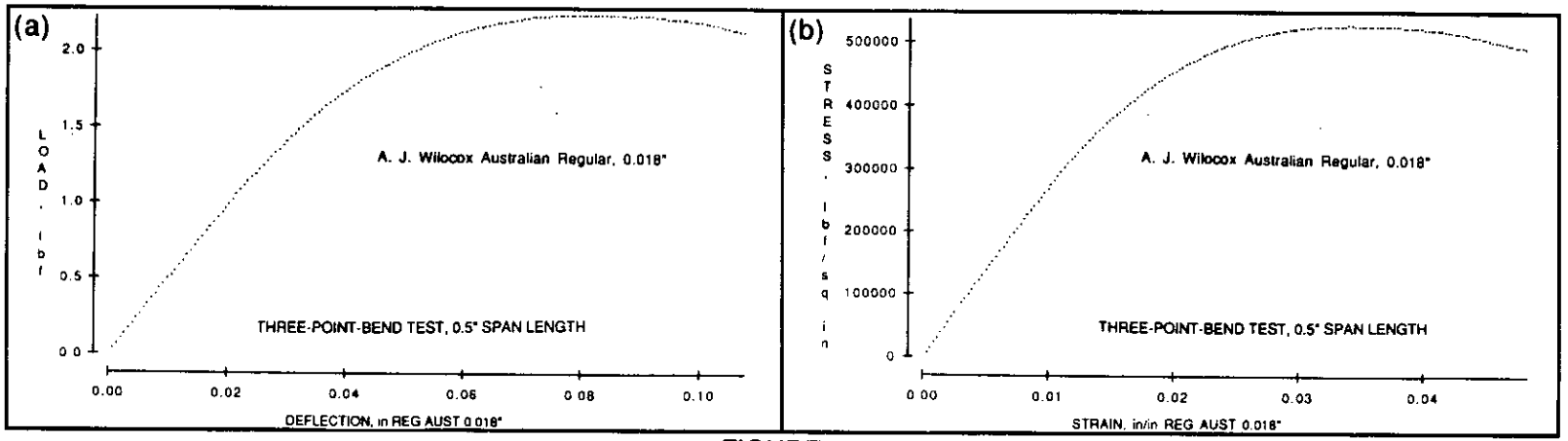
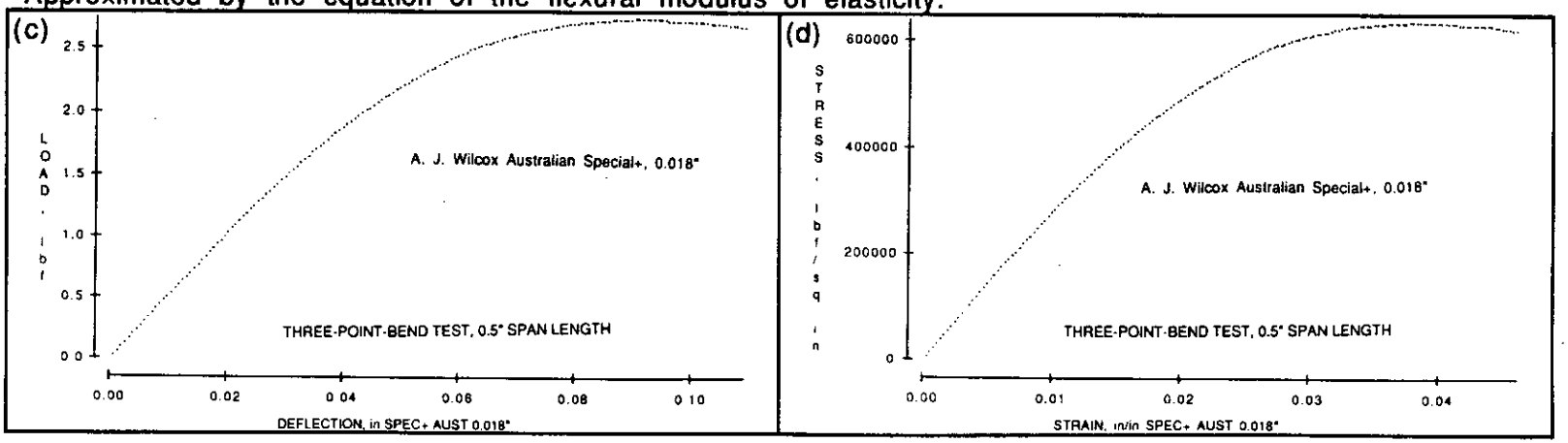


FIGURE 39

Three-point-Bend Test Load/Deflection [L/D] and *Approximated Flexural Stress/Strain [S/S] Diagrams for Individual Materials -- (a) [L/D] Diagram of A. J. Wilcox Australian Regular 0.018", (b) *Approximated Flexural [S/S] Diagram of A. J. Wilcox Australian Regular 0.018", (c) [L/D] Diagram of A. J. Wilcox Australian Special+ 0.018", and (d) *Approximated Flexural [S/S] Diagram of A. J. Wilcox Australian Special+ 0.018"

*Approximated by the equation of the flexural modulus of elasticity.



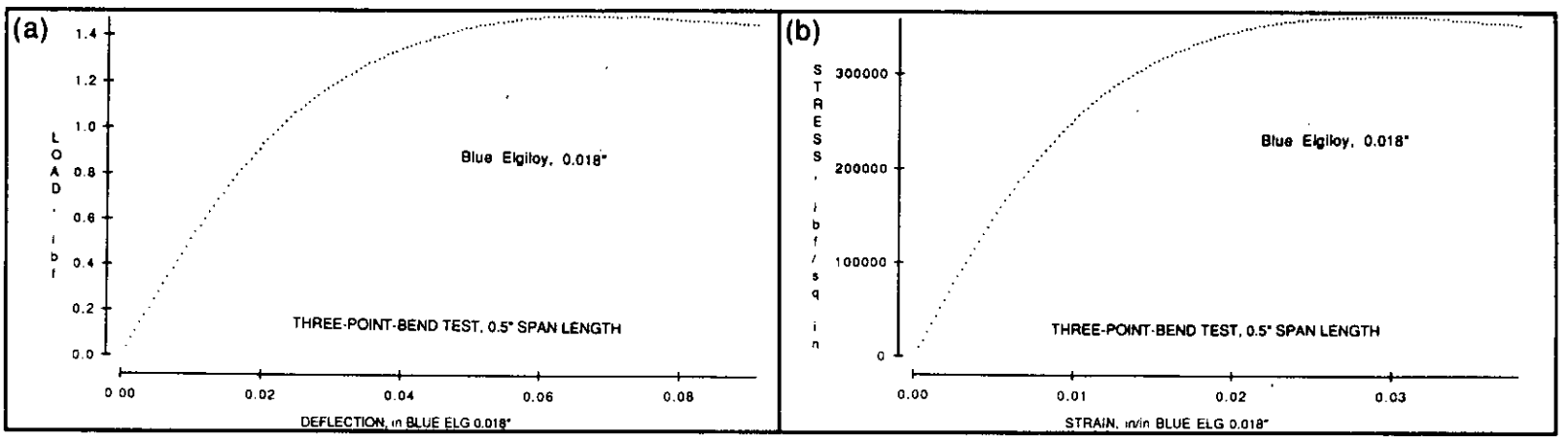
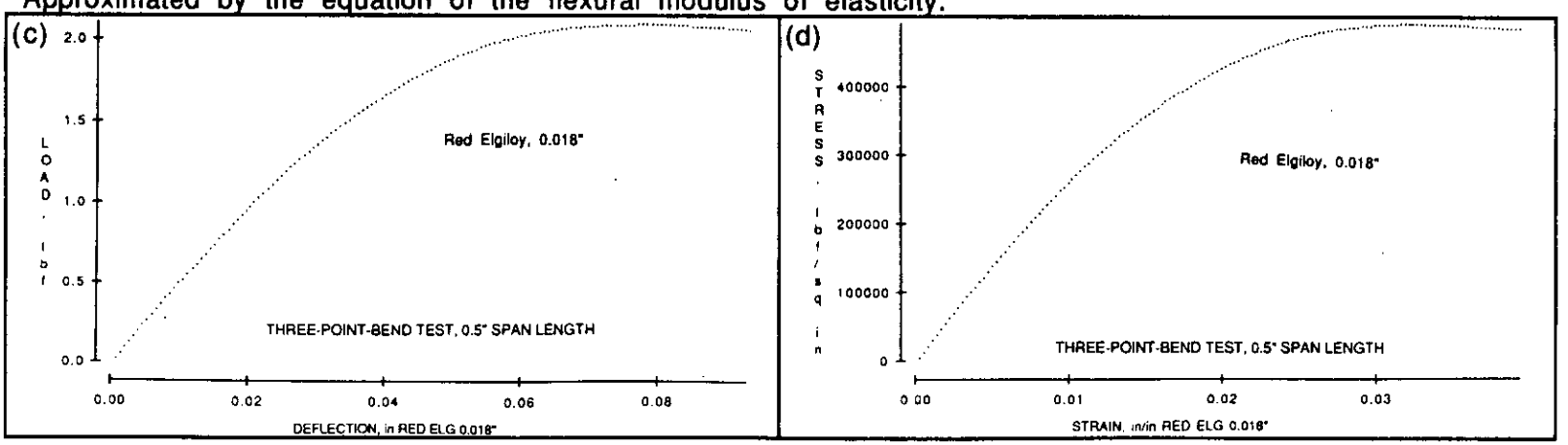


FIGURE 40

Three-point-Bend Test Load/Deflection [L/D] and *Approximated Flexural Stress/Strain [S/S] Diagrams for Individual Materials -- (a) [L/D] Diagram of Blue Elgiloy 0.018", (b) *Approximated Flexural [S/S] Diagram of Blue Elgiloy 0.018", (c) [L/D] Diagram of Red Elgiloy 0.018", and (d) *Approximated Flexural [S/S] Diagram of Red Elgiloy 0.018"

*Approximated by the equation of the flexural modulus of elasticity.



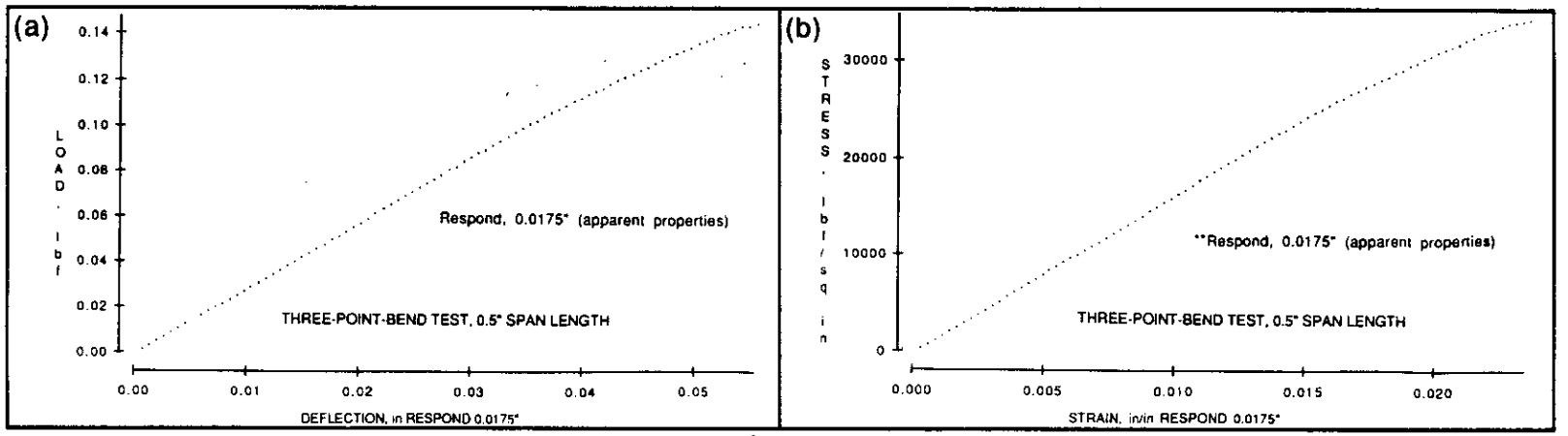
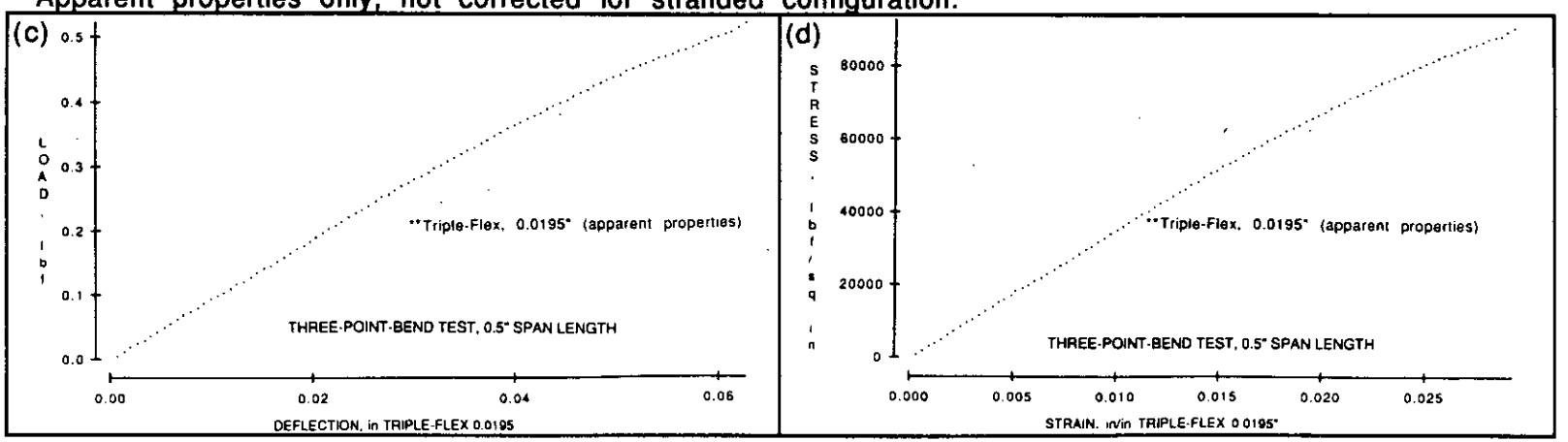


FIGURE 41

Three-point-Bend Test Load/Deflection [L/D] and *Approx. Flexural Stress/Strain [S/S] Diagrams for Individual Materials -- (a) [L/D] Diagram of **Respond 0.0175", (b) *Approx. Flexural [S/S] Diagram of **Respond 0.0175", (c) [L/D] Diagram of **Tripleflex 0.0195", and (d) *Approx. Flexural [S/S] Diagram of **Tripleflex 0.0195"
*Approximated by the equation of the flexural modulus of elasticity.
**Apparent properties only, not corrected for stranded configuration.



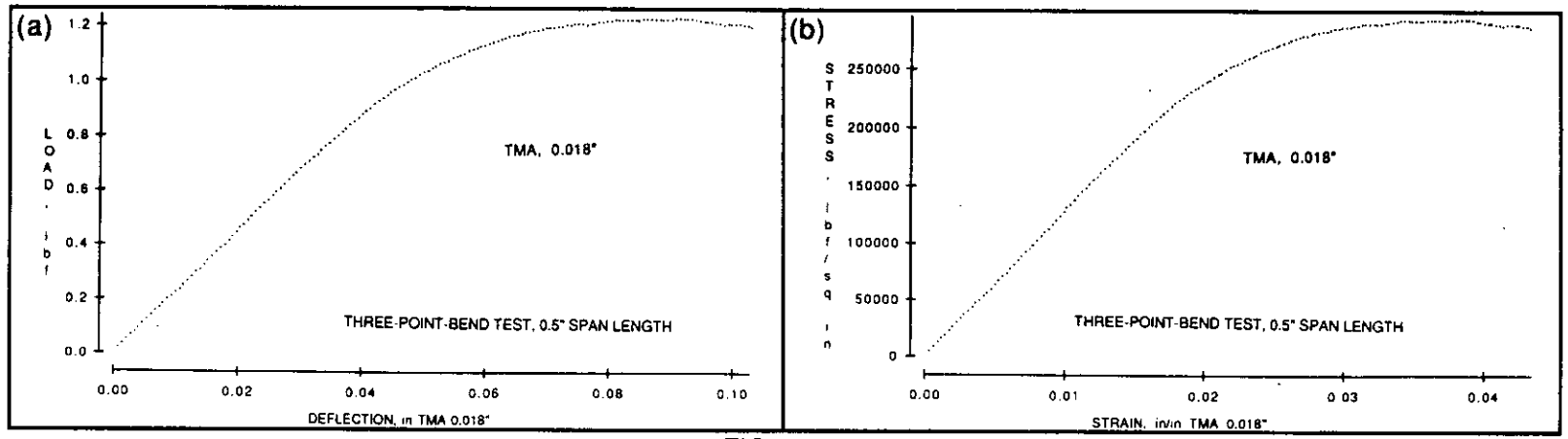
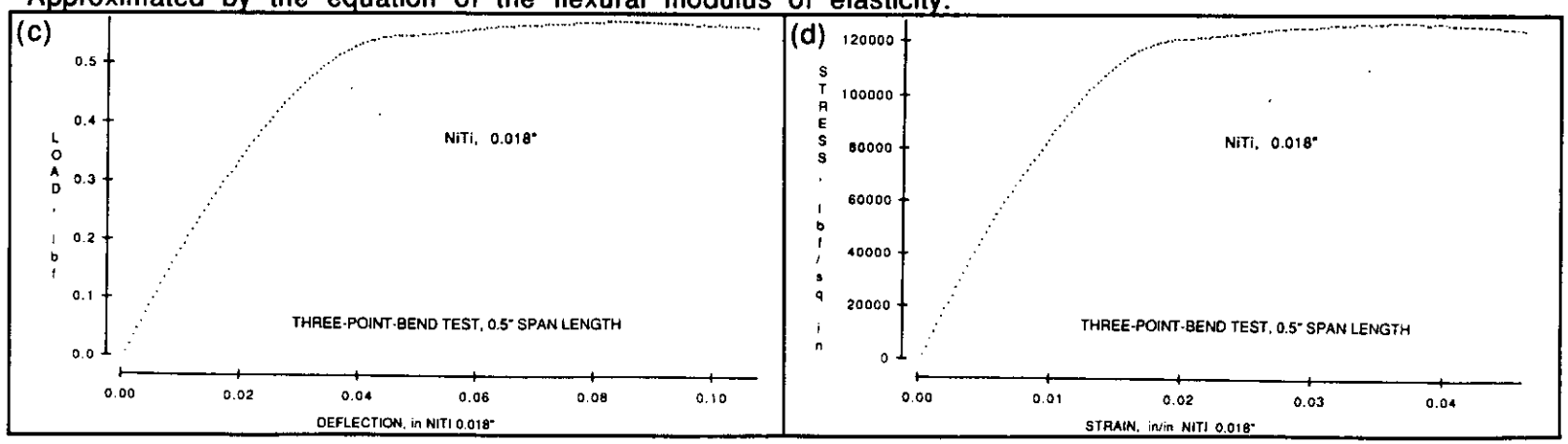


FIGURE 42

Three-point-Bend Test Load/Deflection [L/D] and *Approximate Flexural Stress/Strain [S/S] Diagrams for Individual Materials -- (a) [L/D] Diagram of TMA 0.018", (b) *Approximate Flexural [S/S] Diagram of TMA 0.018", (c) [L/D] Diagram of NiTi 0.018", and (d) *Approximate Flexural [S/S] Diagram of NiTi 0.018"

*Approximated by the equation of the flexural modulus of elasticity.



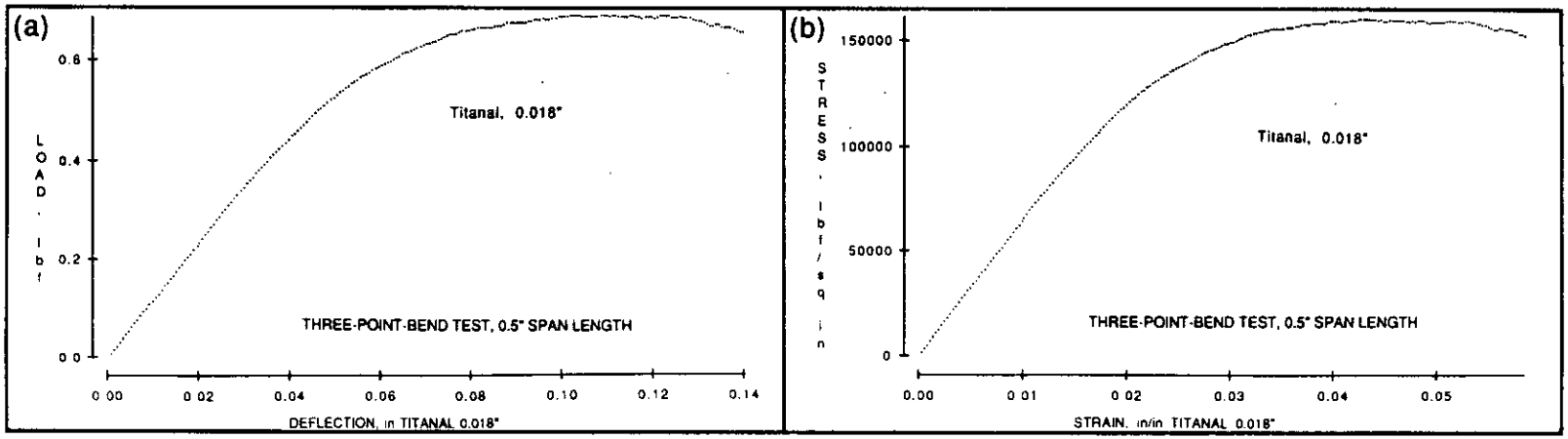
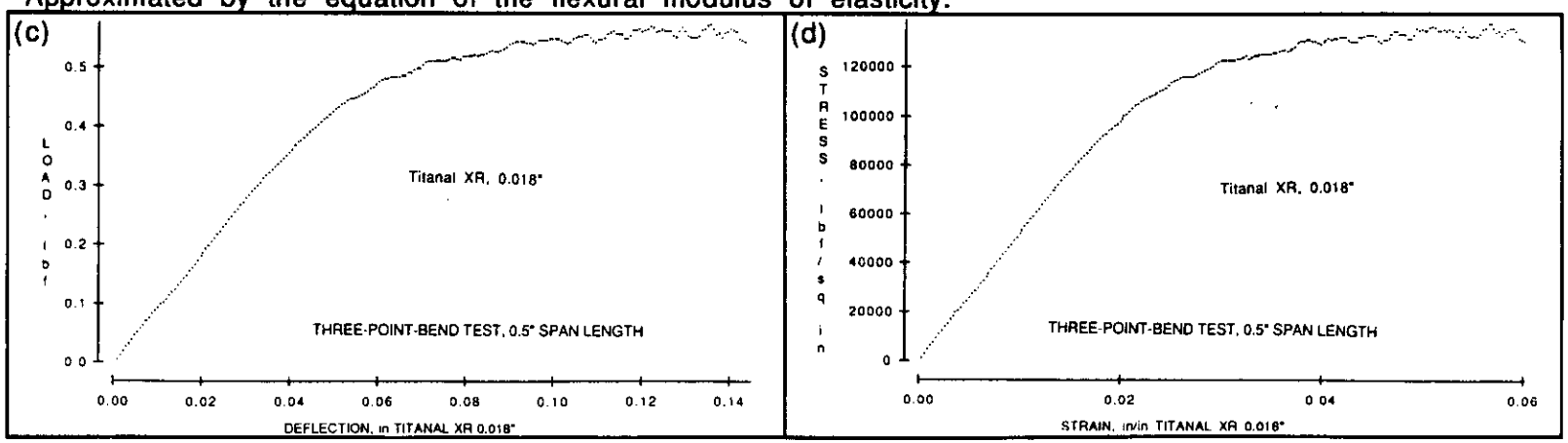


FIGURE 43

Three-point-Bend Test Load/Deflection [L/D] and *Approximate Flexural Stress/Strain [S/S] Diagrams for Individual Materials -- (a) [L/D] Diagram of Titanal 0.018", (b) *Approximate Flexural [S/S] Diagram of Titanal 0.018", (c) [L/D] Diagram of Titanal XR 0.018", and (d) *Approximate Flexural [S/S] Diagram of Titanal XR 0.018"

*Approximated by the equation of the flexural modulus of elasticity.



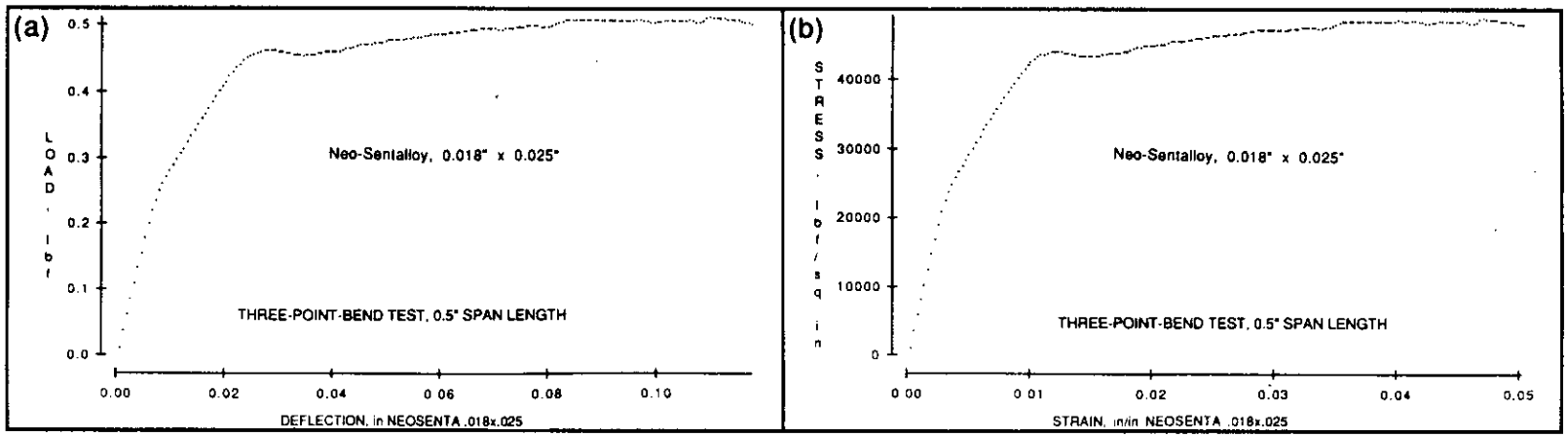
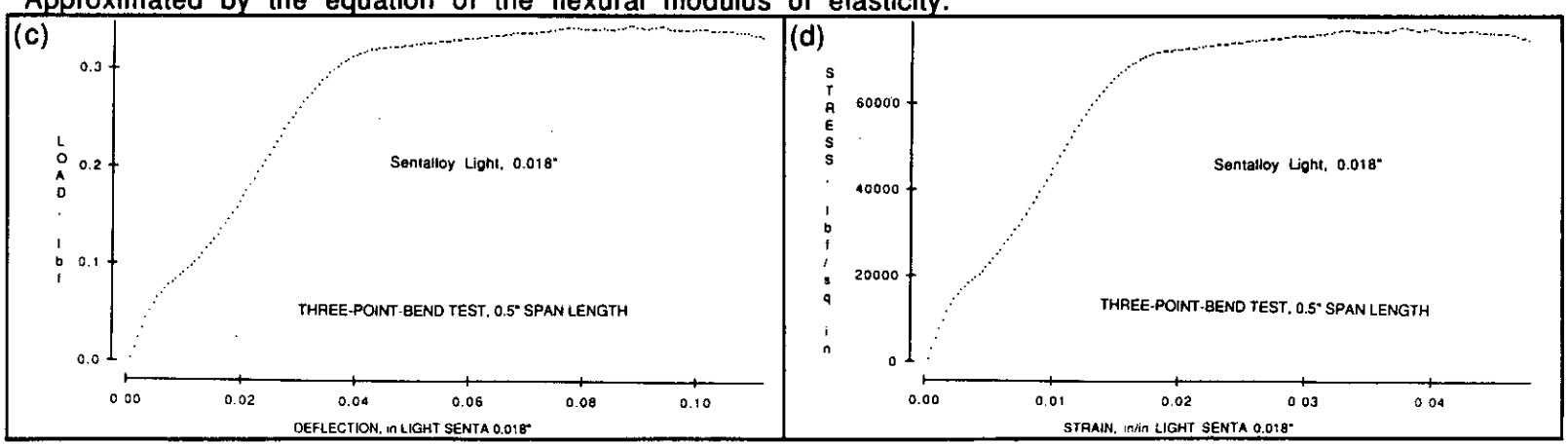


FIGURE 44

Three-point-Bend Test Load/Deflection [L/D] and *Approximate Flexural Stress/Strain [S/S] Diagrams for Individual Materials -- (a) [L/D] Diagram of Neo-Sentalloy 0.018" x 0.025", (b) *Approximate Flexural [S/S] Diagram of Neo-Sentalloy 0.018" x 0.025", (c) [L/D] Diagram of Sentalloy Light 0.018", and (d) *Approximate Flexural [S/S] Diagram of Sentalloy Light 0.018"

*Approximated by the equation of the flexural modulus of elasticity.



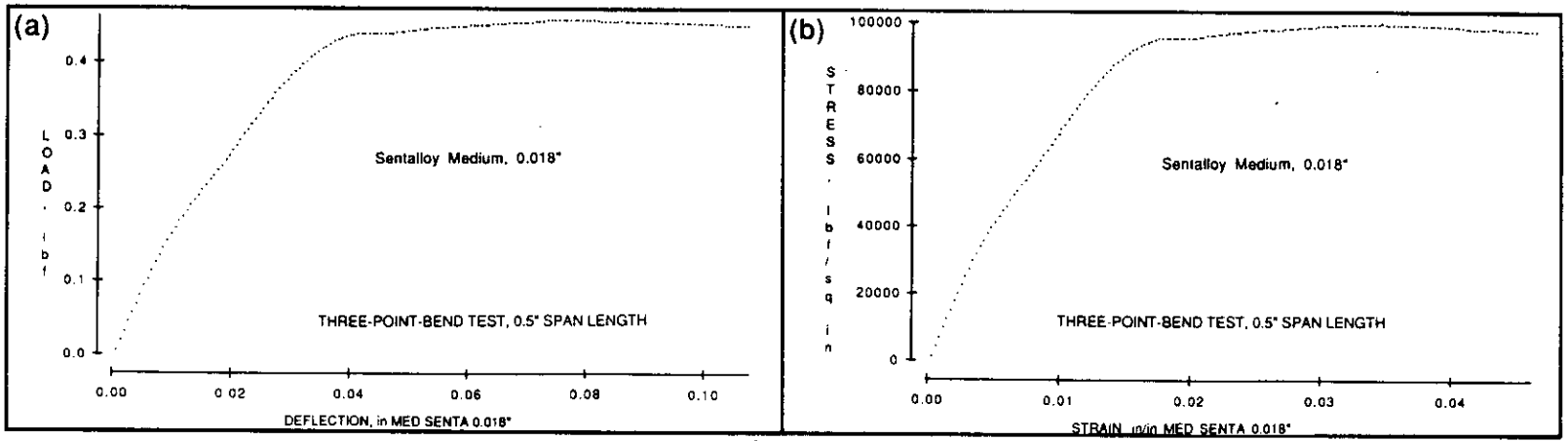
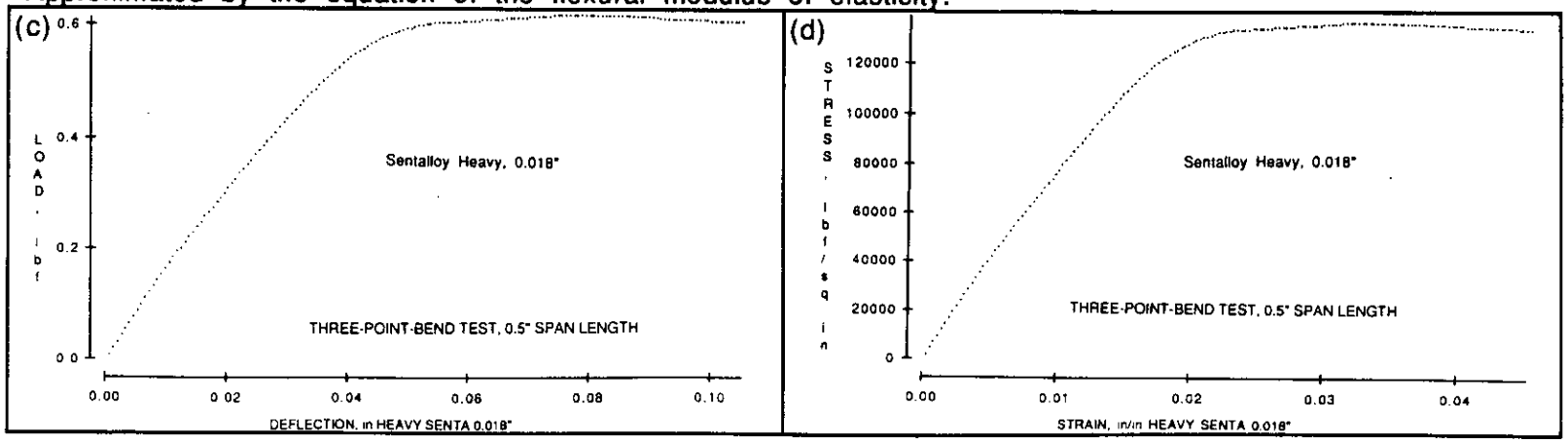


FIGURE 45

Three-point-Bend Test Load/Deflection [L/D] and *Approximate Flexural Stress/Strain [S/S] Diagrams for Individual Materials -- (a) [L/D] Diagram of Sentalloy Medium 0.018", (b) *Approximate Flexural [S/S] Diagram of Sentalloy Medium 0.018", (c) [L/D] Diagram of Sentalloy Heavy 0.018", and (d) *Approximate Flexural [S/S] Diagram of Sentalloy Heavy 0.018"

*Approximated by the equation of the flexural modulus of elasticity.



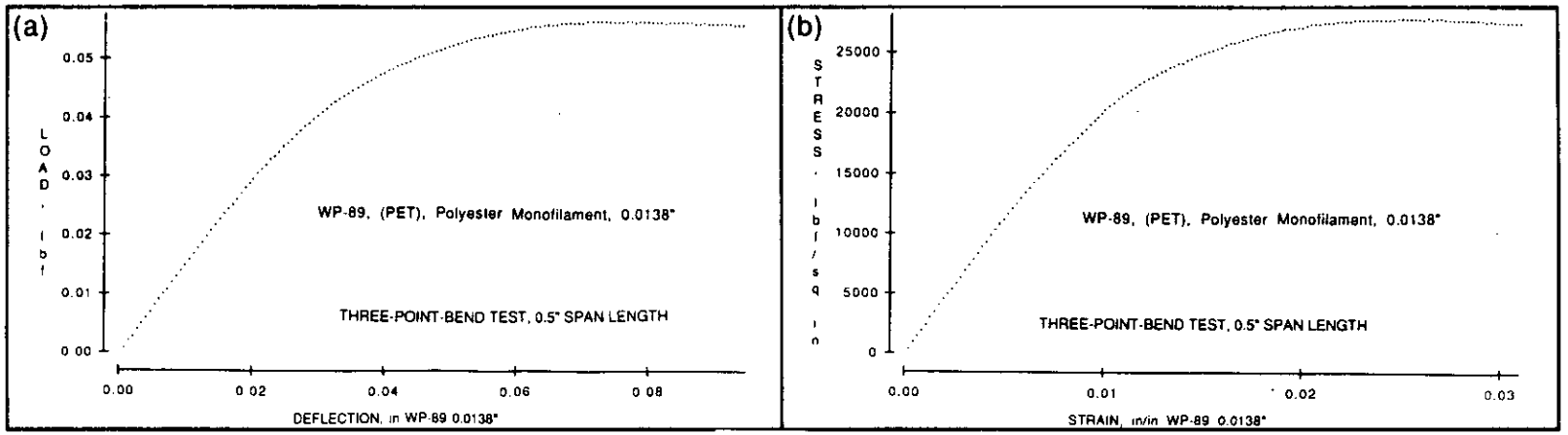
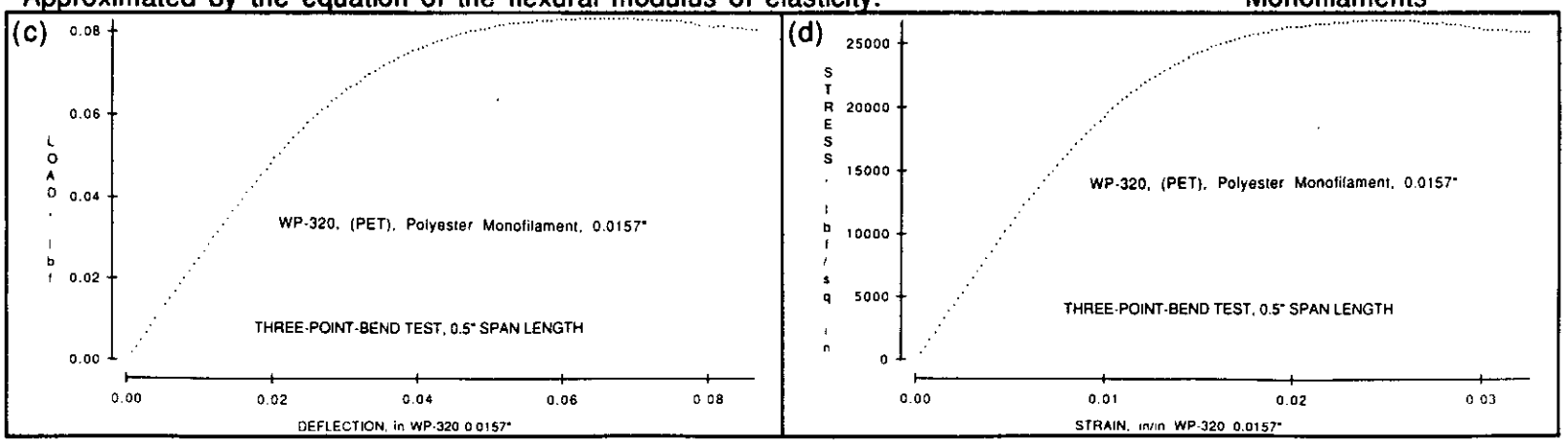


FIGURE 47

Three-point-Bend Test Load/Deflection [L/D] and *Approximate Flexural Stress/Strain [S/S] Diagrams for Individual Materials -- (a) [L/D] Diagram of **WP-89 (PET) Polyester 0.0138", (b) *Approximate Flexural [S/S] Diagram of **WP-89 (PET) Polyester 0.0138", (c) [L/D] Diagram of **WP-320 (PET) Polyester 0.0157", and (d) *Approximate Flexural [S/S] Diagram of **WP-320 (PET) Polyester 0.0157"

*Approximated by the equation of the flexural modulus of elasticity. **Monofilaments



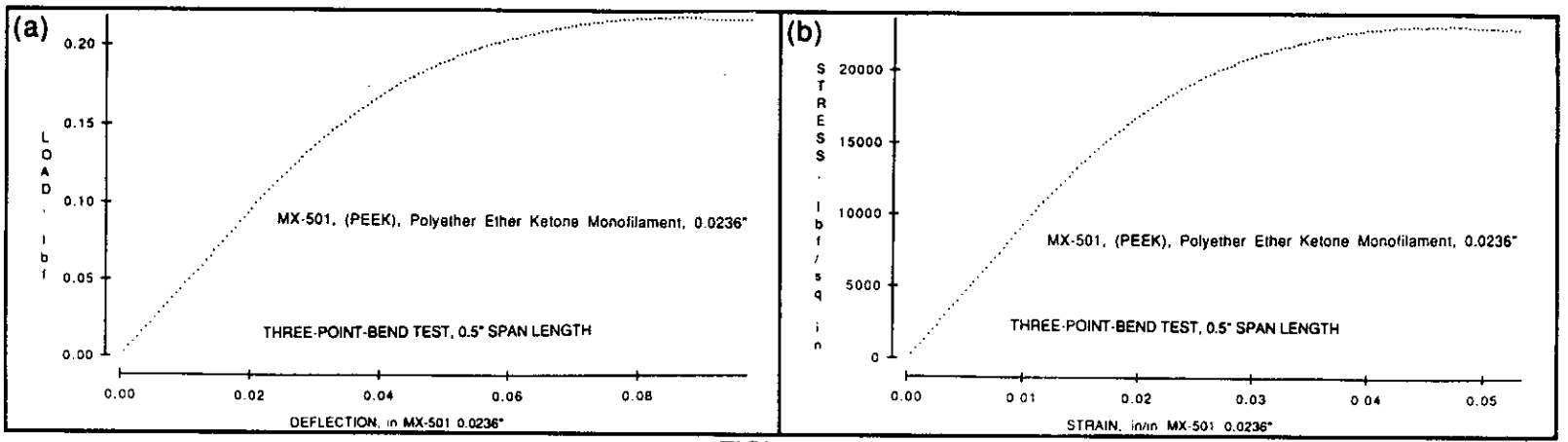
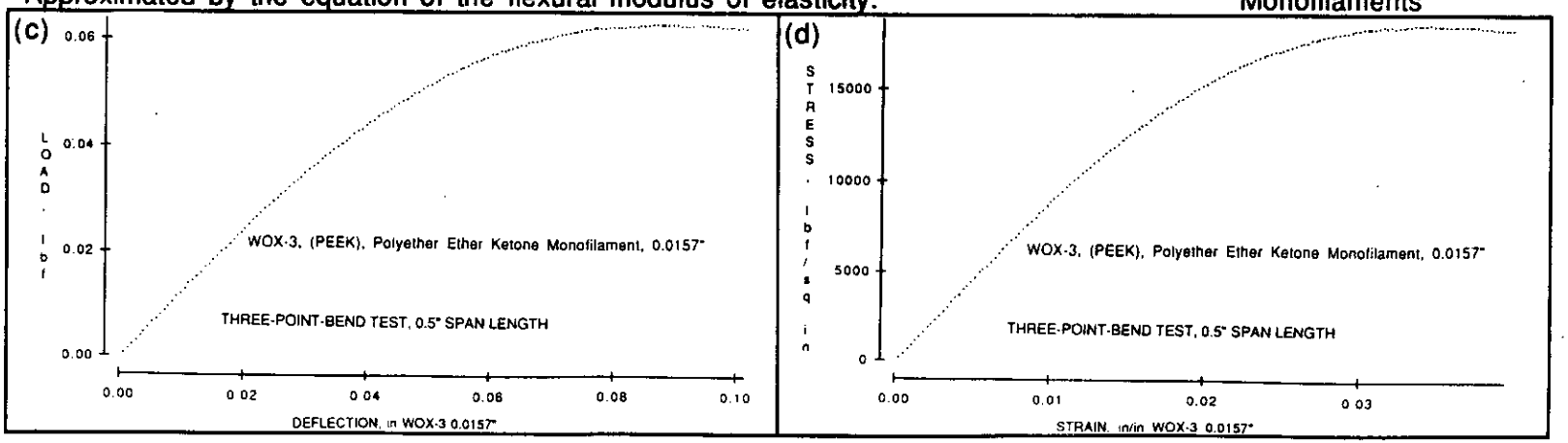


FIGURE 46

Three-point-Bend Test Load/Deflection [L/D] and *Approximate Flexural Stress/Strain [S/S] Diagrams for Individual Materials -- (a) [L/D] Diagram of **MX-501 (PEEK) 0.0236", (b) *Approximate Flexural [S/S] Diagram of **MX-501 (PEEK) 0.0236", (c) [L/D] Diagram of **WOX-3 (PEEK) 0.0157", and (d) *Approximate Flexural [S/S] Diagram of **WOX-3 (PEEK) 0.0157"

*Approximated by the equation of the flexural modulus of elasticity. **Monofilaments



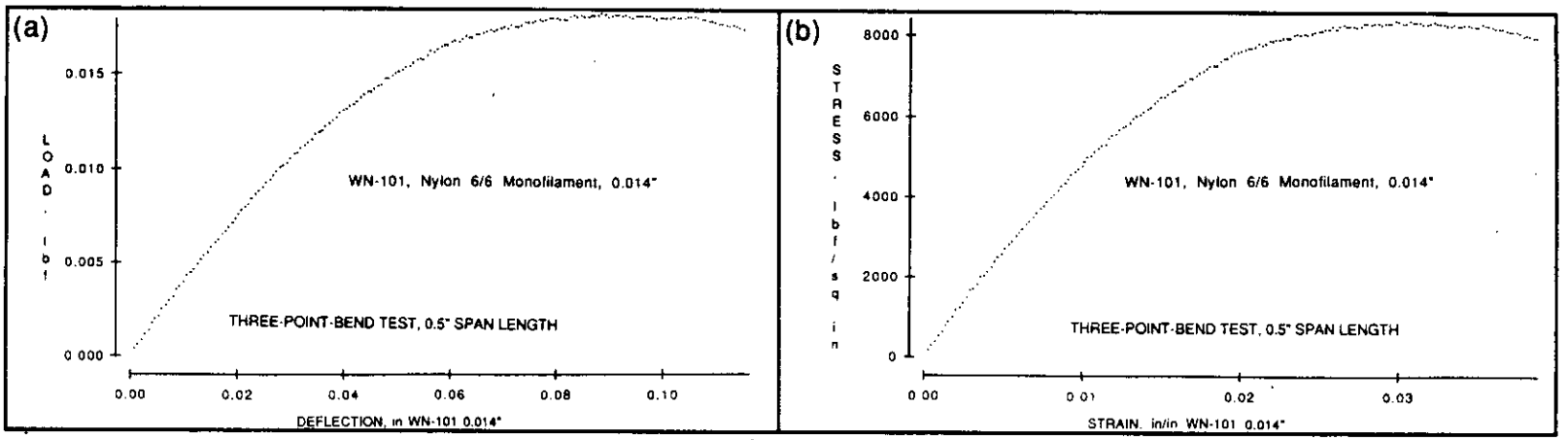
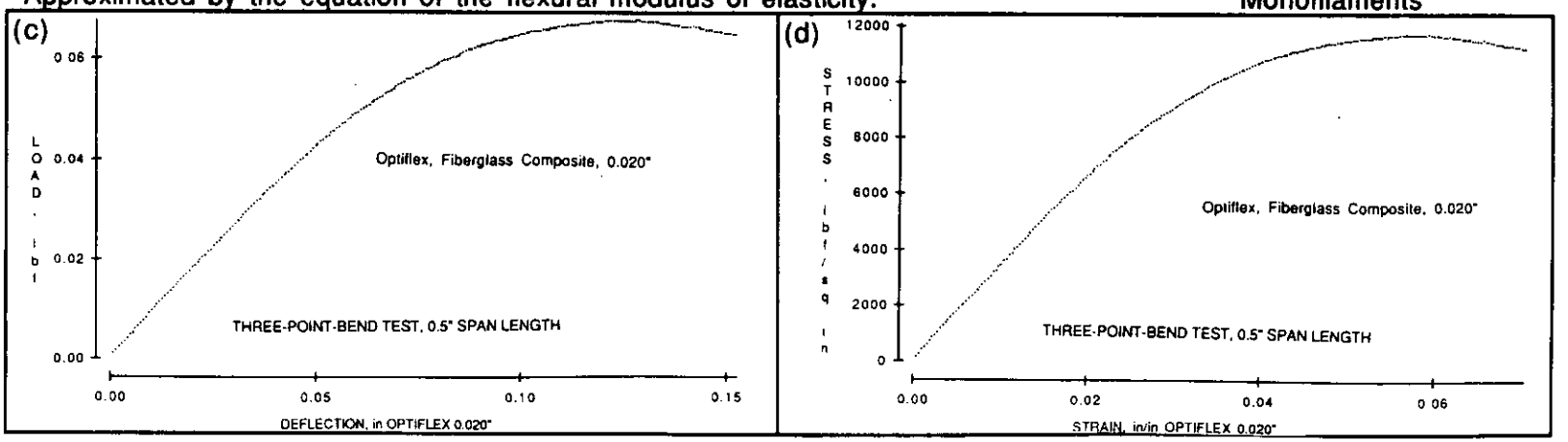


FIGURE 48

Three-point-Bend Test Load/Deflection [L/D] and *Approximate Flexural Stress/Strain [S/S] Diagrams for Individual Materials -- (a) [L/D] Diagram of **WN-101 Nylon 6/6 0.014", (b) *Approximate Flexural [S/S] Diagram of **WN-101 Nylon 6/6 0.014", (c) [L/D] Diagram of Optiflex Fiber Glass Compsite 0.020", and (d) *Approximate Flexural [S/S] Diagram of Optiflex Fiber Glass Composite 0.020"

*Approximated by the equation of the flexural modulus of elasticity. **Monofilaments



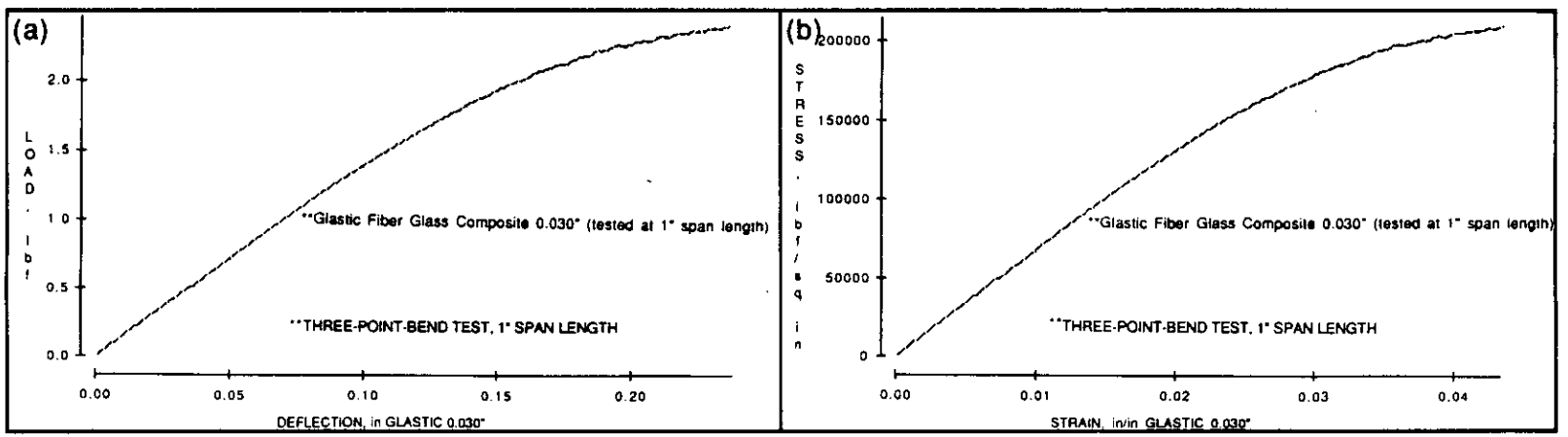


FIGURE 49

Three-point-Bend Test Load/Deflection [L/D] and *Approximate Flexural Stress/Strain [S/S] Diagrams for Individual Materials -- (a) [L/D] Diagram of **Glastic Fiber Glass Composite 0.030", and (b) *Approximate Flexural [S/S] Diagram of **Glastic Fiber Glass Compsite 0.030"

*Approximated by the equation of the flexural modulus of elasticity.

**Glastic tested at a span length of 1" instead of 0.5" (not directly comparable to other materials tested).

DISCUSSION

The mechanical properties of the various commonly used metal alloy orthodontic arch wires, and wires made of esthetic materials, were determined by means of a uniaxial tensile test and a three-point-bend test. By comparing results from the tensile and bend tests, not only were the unique mechanical characteristics of the materials identified, but certain characteristics of the tensile and bend test techniques became evident. On the basis of comparison of the mechanical properties of the various types of metal alloy wires, which have known clinical efficacy when used for specific treatment purposes, judgments as to whether the esthetic materials tested had potential from the point of view of mechanical properties were made.

Comparison of The Tensile Test and Bending Test

Since in the ideal tensile test involved the uniaxial, centroidal loading throughout the cross sectional area of the specimen, homogenous tensile characteristics of the material are isolated. In the case of the bending test, loading the specimen results in a blend of compression and tensile characteristics because stresses are more variable throughout the specimen cross section. On the basis of this fact, information derived from the bend test may be more difficult to understand. While the calculation of data from the tensile test and the actual theoretical modeling of pure tensile deformation phenomenon is simpler than the bend test, the experimental technique of the tensile test is more complicated then the bend test do

to the testing apparatus involved. The inherent mechanical complexity of the test grips, clamps, the universal joint connecting the load cell to the upper grip, and the extensometer with its specimen clips makes the tensile test a physically more complicated procedure, as apposed to the simplicity of the three-point-bend test design. All these complicating factors may influence the exact repeatablility of test condions during the tensile test. Although the instrumentation used in the tensile test is more complicated that the bend test, the tensile test is much more sensitive in separating the material characteristic of specimens tested.

The repeatability of experimentation was compared between the tensile and bend tests by taking the standard deviation and dividing by the mean of the various reported values and multiplied by 100%, {(std. dev./mean)x100%}, for each test condition, and then the summation of this ratio for all test conditions was divided by the number of test conditions, [Σ{(std. dev./mean)x100%}/(# of test conditions)]. This value is the overall average percent of the standard deviation divided by the mean. For the bend test, the values for the flexural modulus of elasticity (E_f), the approximated flexural yield strength (FYS) at the 0.2% offset and the corresponding approximated flexural strain at the 0.2% offset are 2.52%, 4.39% and 3.96%, respectively. For the tensile test, the value for the tensile modulus of elasticity (E_t), the yield strength at the 0.2% offset and the corresponding strain at the 0.2% offset are 5.9%, 5.62%, and 8.9%, respectively. From these values it can be seen that the bend test is more repeatable that the tensile test, thus giving less variation in data for a given test condition. The value of 8.9% for the corresponding strain at the 0.2% offset demonstrates that there may considerable error in determining the exact abscissa (horizontal) origin of the plot do to

such artifacts (view the very initial nonlinear portions of Figures 21c and 23a as opposed the linear origins of the bend test data) as slack in the specimen and gripping apparatus, and/or in the case of very light and flexible wires, some torsional component cause by the weight of the extensometer and its cored at the beginning of the test.

The results of the tensile test for the metal alloy wires tested are in very good agreement with values reported in recent orthodontic investigations for both value of the tensile modulus of elasticity (E_t) and the yield strength (YS) at the 0.2% offset (see Table 1). There is more variability in the values of yield strength (YS) than the modulus of elasticity (E) as reported by various authors because the method of determination of the yield strength (YS) involves the selection of a arbitrary offset or actually determining the linear limit of the initial linear portion of the stress-strain curve which has not been standardized among the investigators. Burstone and Golberg (1982) reported the yield strength at a 0.1% offset so it is expected that their yield strength value of 239,000 ± 26 psi would be lower than the value of yield strength reported here at the 0.2% offset which is 272,000 ± 27 psi. Considering this source of variation, the yield strength at a 0.2% offset reported here is within the ranges reported for the various metal alloy wires by other investigators.

The results presented here for the tensile modulus of elasticity (E_t) are in particular close agreement with the work of Goldberg and Burstone (1982) and Asgharnia and Brantley (1986) who used a tensile test instrumentation that is very similar to the one used herein. There values for the tensile modulus of elasticity (E_t) for stainless steel was 25.0×10^6 and 24.4×10^6 psi, respectively, and the overall average of all sizes of Tru-Chrome® stainless steel

reported here is $24.2 \times 10^6 \pm 1.4 \times 10^6$ psi. By comparing the tensile test results of this study to the range of values present for the spectrum of metal alloy wires in Table I, it is obvious that the test protocol developed here is sufficiently accurate isolate the mechanical properties of the tensile modulus of elasticity (E_t) and yield strength (YS) for a given material.

The values reported herein for the flexural modulus of elasticity (E_f) and the flexural yield strength (FYS) at the 0.2% offset were higher than for the corresponding values reported for the tensile test. The proportions that the values in bending test are higher than opposed to the tensile test are consistent with the findings of other investigators (Ashgarnia and Brantley, 1986).

The values of the tensile modulus of (E_t) reported herein for the various brands of nickel-titanium tested here were within the established range of values for the tensile modulus of elasticity (E_t), 4.3×10^6 to 8.5×10^6 psi (Drake *et al.*, 1982; Miura *et al.*, 1986, respectively), for *Nitinol™ brand nickel-titanium wire. The value of the modulus of elasticity of NiTi™ brand nickel titanium was the highest at 8.9×10^6 psi and information about the specific modulus of elasticity (E) for this brand was not found in the literature. As can be see from Tables IV and VII there is considerable variation in the modulus of elasticity (E) between nickel-titanium wire brands. Exact reference values of the modulus of elasticity and yield strength for all the brand of nickel titanium wire studied here are not available in the literature.

Of interest is the varying degree of discontinuous yield each brand of the nickel-titanium

*Unitek Corp., Monrovia, Calif.

wires undergoes when deformed. The discontinuous yield region of the nickel-titanium stress strain diagrams is were there is a relatively constant stress, but the strain is increasing. This region is seen of the stress-strain diagrams of nickel-titanium as a nearly horizontal region after the wire has encountered stresses that are beyond the linear elastic portion. This region is what gives these nickel-titanium wires their "superelastic" properties (Miura *et al.*, 1986). This phenomenon is due to the stress induced martinsitic phase transformation. Rather than going through a lattice slip that induces deformation of most metals, nickel-titanium undergoes a martinsitic phase transformation which induces the material deformation. During the discontinuous yielding region, more elements of the nickel-titanium wire are recruited from the austenitic to martensitic phase. When the wire is exposed to temperatures at its temperature transition range (TTR), the wire can return to its austenite phase and to its original shape without permanent deformation (Muira *et al.*, 1986). Of great clinical significance is that, by nature of their composition (Khier, 1988), certain nickel-titanium wires have the temperature transition range (TTR) at body temperature and there their most optimal "superelastic" properties can be obtained when the wire is in the mouth. This discussion of nickel-titanium wire was done so that the exceptional "superelastic" properties of nickel-titanium wires be understood, its clinical efficacy better appreciated, and to realizes that the ability of nonmetal materials, such as polymers, to possess such ideal "superelasticity" is unlikely do to non-metallic molecular structure.

The "superelastic" properties of the nickel-titanium wires as reflected in the discontinuous yielding region on the tensile test stress-strain diagram are not obvious on stress-strain

diagram from the bend test (see Figures 23d, 24a, 24b, 24c, 24d, 25a, and 25b as compared to Figures 42d, 44b, 44d, 45b, 45d, 43b, and 43d, respectively). This unique property could not be explained if only bend tests were done. This demonstrates that tensile test has a better inherent ability to characterize material properties than the bend test. The tensile test, because it involves the uniaxial, centroidal stressing of all elements of the wire in a homogenous manner, it tends to separate various characteristics of deformation phenomenon. In the case of the bend test, both compression and tensile behavior is occurring simultaneously in a non-homogeneous manner, when considering the cross section of the specimen. Thus deformation phenomenon as observed on the bend diagrams tends to present an obscured blend (gradient) of characteristics.

A good illustration of what may be a blending of deformation phenomenon (a gradient of different phenomenon at various points in the cross section of the wire) during the bend test is seen in the load-deflection and approximated flexuralstress-strain diagrams of the bend test data for the Sentalloy® wires (particularly Figures 44c and 44d), where it appears that there are two distinct linear portions of the curve before the maximal bending load is reached). As was the case, the very initial linear portions of the diagrams of these materials gave values of the flexural modulus of elasticity (E_f) of 8.2×10^6 to 9.2×10^6 psi. These values tended to be on the high side of the range of values for the tensile modulus of elasticity (E_t) of 4.3×10^6 to 8.5×10^6 psi as previously reported (Drake *et al.*, 1982 ; Miura, *et al.*, 1986, respectively) for another brand of nickel-titanium, Nitinol™. Especially in the case of the Sentalloy® Light wires, there seemed to be two distinct linear regions originating from the origin before the

discontinuous maximal bending load had been reached. In the particular case of Sentalloy® Light, the most initial linear portion originated at the origin and the secocodary linear portion, occuring before the maximal bending load had been placed, could be extrapolated to the origin. Since the definition of the modulus of elastic (E) involves the "initial" linear portion of the stress-strain curve, values for the flexural modulus of elasticity (E_f) were reported by means of analyzing the most initial linear portion.

Since Sentalloy® Light wires were the most obvious case of this phenomenon, the secondary linear portion, which occurred before the maximal bending stress was reached, was extrapolated to the origin and the slope was calculated in order to determine what may be the cause of this double linear portion phenomenon that occurred before the maximal bending load was obtained (see Figures 44c and 44d). Finding the slope of this secondary linear portion before the maximal bending load was reached, with extrapolation to the origin, would roughly approximate of the "flexural modulus of elasticity (E_f)" in this portion of the curve. It was found to be $4.7 \pm 0.07 \times 10^6$ psi and this is more consistent with the values found for the modulus of elasticity (E_t) in the tensile test for actual initial linear data. The unusual initial linear portion in the bend test that gave these wires a higher flexural modulus of elasticity (E_f) was thought to be due to the fact that some elements in the wire may be transforming to the martinsitic phase earlier that others because stresses are unevenly distributed in the specimen while undergoing bending.

In order to investigate this hypothesis, tensile data for the Sentalloy® Light wire was examined since this may give a clearer picture of what may be causing this phenomenon in

this particular bend test data. To further investigate if phase transformations may result in this phenomenon, the slope of the line that occurs after the discontinuous yielding region of the tensile stress-strain diagram (the portion of the curve after a strain of 0.05 ln(in/in) on Tensile Figure 24b) was measured because this would indicate the "modulus of elasticty" of the more wholly martinsitic material. Surprisingly, the slope (the martensitic "modulus of elasticity") at this portion of the tensile curve was lower than the tensile modulus of elasticity (E_t) for the initial linear portion of the curve (a more austenitic material) and would probably not account for early increases in the flexural modulus of elasticity (E_f) as found in the initial linear portion of the bend test data. As was the case with the Sentalloy® wires, if some elements of the wire were transforming early and reflecting this martensitic "modulus of elasticity" earlier in deformation it would tend to lower the initial slope rather than increase it as suggested by the corresponding tensile data. As seen from the bend test diagrams of other materials, this curve shape in the bend test was unique to the Sentalloy® wires and was not taken as an artifact (the flexural modulus of elasticity (E_f) was still taken from the most initial linear portion although the values of the flexural modulus of elasticity (E_f) tended to be higher than expected when considering the reported values for another brand of nickel-titanium, Nitinol™).

Another material characteristic that was well demonstrated on the tensile test is the amount of elongation a specimen will tolerate before it fails. The area under the curve from the onset of the load to the point of failure indicates the toughness of the materials. It can be seen in Figure 17b that the Tru-Chrome®, stainless steel specimen failed at an approximate

strain of 0.02 or 2%, Sentalloy® Light, nickel-titanium failed at an approximate strain of 0.13 or 13%, and WOX-3 (PEEK) monofilament failed at an approximate strain of 0.23 or 23%. Specimens did not exhibit failure during the bend test because they were all too flexible the break under the loading conditions of the bend test. They always would slip done through the supports before the necessary stresses could develope to fracture the material. Recording of bend test data stopped before specimen failure, because slippage through the supports occured at a fraction of the failure strain that could only be demonstrated on the on the tensile diagrams. The failure of the material notates the end of the stress-strain curve in the tensile test, where in the bend test, the curve was stopped at an arbitrary and variable point were the specimen appear to slip through the supports or an obvious maximal bending load had been found (Figures 43a and 43b demonstrate what slippage of the specimen through the three-point-bend test supports looks like, this portion of the curve was usually deleted if it happen to occur during a particular trial. Some specimens obtained obvious maximal loads and then would show a decreased load as the test progressed beyond this point, and still before any slippage behavior was noticed. In these cases the test was stopped here before slippage was seen, but after the maximal bending load was obtained, see Figures 37a and 37b). Figures 33a and 33b shows that because of the arbitrary ending of the bend test data collection, no information about specimen failure is demonstrated about the various materials shown in this diagram of bend test data. These materials all had distinctive failure points as see on Figure 18b for the tensile data.

It can be seen that stress-strain diagrams tend to factor-out influences of varied wire

sizes of a given material, because as seen on Figure 13a, which is tensile data for four different diameters of Tru-Chrome® arch wires, the different curves tend to be grouped together and of relatively the same shape. Conversely, the bend test tends to separate the curves of the archwires of different sizes when load-deflection diagrams are constructed, because these diagrams are influenced by the size of the specimen (compare Figures 28a to 13a for the same test conditions). When the bending load-deflection diagram is transformed in to an approximated flexural stress-strain diagram by using the definition of the modulus of elasticity, $E=\sigma/\varepsilon$, and values of load and deflection are plugged in to the respective stress, σ, and strain, ε, coefficients (see Methods section for equations used), the curves plotted on this approximated flexural stress-strain diagram tend to become more independent of wire sizes just like the actual stress-strain diagrams derived from the tensile test (compare Figures 28b ans 13a, repectively). By comparing the load-deflection Figure 28a (four different Tru-Chrome® wire sizes tested), to Figure 28b which is the approximate flexural stress-strain diagram draw by converting the load-deflection data of these four wire sizes, it is demonstrated that stress-strain curves tend to factor-out wire size influences. The approximated flexural stress-strain Figure 28b also demonstrates that the initial linear portions of these four curves have almost been transformed into a single line which defines the linear characteristics of the Tru-Chrome® material. Deviations from these closely grouped lines of the linear portion tend to diverge as the curve becomes curvilinear, this is because the equation used to convert this data from load-deflection to approximated flexural stress-strain data is only valid for initial linear portions of the curve. Errors tend to become more

significant as the curve becomes more nonlinear. The constructed approximated flexural stress-strain curves from the bend test offer the wire designer the ability to enter variable parameters such any wire size of immediate interest into calculations and determine stress-strain behavior without requiring a separated load-deflection diagram for specific wire size he wants to consider. The orthodontic clinician may fine it convenient to look at load-deflection diagrams since only four standardized wire sizes are usually offer for orthodontic arch wires.

During the literature review it was noticed that there was variation in selecting a value for the amount of yield strength offset. Values of yield strength at 0.01% (Goldberg *et al.*, 1977), 0.1% (Goldberg *et al.*, 1977; Drake, *et al.*, 1982; Asgharnia and Brantley, 1986), 0.2% (Burstone and Goldberg, 1983) offsets and at the proportional limit (Asgharnia, 1983) have been reported by the various orthodontic researchers. The decision where to the select the yield strength offset should be carried out on the basis of whether it has clinical significance, and therefore providing useful information, rather than accepting offsets which were selected by other investigator with interests other than orthodontics. For example, the standard 0.2% yield strength offset used in general engineering purposes was selected specifically as it related to specific parameters of importance to engineering design applications. These parameters may not have the same significance when trying to define useful deformation parameters of orthodontic arch wire. Several values for the arbitrary yield point offset were investigated here prior to choosing the 0.2% offset in this study, which in itself was initially selected here in order to be consistent with engineering and other orthodontic reference values. It was noticed while trying to determine yield strengths at exactly the proportional

clinically visible. The approximated flexural yield strength (FYS) at the 0.2% offset for all the materials studied here fell in the range between 0.0215 in (0.55mm) to 0.0595 in (1.51mm). The difference between the approximate location of the proportional limit (not reported herein because of difficulty in locating it accurately, but was approximately graphically just for the sake of this discussion on where to select an appropriate yield strength offset) and the approximated flexural yield strength (FYS) at the 0.2% offset, was calculated in terms of difference in deflection between the two points. The difference between these two points for all the materials tessted fell within the range of about 0.005 in (0.127 mm) to 0.030 inch (0.762 mm) with the majority of trials falling between 0.015 inch (0.381 mm) and 0.030 inch (0.762 mm). This demonstrates that with the selection of a 0.2% strain offset, the clinician can approximate the 0.2% yield offset to within a visible error in the visual detection of the actualdeflection of the wire between 0.015 inch (0.381 mm) and 0.030 inch (0.762 mm) and still not dramatically underestimate were the proportional limit of the wire. However, this depends on were the particular wire type fell in the above range of difference between the proportional limit and the approximated flexural yield strength (FYS) at th 0.2% offset in terms of deflection (a clinically noticeable parameter).

Goldberg *et al*., (1977) felt that the orthodontic wires he tested had exceeded their elastic limit at the 0.01% offset, so he felt that any larger offset would not be a good design parameter for elastically linear orthodontic appliances. The selection of the 0.2% yield strength was made herein so as to be consistent with data reported in the engineering literature and other orthodontic references, and in addition, there was interest in selecting a

yield offset that would somehow be detectable clinically (*e.g.* by visually approximating the amount of deflection that was occurring for a given bracket engagement and checking reported values to see if the deflection corresponding to the approximated 0.2% strain offset has been exceeded).

The Material Properties of the Esthetic Wires Tested and The Likelihood of Their Potential Efficacy as Esthetic Orthodontic Arch wires

As the search for esthetic materials began, it became obvious that polymers were being used to produce common place items such as fishing line, broombristles, tire cord, and many other products, resembled the dimensions and shapes of orthodontic arch wires. The flexibility and esthetic quality found in some of these common products encouraged investigation of the mechanical properties of various polymers. References on the mechanical properties of polymers immediately demonstrated that they could not provide a modulus of elasticity (E) in the range of stainless steel, the most common used orthodontic wire. In addition, it was found that polymers generally lacked the property of formability, which is important for wires used later in treatment in order to be bent in to wire configurations which induce torque, detailing movements, intrusive/extrusive forces, and space closing mechanics.

While initial investigations generally ruled out obtaining a clinically effective polymer or composite wire with a modulus of elasticity near the stainless steel range, interest was focus on the metal alloy wire that had established their clinical efficacy of the basis of delivering

light, consistent forces to teeth. Such wires included the nickel-titanium and multistranded stainless steel wires. It seemed more likely that a polymer wire could be deliver force in these lower ranges. The material search became more directed at finding an esthetic material that could produce an initial leveling and aligning wire, since this type of wire involves the simplest application where formability and the ability to produce heavy forces is not necessary. Further more round wire configurations are usually used in this application and other polymer products on the markets were more available in this round wire shape than in rectangular wire form.

As esthetic material samples were obtained, tested and compared to the metal alloy in terms of mechanical properties it became obvious that stainless steel was not the best standard of comparison because it's properties were not of the magnitude of the polymers tested (see Figures 16a, 16b, 17a, 17b, 18a, 19a, 34a, and 34b). The nickel-titanium and in particular the multistranded stainless steel wires proved to be in a range of mechanical properties (modulus of elasticity (E) and yield strength (YS)) lend themselves to be better standards of comparisons for the polymer materials (see Figures 16a, 16b, 17a, 17b, 18a, 19a, 34a, 34b, 35a, and 35b).

It was particularly encouraging to find that the apparent or effective flexural modulus of elasticity (E_f) of the Respond® 6-strand multistranded stainless steel wire was only 1.64 ± 0.02x10^6 psi. From examining the reference values (The Modern Plastics Encyclopedia, 1990) of the modulus of elasticity for various polymers, it was found that many polymers, particularly fibers reinforced composites with fiber glass, graphite or other filler exceeded this

range. Further investigation discovered that while fillers such as graphite tremendously increased the flexural properties of polymers, some of them were incompatible with esthetic considerations, since their color cannot be used to make a clear wire or one that is at least tooth colored. Fiber glass is a readily available fiber reinforcement that would satisfy esthetic demands and although it dramatically modulus of elasticity (E) of the polymer composite, the drawback is that it produces a composite material that is brittle.

Polymers, as a broad class, usually have a flexural modulus of elasticity (E_f) of somewhere in the range of 5,000 to 650,000 psi in their unfilled state (The Modern Plastics Encyclopedia, 1990). These values may not take into consideration the dramatic increase in the modulus of elasticity do the increasing the molecular orientation of the polymer during some formation processes. With the addition of 30% volume percent of fiber glass the flexural modulus of elasticity (E_f) of many polymers can be boosted to over 1,000,000 psi, however the composites become too brittle for the intended purposes. With the addition of 40% volume percent PAN carbon fibers in composites, they can approach 5,000,000 psi. Unfortunately these fillers and various other fillers because of their coloration, may have limited esthetic potential if used in the production of arch wires. Composites with such high volumes of filler would likely be to brittle for use in producing effective arch wires, however, this information was included to demonstrate that even if the most extreme amount and type of modulus of elasticity (E) increasing fillers were used, a wire of low mechanical properties in comparison to most metal wires would still be produced.

The esthetic materials that were tested herein represented two basis categories of

polymer products. The Glastic® and Optiflex™ wires are fiber glass reinforced composites, and the MX-501 (PEEK) polyether ether ketone, WOX-3 (PEEK) polyether ether ketone, WP-89 (PET) high molecular weight polyester, WP-320 (PET) high molecular weight polyester, and the WN-101 Nylon 6/6 wires are unfilled and extruded monofilaments (see Tables IV to XI for the values of mechanical properties reported for the esthetic materials in this study). The Glastic® wire had an impressive flexural modulus of elasticity (E_f) of $7.32 \pm 0.37 \times 10^6$ psi and a tensile modulus (E) of $7.81 \pm 0.12 \times 10^6$ psi (consistent with the 7 to 8 million psi range for both moduli as given by the manufacturer; Goeden, 1990). The tensile modulus of elasticity (E_t) in this case is the longitudinal elastic modulus of the composite because of the longitudinal orientation of the continuous glass fibers. The longitudinal modulus of elasticity ($E_{comp.\ long.}$) could be calculated from the equation (Weeton, Peters, and Thomas, 1987) for specimens in elastic deformation by the following equation (only valid if void are considered equal to zero, other wise corrections for voids must be made, see Weeton, Peters, and Thomas, 1987),

$$E_{comp.\ long.} = k_{fiber} * E_{fiber} + k_{matrix} * E_{matrix}$$

where K=respective volume fraction of filler or composite, volume fraction, and

E=respective longitudinal elastic modulus of the filler or the modulus composite, psi.

Taking the fiber glass filler in the Glastic® as a type E-glass with a longitudinal modulus of 12.4×10^6 psi and the modulus of the arcylated epoxy matrix of 400,000 psi, the calculated longitudinal modulus of elasticity is 7.96×10^6 psi for a 63% glass filled Glastic® wire. Equations are also available to estimate the transverse modulus of elasticity of the composite

which is more important to know since this is the direction in which longitudinal fibers would be are stressed during orthodontic procedures. Fiber glass is unique as far as fillers go because its longitudinal modulus of elasticity is reported as equal to its transverse modulus of elasticity and since most fillers have a dramatic difference between the two, many longitudinally oriented fillers while adding greatly to the longitudinal modulus may not add very significantly to the transverse modulus (in the case of *Kevlar fibers the transverse modulus is only 3% of longitudinal modulus (Weeton, Peters, and Thomas, 1987)). The difference between the longitundintal and tranverse moduli of elasticity of certain materials is a manifestation of thier unique molecular structure (*e.g.*, ploymers fillers have a high longitundinal modulus of ealsticity because of thier longitudinally oriented molecular chain structure). The orientation of the filler fibers is critical when designing a composite system.

The Glastic® wire was only available in a specimens that were as small as 0.030" in diameter so it is unknown how this material would respond if it were in the archwire size range. The Glastic® wire is similar to the Optiflex™ wire experiences at least partial breakage of the fiber glass filler fibers when it is bent sharply or to the extend on some clinical applications would necessitate. If the wire is bent too sharply, the nylon matrix over the fiberoptic core of the Otpiflex™ wire tends to hold the fragment core in place, but in the case of the Glastic® wire, were the acrylated epoxy matrix is a more brittle than nylon, the glass fibers tend to break out of the matrix and splinter at the surface of the composite.

---

*Dupont Co., Wilmington, De.

The Optiflex™ wire has a 190 micron fiberoptic core in the center of a 0.020" or 0.017" overall diameter wire with the balance of the wire made of the surrounding nylon matrix (Farzin'nia, 1990). This is an approximately 37% fiber glass volume percent filler. The flexural modulus of elasticity (E_f) of the Optiflex™ wire unexpectedly low for a reinforced composite at 360,000 ±4,000 psi. This concurs with the manufacturer reported the flexural modulus of elasticity to be in the 400,000 to 500,000 psi range. The tensile modulus of elasticity (E_t) for the Optiflex™ wire was unreliable since the fiberoptic core was pulled through the nylon matrix, which was left compressed between the tensile clamps, as the tensile test progressed. One may envision that the Optiflex™ wire may be better described as a nylon-coated fiber glass core wire. The Glastic® wire has multifilamentous fiber glass strands embedded throughout the diameter of the wire in the arcrylated epoxy matrix. Because of the nature of the fiber glass in these two wires, some breakage of fibers maybe expected if they were deformed under certain conditions that may arise in clinical use. The obvious advantage of using fiber glass as a reinforcing filler is that it is clear and provides optimal esthetics. Also the addition of fillers improves the creep properties of the polymer matrix, so the wire may be more protected from losing flexural properties while sustaining a load over a period of long time intervals (Nielsen, 1974).

The polyether ether ketone (PEEK) monofilament wires, MX-501 and WOX-3, which are the same material but processed differently to give different surface texture, behaved similarly in the tensile and bending test. The MX-501 PEEK monofilament which was air quenched provided a very smooth surface, and the WOX-3 PEEK monofilament is water cooled. The

flexural modulus of elasticity (E_f) these materials is approximately 1 million psi (0.97 ± 0.03 x10^6 psi and 1.05 ± 0.11x10^6 psi, respectively) and that is approaching the 1.6 million apparent flexural modulus 0175" Respond® 6-strand multistand initial leveling and aligning wire. The reported the flexural modulus of elasticity (E_f) from the reference is 560,000 psi (The Modern Plastics Encyclopedia, 1990).

The increased values for the tensile and flexural moduli of elasticity, (E_t) and (E_f), seen in the values reported herein, maybe due to a high degree of molecular orientation which is a critical factor influencing the elastic moduli of polymers. Hot stretching of the polymer, followed by rapidly cooling of the melt or by drawing , the moduli of elasticity can be increased parallel to the uniaxial orientation (Nielsen, 1974). The shape of the stress-strain diagram (Figures 26a and 26b) where there is an initial linear portion followed by a curvilinear portion, a "knee", and then continuation of another upwardly progressing linear portion indicates a high degree of molecular orientation for polymer (Nielsen, 1974). Molecular orientation explains the greater value of moduli for these extruded monofliment wires. Polyether ether ketone (PEEK) tends to have an inherent brownish color that may interfere with producing wires of esthetic quality. In addition, PEEK is a high temperature thermoplastic with a melt temperature of 633°F and this may make the coloration process difficult with the commonly used polyolefins coloring agents, which have a melt temperature of about 340°F (Riddle, 1990). The manufacturer can produce PEEK monofliments in any requested size, although esthetic coloration may be difficult (Riddle, 1990).

Burstone *et al.* (1983) reported an apparent flexural modulus of elasticity (E_f) for D-

Rect®, a 9-stranded, interwoven rectangular multistranded stainless steel wire, at 0.89 ± 0.08×10^6 psi when loaded parallel to the larger cross-sectional dimension of a 0.016" x 0.022" rectangular wire and $1.26 \pm 0.16 \times 10^6$ psi when loaded parallel to the smaller cross-sectional dimension of a 0.016" x 0.022" rectangular wire in a cantilever bend test. The D-Rect® wire which has known clinical efficacy, and when compared the flexural modulus of elasticity (E_f) values of the PEEK wires, indicates that the PEEK wire may have a similar level of clinical efficacy when based on approximately equal values for the flexural modulus of elasticity (Ef).

In terms of cost, PEEK is an expensive polymer and in final product form it costs about $200/lbs. For the 0.0236" wire sample tested here, there is 1,270 yards of wire per pound which translates into a cost of about 2.6 cents for a 6" length (Riddle, 1990). The great cost advantage of these materials can be seen when compare to the national average of $4.21 for a preformed nickel-titanium wire (Masel Corporation, 1989).

The Nylon 6/6 monofilament wire, WN-101, had a flexural modulus of elasticity (E_f) of 560,000 ±9,000 psi and the reported reference values 410,000 to 470,000 psi for an unreinforced molding compound (The Modern Plastics Encyclopedia, 1990). A disadvantage to Nylon 6/6 in addition to its comparatively low flexural modulus of elasticity (E_f), is that it has a moderately high moisture absorption of 4.2%. This value for PEEK is only 0.15% and for PET polyester it is only 0.2% (Seymour, 1987). Nylon can have a 50% reduction of modulus of elasticity (E) if significant water absorption occurs. An advantage to Nylon 6/6 is that is available in just about any color including clear and the manufacturer can produce any requested wire diameter (Riddle, 1990). The relatively high flexural moduli of elasticity (E_f)

reported for PEEK and the PET polyester monofilaments make them better candidates for esthetic arch wire materials.

The most impressive esthetic materials studied in this investigation on the basis of relative flexural modulus of elasticity (E_f), were the WP-89 and WP-320 high molecular weight PET polyester monofilaments. These monofilaments are of a high viscosity type which have better abrasion properties compared to low viscosity types (Riddle, 1990). WP-89 and WP-320 polyester monofilaments are essentially the same product, but the where produced with different coloring agents and diameters. These PET polyester monofilaments are available in variable colors including clear and can be produced in any requested size (Riddle, 1990). The reference values for the flexural modulus of elasticity (E_f) for unfilled PET poylester monofilament is between 350,000 and 450,000 psi (The Modern Plastics Encyclopedia, 1990). The flexural modulus of elasticity (E_f) for the WP-89 and WP-320 monofilament wires reported here are $2.43 \pm 0.04 \times 10^6$ and $2.24 \pm 0.02 \times 10^6$ psi, respectively. Factors relating to the molecular orientation that may occur during the processing of these materials may effect considerable changes in the modulus of elastic as discussed in the case of the PEEK monofilaments. Nylons and polyesters used in the tire industry have obtain elastic moduli between 1 and 2 million psi (Litt, 1990). The values of the flexural modulus of elasticity (E_f) of the WP-89 and WP-320 PET polyester monofilaments are 173% and 150% greater than the flexural modulus of elasticity (E_f), $0.89 \pm 0.08 \times 10^6$ psi, reported for a 0.016" x 0.022" D-Rect®, 9-stranded braided multistranded rectangular wire when tested parallel to the large cross-sectional dimension, respectively (Burstone *et al.*, 1983). Compared to the flexural modulus

of elasticity (E_f) of the 0.0175" Respond® 6-stranded multistranded reported here, $1.64\pm0.02x10^6$ psi, the WP-89 and WP-320 PET polyester monofilaments have a flexural modulus of elasticity (E_f) that is 58% and 37% in excess of the Respond® value reported here, respectively.

Based solely on the identification and comparison of the flexural modulus of elasticity (E_f) of the MX-501 and WOX-3 PEEK monofilaments, they may have a clinical efficacy in terms of providing forces in the elastic range of these materials that is approximately equal to the D-Rect® multistranded stainless steel wire, and the WP-89 and WP-320 PET polyester monofilaments may have a clinical efficacy in terms of providing forces in the elastic range of these materials that is greater than that of the Respond® multistranded stainless steel wire.

As was brought out in the literature review, the mechanical properties of polymers, especially non-filled ones, are dependent on time, temperature and the manner of force application (Nielsen, 1974). The parameters examined in this investigation, the moduli of elasticity, and the various yield point data, only give a gross approximation of the actual behavior the polymers will experience when they are subjected to the highly variable conditions when in the desired product form. A critically important parameter is that also must be known is to what extent the mechanical properties of the polymers tested will deteriorate due to creep. Even after a single deflection of the polymer wire, certain fatigue phenomenon may occur that greatly reduce the springback potential of the wire and thus the clinical efficacy and predictability. In order to understand the nature of the fatigue of these materials it is necessary to do tensile strain cycling and bending flexural cycling tests. The mechanical

parameters studied in this investigation can only provide information to the wire designer so he can decide if the materials selected warrants further investigation.

A flexural cycling test may be difficult using the three-point-bend test set-up since as the load is removed from the specimen the wire is free to rotate on the supports and inaccurate springback data occur particularly if permanent deformation of the wire had occurred. Since cantilever bend tests fixtures are designed with easily readable degree scales next to the deformed specimen, this bend test technique may lend itself to easier interpretation of flexural cycling (springback) information.

Although flexural cycling bend tests were not done in this study to address the fatigue properties of materials, the Optiflex™ fiber glass reinforced esthetic wire seemed to have a better ability to maintain its springback properties after repeated bends as opposed to the unfilled polymers. Reinforcement of the polymers increases the creep resistant properties in composite materials (Nielsen, 1974). Reinforcement of the unfilled polymers maybe a consideration if the unfilled polymers prove to have unfavorable fatigue and creep properties that would otherwise limit their clinical efficacy if used to make esthetic orthodontic arch wires. As discussed earlier the shape of the PEEK monofilament tensile stress-strain curve tends to exhibit an initial linear portion then it has a "knee" and the continues upward (see Figures 26a and 26b), this is consistent with plastic behavior (see Figure 4). The PET polyester monofilaments have a higher tensile and flexuralmoduli of elasticity, (E_t) and (E_f), than the PEEK Monofilaments, but their tensile stress-strain curves appear to be more elastomeric (see Figure 4). Again, strain cycling tests would be necessary to truly and more fully

understand the unique deformation properties of these materials.

SUMMARY AND CONCLUSIONS

The uniaxial tensile test and the three-point-bend tests developed in this investigation provided quanitified mechanical parameters for the metal wires studied herein that are consistent with a number of other references. On the basis that these tests provided accurate mechanical properties data for the various metal wires studied, while also while considering their particular clinical efficacy, a mechanical properties testing protocol and a standard of comparison for new esthetic materials was established. Since the mechanical properties of polymers, particularly unfilled polymers, are dependent of time, temperature, and manner of force application, and since the mechanical properties tests done herein do not address these factors, the results from this investigation are only offered as an initial screening measure for potential esthetic arch wire materials. The following conclusions have been drawn from this investigation:

(1) On the basis of comparison with reference values, the uniaxial tensile test and the three-point-bend test developed herein are highly accurate, and have the ability to define the respective mechanical properties of the materials that are tested.

(2) It is possible that polymers can deliver clinical efficacy similar to the D-Rect® 9-stranded 0.016" x 0.022" and the Respond® 6-stranded 0.0175" multistranded stainless steel wires based solely on the experimental values of the instantaneous flexural modulus of the elasticity (E_f) of the (PET) polyester monofilaments and (PEEK) polyether ether ketone monofilaments wires.

(3) Both tensile tests and bending tests are necessary to fully characterize the particular mechanical properties studied herein of any new arch wire materials.

(4) The creep properties of the polymers that are suggested for use as arch wires must be evaluated since they will ultimately be left in place for three or more weeks and it is necessary to determine if their flexural properties will deteriorate over the specified time frame to an extent that would significantly reduce their clinical efficacy.

(5) Factors such as biocompatibility must be determined if esthetic arch wires are to become successful products. The PET polyester monofilaments are already used in plastic bottles and should satisfy biocompatibility requirements.

(6) Close coordination with a polymer expert and a manufacturer maybe necessary to ultimately establish a marketable product.

(7) The search for esthetic materials should not be limited to polymers, since such areas as the metal coating industry are rather sophisticated, in that an esthetic nickel-titanium wire, Spectra-Sentalloy®, has already has been developed which has a titanium nitrate oxidized surface, that provides the wire with improve esthetics and still has uncompromised, if not ideal mechanical properties.

(8) The performance in term of the tensile and flexural moduli of elasticity, (E_t) and (E_f), of the polyether ether ketone (PEEK) and PET polyester monofilament esthetic wires warrants further investigation in order to understand their test condition dependent mechanical properties.

(9) The elevated tensile and flexural moduli of elasticity, (E_t) and (E_f), of the extruded

monofilaments, polyether ether ketone (PEEK) and the PET polyester in particular, over the reference values, which are usually based on polymers in molded form, demonstrates the variability in the mechanical properties of polymers do to the manner of processing.

(10) It may be necessary to reinforce unfilled polymers in order to reduce the creep properties from limiting the clinical efficacy of polymer material.

The information provided by the methods used in this study can be a useful tool in screening the potential material that are being considered for use in the production of esthetic arch wires. The unique mechanical properties of polymers must be understood and further investigations are necessary to quantify the test condition dependent mechanical behavior of the polymers of interest. This information must be obtained if an esthetic polymer arch wire is to be designed that will ultimately yield a predictable clinical efficacy. The following are suggestions for future work:

(1) Make further considerations on which material properties are critical to know when selecting new materials for arch wires. In example, fatigue properties have not been generally reported by orthodontic researchers, but this parameter seems critically important, especially with polymer materials that may behave very differently from metals in this respect.

(2) Design a protocol to study the creep properties of new esthetic material for arch wires.

(3) Design a protocol to study the tensile strain and flexural strain cycling properties (fatigue) of new esthetic materials for arch wires.

(4) Establish a clinical testing protocol to assess the clinical efficacy of the Optiflex™ wire

since it is already on the market and no clinical investigations on its clinical efficacy have been published. This clinical testing protocol can also be used to assess the clinical efficacy of new esthetic arch wire materials once their mechanical properties and biocompatablity are considered favorable .

LITERATURE CITED

American Society of Testing and Materials (ASTM): Designation: A 370-88, Standard Test Methods and Definitions for Mechanical Testing of Steel Products. Annual Book of ASTM Standards, 03.01: 3-39, 1988.

Andreasen, G. F. and Morrow, R. E. : Laboratory and clinical analyses of nitinol wire. Am. J. Orthod., 73: 142-151, 1978.

Asgharnia, M. K. : Refinements of bending mechanics analysis and test methods for orthodontic wires. M.S. Thesis, Graduate School, Marquette University, Milwaukee, Wisconsin, 1983.

Asgharnia, M. K. and Brantley, W. A. : Comparison of bending and tension tests for orthodontic wires. Am. J. Orthod., 89: 228-236, 1986.

Brantley, W. A., Private communication with the Department of Restorative Dentistry, Material Science Division, The Ohio State University, Columbus, Ohio, 1990.

Brantley, W. A., Augat, W. S., Myers, C. L., and Winders, R.V. : Bending deformation studies of orthodontic wires. J. Dent. Res. 57: 609-615, 1978.

Brantley, W. A., and Myers, C. L. : Measurement of bending deformation for small diameter orthodontic wires. J. Dent. Res. 58: 1696-1700, 1979.

Broutman, L. J. and Krock, R. H. : Modern Composite Materials. Reading, Mass.:Addison-Wesley Pub. Co., 1967.

Burstone, C. J. : Variable-modulus orthodontics. Am. J. Orthod. 80: 1-16, 1981.

Burstone, C. J. and Goldberg, A. J. : Maximum forces and deflections from orthodontic appliances. Am. J. Orthod. 84: 95-103, 1983.

Byars, E. F. and Snyder, R. D. : Engineering Mechanics of Deformable Bodies. Scranton: International Textbook Co.,1963.

Council on Dental Materials and Devices of the American Dental Association : New American Dental Association Specification No. 32 for Orthodontic Wires Not Containing Precious Metals. JADA, 95: 1169-1170, 1977.

Dieter, G. E. : Mechanical Metallurgy. New York: McGraw-Hill, Inc.,1976.

Drake, S. R., Wayne, D. M., Powers, J. M., and Asgar, K.: Mechanical Properties of Orthodontic Wires in Tension, Bending, and Torsion. Am. J. Orthod., 82: 206-210, 1982.

Farzin'nia, F. : Private communication with the Metallurgy Department, Ormco Corp., Glendora, Calif., 1990.

Goeden, H. A. : Private commumnication with the manager of the Fiber Optic Group, Glastic Corp., Cleveland, Ohio, 1990.

Goldberg, A. J. and Burstone, C. J. : An evaluation of beta titanium alloys for use in orthodontic appliances. J. Dent. Res. 58: 593-599, 1979.

Goldberg, A. J. and Burstone, C. J. at the request of the Council on Dental Materials, Instruments, and Equipment of the American Dental Association: Status report on beta titanium orthodontic wires. JADA, 105: 684-685, 1982.

Goldberg, A. J. Morton, J. And Burstone, C. J. : The flexure modulus of elasticity of orthodontic wires. J. Dent. Res. 62: 856-858, 1983.

Goldberg, J., Vanderby, R., Jr., and Burstone, C. J. : Reduction in the modulus of elasticity in orthodontic wires. J. Dent. Res. 56: 1227-1231, 1977.

Gosney, M. B. E. : An Investigation into Factors Which May Deter Patients from Undergoing Orthodontic Treatment. British J. Orthod., 12: 133-138, 1985.

Griffel, W. : Handbook of Formulas for Stress and Strain. New York: Frederick Ungar Publishing Co., 1966.

Howe, G. L., Greener, E. H., and Grimmins, D. S. : Mechanical properties and stress relief of stainless steel orthodontic wire. Angle Orthod. 38: 244-249, 1968.

Ingram, S. B., Gipe, D. P. , and Smith, R. J. : Comparative Range of Orthodontic Wires. Am. J. Orthod. 90: 296-307, 1986.

Kapila, S. and Sachdeva, R. : Mechanical properties and clinical applications of orthodontic wires. Am. J. Orthod. 96: 100-109, 1989.

Khier, S. E. : Structural characterization, biomechanical properties, and potentiodynamic polarization behavior of nickel-titanium orthodntic wire alloy. Ph. D. Dissertation, Graduate School, Marquette University, Milwaukee, Wisconsin, 1988.

Kusy, R. P. and Dilley, G. J. : Elastic modulus of a triple-stranded stainless steel arch wire via three- and four-point bending. J. Dent. Res., 63: 1232-1240,1984.

Kusy, R. P., Dilley, G. J. and Whitley, J. Q. Mechanical properties of stainless steel orthodontic arch wires. Clin. Mater. [in press, 1989].

Kusy, R. P. and Stush, A. M. : Geometric and material parameters of a nickel-titanium and a beta-titanium orthodontic archwire alloy. Dent. Mater. 3: 207-217, 1987.

Litt, M. : Private communication with the Macromolecular Science Department, Case Western Reserve University, Cleveland, Ohio, 1990.

MacDermott, C. P. : Selecting Thermoplastics for Engineering Applications. New York: Marcel Dekker, Inc., 1984.

Masel Orthodontics, Inc. : Masel Orthodontic Supply Catalog. Bristrol, Pa. : Masel Orthod. Inc., 1989.

Miura, F., Mogi, M., Ohura, Y., and Hamanaka, H. : The super-elastic property of the Japanese NiTi alloy wire for use in orthodontics. Am. J. Orthod., 90: 1-10, 1986.

Nielsen, L. E. : Mechanical Properties of Polymers and Composites. Vol. 1 and 2, New York: Marcel Dekker, Inc., 1974.

Nikolai, R. J. : Flexural activation and de-activation responces of orthodontic wires in single-tooth, occlusogingival corrections. Dent. Mater., 5: 339-345,1989.

Nikolai, R. J., Anderson, W. T., and Messersmith, M. L. : Structural responces of orthodontic wires in flexure from a proposed alternative to the existing specification test. Am. J. Orthod. 93: 496-504, 1988.

O'Toole, J. L., revised and updated by Carley, J. F. : Designing with plastics. In: Modern Plastics Mid-October Encyclopedia Issue. New York: McGraw-Hill Inc., 1990.

Popov, E. P. : Mechanics of Materials. Englewood Cliffs: Prentice-Hall, Inc., 1963.

Powell, P. C. : Engineering with Polymers. London: Chapman and Hall Ltd., 1983.

Riddle, J. : Private communication with the Industrial Lines Division, Sheakespeare Monofilament Co., Columbia, S. C., 1990.

Seymour, R. B. : Polymers for Engineering Applications. ASM International, Inc.,1987.

Tayer, B. H. and Burek M. J. : A survey of adult's attitudes toward orthodontic therapy. Am. J. Orthod., 79: 305-315, 1981.

Van Krevelen D. W. : Properties of Polymers: Their Estimation and Correlation with Chemical Structure. Amsterdam: Elsevier Scientific Publishing B. V., 1976.

Wheeton, J. W., Peters, D. M., and Thomas, K. L. : Engineers' Guide to Composite Materials. American Society for Metals, by Carnes Publication Services, Inc., 1987.

Yoshikawa, D. K., Burstone, C. J., and Morton, J. : Flexure modulus of orthodontic stainless steel wires. J. Dent. Res. 60: 139-145, 1981.

49 91 355GS 0 104 7 TH